POLITECNICO DI MILANO
DIPARTIMENTO DI ELETTRONICA, INFORMAZIONE E BIOINGEGNERIA
DOCTORAL PROGRAM IN INFORMATION TECHNOLOGY

SAFE AND ADAPTIVE SOCIAL ROBOTS FOR CHILDREN WITH AUTISM

Doctoral Dissertation of:
Ahmad Yaser Alhaddad

Supervisors:
Prof. Andrea Bonarini
Prof. John-John Cabibihan

Tutor:
Prof. Francesco Amigoni

The Chair of the Doctoral Program:
Prof. Barbara Pernici

2020 – Cycle XXXI

Acknowledgements

I have left this part of my dissertation to be written last, not because of the lack of delicacy or etiquette, but because it is the hardest to write. Indeed, it is truly difficult to enumerate all the persons and individuals that have influenced and supported me throughout these years.

I am very grateful to have John-John Cabibihan and Andrea Bonarini as my mentors. Their continuous support, help, and guidance have made many accomplishments possible and rendered many obstacles obsolete.

One can not truly succeed without the unconditional love and support of his family and loved ones. Thank you to the late Abdul Sattar, Amal, Fouad, Eiad, Bashar, Aslan, Fedae, Ghaidaa, Hadia, Mahde, Walaa, Little Amal, Sultan, Suleiman, Salma, Omar, and Mousa. A special thank you to my sister Yousra for her artistic help and support. Thanks to Teab, Sanaa, Khalid, Yossuf, and Maryam for making my Saturdays truly joyful.

One can not forget to thank his colleagues Lutfi, Atif, Shahnaz, Tahir, Ahmad, Adel, Alaa, Davide, Carlos, Ewerton, Nico, Mirco, Suka, Lorenzo, Fabiano, Luca, Cibo, Saniorita, Alessio, and many others. Truly, their support and friendship have made this journey very interesting.

Abstract

Social robots are being considered to be a part of the therapy for children with autism due to the reported efficacy of such technology in improving the outcomes. However, children diagnosed with autism exhibit challenging behaviors that could cause harm to themselves and to others around them. Throwing, hitting, kicking, and self-harming are some examples of the challenging behaviors that were reported to occur among this population. The occurrence of such behaviors during the presence of a social robot could raise some safety concerns. For this reason, the research presented in this dissertation attempts to identify the potential for harm due to the diffusion of social robots and investigate hardware and software means to mitigate them. Considering the advancement in technology and the progress made in many computer science disciplines are making small and adaptable social robots a foreseeable possibility, the studies presented in this dissertation focus on small robotic form factors. The first study quantifies the potential harm to the head due to one of the identified risky scenarios that might occur between a child and a social robot. The results revealed that the overall harm levels based on the selected severity indices are relatively low compared to their respective thresholds. However, the investigation of harm due to the throwing of a small social robot to the head revealed that it could potentially cause tissue injuries, subconcussive or even concussive events in extreme cases. The second two studies are aimed to make small robots safer by optimizing their design. Hence, studies are conducted investigating how robot design can be made safer by investigating different design factors. The first study investigated the

influence of the mass and shape on the linear acceleration of a developed dummy head. The results revealed that the two design factors considered (i.e. mass and shape) affected the resultant response significantly. The second study investigated the influence of the storage modulus and thickness of three different soft materials on the same response. The findings showed that the control factors considered are not statistically significant in attenuating the response. Finally, the last two studies attempt to make small robots more adaptable to promote safer interactions. This is carried out by embedding the recognition of unwanted physical interactions into companion robot with the appropriate timing of responses. The findings of the first study highlight the possibility of characterizing children's negative interactions with robotic toys relying on an accelerometer sensor. The second study showed that producing a late response to an action (i.e. greater than 1.0 s) could negatively affect the children's comprehension of the intended message. The work presented in this dissertation is multidisciplinary that involves the field of Mechanical Engineering and Information Technology.

Contents

List of Figures

List of Tables

Abbreviations

ASD	Autism spectrum disorder
TBI	Traumatic Brain Injury
ATD	Anthropomorphic Test Dummy
HIC	Head Injury Criterion
AIS	Abbreviated Injury Scale
EnuroNCAP	European National Car Assessment Protocol
PLA	Peak Linear Acceleration
DOE	Design of Experiment
OA	Orthogonal Array
FEM	Finite Element Method
AI	Artificial Intelligence
IFR	International Federation of Robotics
DMA	Dynamic Mechanical Analysis
ANOVA	Analysis of Variance
S/N	Signal to Noise
APA	American Psychological Association
LSTM	Long Short-term Memory
MLP	Multi-layer Perceptron
RNN	Recurrent Neural Network

CHAPTER 1

Introduction

Autism spectrum disorder (ASD) is a condition that is diagnosed during early childhood and affects the neurodevelopment. Traditionally, intervention sessions for ASD have been carried out through a human therapist. However, there has been a promising potential of using social robots in interventions based on the evidence reported by many individual studies [47], [171]. Most of the studies conducted in robot-mediated interventions, if not all, did not address some of the safety concerns regarding the diffusion of social robots into therapy. The interaction between children with autism and social robots will introduce some safety concerns and issues (Fig. 1.1).

Children with ASD often exhibit aggressive behaviors that cause a lot of troubles to their families and caregivers. The extent of such aggressive behaviors could even affect their peers and the people around them. Children diagnosed with ASD often exhibit stereotypical repetitive and stimming behaviors as a response to a sensory overload. When their body's senses are overwhelmed by too many stimuli in the environment, they might exhibit shut down, loud outbursts or aggressive behaviors in an attempt to escape from unpleasant sensations. This response could intensify to meltdowns, that is the temporary loss of behavioral control. Biting, hitting, throwing

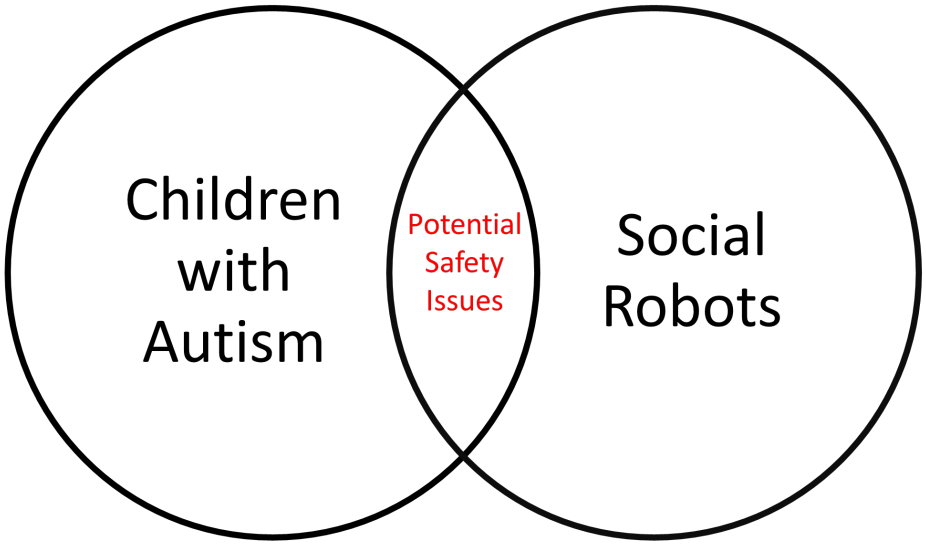

Figure 1.1: *The interaction between children with autism and social robots raises potential safety issues that need to be addressed early on.*

objects, and others are physical signs that are usually associated with meltdowns.

1.1 Overview

Many studies have been conducted on using robots in the therapy sessions with children with ASD. There have been many designs with various shapes, functionalities, sizes, and therapeutic objectives. Most of the existing designs, if not all, were designed initially for research purposes to target a single or a set of objectives; hence, they have been limited in terms of functionality; were not flexible to re-adjust to target different or new objectives; and lacking the feasibility to be deployed to the end-users. When it comes to design features of a robot, there are many important requirements that should be considered, such as safety, adaptability, functionality, and autonomy [82].

Children with autism often show aggressive behaviors that should be

accounted for when designing robots for them. The robot design should be made safe enough not to harm the child and others in case of the occurrence of such behaviors. Few previous designs have paid attention to that aspect, but as a trade-off, the overall functionality of the robot has been limited. Other than the safety of the child and people around them, the robot must be designed to be robust enough to withstand any aggressive behaviors. The overall robot design should be safe and robust at the same time.

Most existing social robots that have been used in therapy were either controlled through a therapist with a hidden controller or through an operator within the same room or at a different room. The adaptability of the robot in that case was limited to the person controlling it. They might have to control every simple set of interactions manually and try their best to select the next appropriate action to be performed by the robot. The robot by itself should at least have some sort of sensing to enable more autonomy and adaptability during the sessions, especially to unwanted and aggressive interactions. The current state of a robot's autonomy that is meant for therapy has not reached a high level of complexity and it is still lagging. The development in robots that sense and respond to unwanted interactions is still needed to achieve safer interactions.

How can small social robots be made safer? In order to answer this question, this research has three main objectives as follows:

1. To quantify the potential harm due to one of the identified potential risky scenarios that might occur between a child and a social robot.
2. To investigate how a robot design can be made safer by investigating some design parameters and their influence on a selected severity index.
3. To investigate the possibility of recognizing and classifying unwanted interactions and to evaluate the influence of the emotional reaction time of a robot's response on the interactions.

1.2 Contributions

The three major contributions of this research are related to safety aspects of small robotic form-factor as follows:

1. The identification of potential harm and risks due to the introduction of social robots to children with autism. The risks are intensified due to the challenging behaviors that exist within this population as compared to neurotypical children. The risks are also dependent on the

form-factor of the robot involved. Several severity indices were used to quantify the potential harm due to one of the identified risky scenarios.

2. The investigation of hardware approaches to optimize small robotic design to improve safety by reducing the potential harm to the head. The influence of different design parameters on a selected severity index were considered. Two different studies were conducted that considered different parameters. The first study considered the influence of the shape and mass of a robotic design while the second study considered the potential of incorporating soft materials in mitigating the potential harm. The optimal settings for the investigated parameters were identified based on Taguchi method.

3. The embedding of unwanted interactions recognition into small companion robots with the appropriate timing of responses. The first study demonstrated the application of an embedded accelerometer inside a robotic toy to detect and classify a set of interactions based on a machine learning algorithm. The second study investigated the influence of reaction time of the emotional response of a robot to unwanted behavior on the interactions. This study identified the appropriate reaction time window that should deliver the right message to the user.

1.3 Dissertation Outline

The rest of the dissertation is organized as follows:

Chapter 2 provides a background about the core topics in this research. This chapter starts with describing autism, the associated symptoms, and some of the prevalence rates. Next, it moves to describe the challenging behaviors that are exhibited by this population and the application of social robots in therapy. Furthermore, this chapter provides the severity indices of the head that are used to quantify the potential harm. Next, this chapter presents Taguchi method that is used in the robotic design optimization. Finally, this chapter provides studies on activity recognition that are related to make a robot more adaptive in recognizing unwanted interactions.

Chapter 3 presents exploratory experiments for children with autism interacting with different toys and two social robots. This chapter highlights some key interactions between the children with the different robotic form factors. The experiments described in this chapter reveal some behaviors and observations that represent the motivation behind this research.

Chapter 4 identifies the potential risky scenarios between a child and a companion social robot. This chapter highlights some of the challenging behaviors that could cause harm when interacting with social robots. Furthermore, it provides the development of the experimental setup that is used to conduct the impact experiments. Finally, it quantifies the potential harm for one of the identified scenarios based on the relevant severity indices.

Chapter 5 presents two parametric studies aimed to make small robotic design safer. Based on Taguchi's method, the first study investigates the influence of shape and mass of a small robot on the linear head acceleration (i.e. severity index) of a dummy head. The second study in this chapter explores the potential of soft materials embedded into a robotic design in mitigating potential harm based on the same severity index. The optimal conditions for all the investigated parameters are also discussed.

Chapter 6 explores the possibility of recognizing six different possible interactions between a child and a small robotic toy based on an embedded tri-axial accelerometer. This chapter first describes a study presenting the adopted approach to acquire the data and the development of a neural network algorithm to classify the unwanted interactions. The study demonstrates the possibility of recognizing behaviors relying on low-cost and simple approaches. The influence of reaction time in the emotional response of a companion robot to a child's unwanted interaction is explored. The second study in this chapter presents the findings of experiments with children interacting with different robotic toys programmed with different reaction timings. The study finds that the right reaction time of a robot's response is essential to deliver the right message to the user.

Chapter 7 provides the conclusions for all of the studies presented in the previous chapters and their implications on safety in robotic design. This chapter also provides directions for potential future research in this domain.

CHAPTER 2

Background

This chapter provides a theoretical background about the core topics in this research. This chapter starts with describing autism, the associated symptoms, and some of the prevalence rates. Next, it moves to describe the challenging behaviors that are exhibited by this population and the application of social robots in their therapy. Furthermore, this chapter provides the severity indices of the head that are used to quantify the potential harm. Next, this chapter presents Taguchi method that is used in the robotic design optimization. Finally, this chapter provides studies on activity recognition that are related to make a robot more adaptive in recognizing unwanted interactions.

2.1 Autism

Characterized by lifelong difficulties and impairments in communication, social interaction, and the exhibition of restricted interests or behaviors, Autism Spectrum Disorder (ASD) is a condition that is diagnosed during early childhood and affects the neurodevelopment [26], [203], [22]. Furthermore, children face a multitude of daily behavioral challenges as compared to neurotypical children [55], [61]. There has been a growing con-

cern worldwide pertaining the rate of ASD among children. For example, the pervasiveness rate of ASD among children is found to be 1 out of 45 in the United States [199], 1 out of 100 in the United Kingdom [85], and 1 out of 38 children in South Korea [118]. Up to date, the research to find the exact causes of ASD is still on going.

Due to the diverse nature of ASD, the manifestation of behaviors among children on the spectrum varies greatly in their degree. Such children face a lot of daily behavioral challenges as compared to neurotypical children, such as avoiding eye contact, poor motor skills, understanding gestures, interpreting facial expressions, feeding problems and others. Their inability to understand the behaviors, social cues, and feelings of others are among the contributing factors to their impairments in social relationships and interactions [55], [61]. Lack of intonation, inability to understand verbal and nonverbal languages, repetitive and obsessive thoughts, and limited understanding of emotions are some of the deficits in communication among children with ASD [55]. Early intervention, especially during the early years, seems to play a great role in the treatment, or at least the mitigation, of such behaviors and make them more independent in their lives [164].

2.2 Challenging Behaviors

Individuals on the spectrum are very unique and complex in their dispositions and their manifestation of ASD. Autism affect such individuals and causes a lot of deficits and challenges in their communication skills, interactions with others, behaviors, sensory inputs perception, and social life [55]. Furthermore, they exhibit self-stimulatory behaviors, perfectionist tendencies, meltdowns, and delayed echolalia [70]. Due to the nature of ASD, children diagnosed with it tend to exhibit more challenging and aggressive behaviors than their neurotypical peers. For example, those with perfectionist tendencies and emotional regulation deficiencies have shown higher level of aggressive behavior, anxiety, and depression [23], [21].

Frustration is another contributing factor toward the exhibition of more challenging behaviors. Children with ASD might face frustration when being exposed to new unpredictable, overwhelming, and noisy environments as that found in hospitals [115], [170]. In addition, such environments are rich in stimuli that might overload their body's senses, and that would make meeting their needs even harder due to increased struggle with the new environmental changes [142], [170]. Challenging behaviors take on many different forms, such as withdrawal, repetitive and stereotypes habits, aggression against others, self-injury, tantrums, meltdowns, and property

destruction (Fig. 2.1). Not only such behaviors pose risks on the children themselves, but also pose a lot of risk on others around them, such as other children, nurses, patients, care givers, parents, and family members [115], [156].

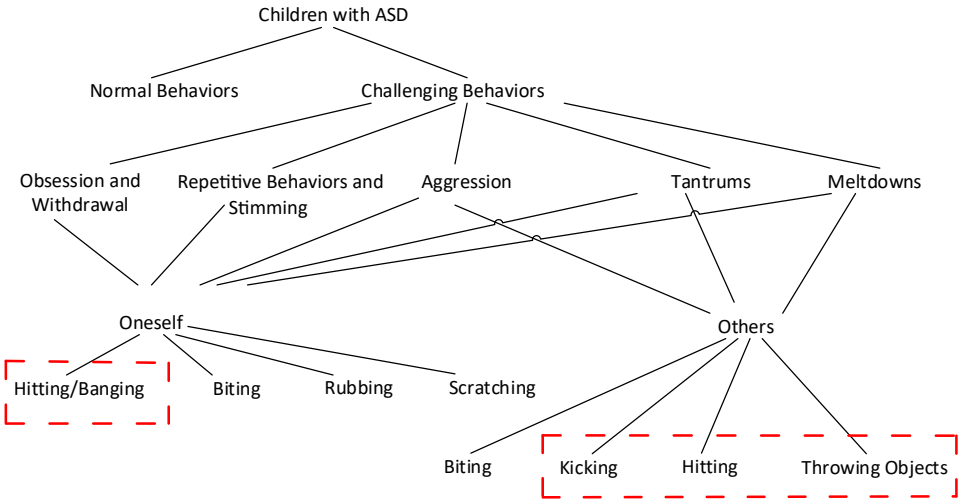

Figure 2.1: *Different forms of challenging behaviors that are exhibited by children with ASD [115], [131], [128], [77].*

Among all the children without and even with developmental disabilities, challenging behaviors and anxiety problems seem to have higher prevalence rates among children with autism [72], [88]. Even within children on the spectrum themselves, those with more severe ASD have showed higher rate of challenging behaviors as compared to those with less ASD severity [141], [132]. Furthermore, studies have shown that even infants or toddlers that are diagnosed with ASD do exhibit challenging behaviors at a higher rate compared to their neurotypical counterparts [77], [122]. Due to difficulties in using proper communication to satisfy their needs, children with autism might turn to challenging behaviors as a form of communication to express themselves [106].

The pervasiveness of challenging behaviors among individual with autism is relatively high. One study surveying 222 children reported 50% oc-

currence rate while another study surveying 32 adults reported a rate of 69% [25], [34]. A more recent study with larger sample size of 1,380 children has reported a high aggression prevalence rate of 68% against caregivers and 49% against others [116]. The majority of previous studies have reported the occurrence of at least one or more challenging behaviors among at least half of the individuals with ASD [77]. The existence of such behaviors has many implications on those providing treatments and services to individuals with ASD [106].

2.3 Social Robots

The traditional intervention sessions for ASD have been usually conducted relying on human therapists. However, the advancement in technology is providing added tools for improved therapeutic sessions (e.g. independent learning, hands-on learning, and skills training [71]). Several technologies have been explored in supporting therapeutic and educational initiatives for children with ASD [83], [158]. Furthermore, previous studies have shown that children on the spectrum have strong interest in technology, such as computer applications [96], virtual environments [152], and robots [47], [171].

There has been a growing interest in using robots clinically to assist in the rehabilitation of children with ASD [65], [103], [31]. The usage of technology, especially robots, for ASD therapy opens many possibilities in the early intervention for children with ASD, and toward more personalized rehabilitation [162], [160]. The application of robots for intervention provides many options and flexibility as it can either be used as an intervention tool to facilitate the therapeutic session, co-therapist with turn-taking with the main therapist or as a sole therapist [31], [68].

Social robots have also been reported to help in improving the outcomes of therapy, such as communication, gestural responses, motor and social skills, eye contact, imitation, and joint attention [47], [178], [53], [93], [193]. Children are found to be more intrigued to interact with robots as compared to humans due to the limited complexity of robots [47]. Many previous studies have demonstrated that robots can be used to elicit many behaviors, such as imitation, joint attention, and eye contact [121], [155], [173]. Many form factors have been developed that took on different looks and shapes that can be broadly categorized as being either anthropomorphic, non-anthropomorphic or non-biomimetic. Kasper (Fig. 2.2a) [62], a minimally expressive robot, and Infaniod (Fig. 2.2b) [120], an upper torso humanoid robot, are examples of an anthropomorphic robotic design. Keepon

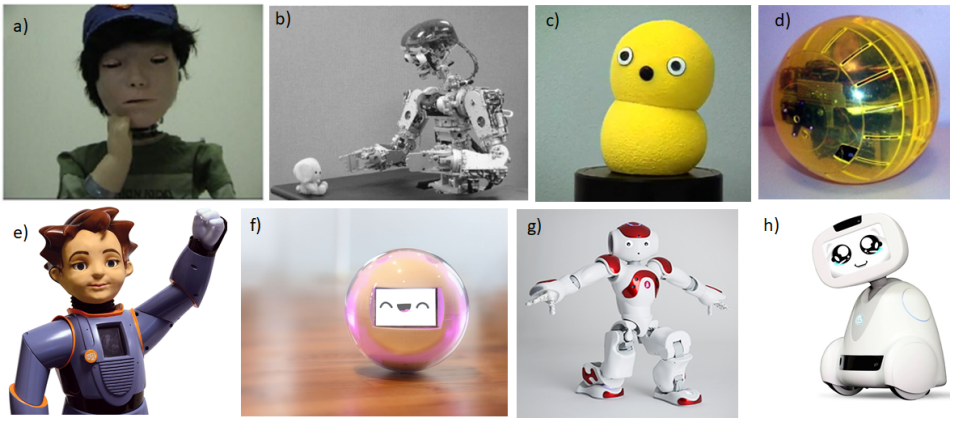

Figure 2.2: *Some of the social robots that have been considered or have the potential for ASD intervention: a) Kasper, the minimally expressive robot. b) Infanoid, the upper torso humanoid robot. c) Keepon, the yellow snow-life robot. d) Roball, the spherical robot. e) Milo, the humanoid robot. f) Leka, the ball-like robot. g) Nao, the humanoid robot. h) Buddy, the companion robot.*

(Fig. 2.2c) [121], a yellow snowman-like robot, is an example of a non-anthropomorphic design while Roball (Fig. 2.2d) [134], the sepherical robot, is an example of non-biomimetic design. There are new emerging, promising, and commercially available robots, such as Milo (Fig. 2.2e), Leka (Fig. 2.2f), Nao (Fig. 2.2g), and Buddy (Fig. 2.2h), that have a great potential to be considered in ASD therapy.

2.4 Quantifying Harm

2.4.1 Overview

The human brain is protected by floating in the cerebrospinal fluid that acts like a cushion to reduce any potential harm. However, the human head is susceptible to traumatic brain injury (TBI) when it is receiving blows or bumps, or subjected to impacts with projectiles, such as a baseball [33]. TBI is categorized as either being mild or severe, and could cause permanent disability or, in severe cases, death. Most occurring type of mild TBI is concussion. It is not considered a life threatening, however, the results on the affected can be serious [79].

In the United States and in 2013 alone, a total of 2.8 million (i.e. 50,000 deaths, 282,000 hospitalizations, and 2.5 million emergency department

visits) cases of TBI have been reported with falls being the lead cause followed by getting struck by or against an object [188]. Furthermore, it has been reported that 1 in 5 cases of TBI occurred among children (age < 15 years old) to the second leading cause.

TBIs among young children may impair the neurological development and cause a multitude of challenges, such as depression, attention deficit hyperactivity disorder, and in attaining academic achievements [16], [17], [159], [197]. Furthermore, data showed that those affected with TBI and ASD share some of the biologic mechanisms that cause both conditions to have similar symptoms. Hence, studying and reducing the occurrence of TBI is very vital.

Challenging behaviors that are exhibited by children on the spectrum pose a potential harm to themselves and to the ones around them. With the presence of a robot, the child might involuntary use it to harm others. Throwing objects, especially in the case of small robots, pose a great risk to the head and need to be quantified. One objective of this research is to simulate objects (i.e. representing a small robot) being thrown at the head to quantify harm levels. Hence, this section describes related studies and relevant severity indices.

2.4.2 Related Studies

Laboratory settings using anthropomorphic test dummies (ATD) are typically used to simulate potentially dangerous scenarios to evaluate the possible harm to a human, such as that used in car crash tests. Furthermore, similar setups have been used to quantify harm due to impacts in some sports and to evaluate protective gears, such as helmets [133], [196], [150]. One study used similar settings to assess the influence of taekwondo kicks and peak velocity of the foot on the dynamics of the head [76]. In that study, a crash test dummy head was secured to an aluminum frame and it was used as a target for the kicks performed. The head form was equipped with an accelerometer to measure the dynamics of the head (i.e. changes in acceleration) as it was being hit by the participants. The data generated was used to assess the potential of concussion based on the head injury criterion (HIC).

Similar studies were conducted in industrial robotics to quantify the potential harm due to different possible impact scenarios between a human and robotic arm. For example, few studies have conducted impact tests of a manipulator to a dummy at a standard automobile crash test facility [90], [92], [91]. In such studies, impacts by robotic arms using flat sur-

Table 2.1: *Abbreviated Injury Scale (AIS) and the corresponding injury classification*

AIS score	Injury classification
1	Minor
2	Moderate
3	Serious or severe, but not life threating
4	Severe and life threating
5	Critical and uncertain survivial
6	Unsurvivable

face impactors were performed against a standard crash test dummy in three regions (i.e. head, chest, and neck). The potential of injury or harm levels were evaluated based on the respective severity index or indices for each region. The evaluations were based on varying some robotic-dependent variables, such as mass and velocity, and their relation on the resultant severity indices. In some studies, low-cost body part models, such as using a head model or an arm model, and low-cost sensors were considered and used to carry out experimental tests to evaluate human-robot impacts [60], [91].

2.4.3 Severity Indices

Severity indices are associated with injury scaling, such as the Abbreviated Injury Scale (AIS) [86]. AIS is a tool that provides a simple way to grade the observed injury based on a scoring criteria (Table 2.1). AIS and together with various severity indices give an estimation of the potential for an injury and its respective severity.

The investigation in this study is limited to the head, hence, only relevant head indices, namely, head injury criterion (HIC), 3 ms criterion, peak linear acceleration, impact forces, and tissue injuries are summarized.

Head Injury Criterion (HIC)

One of the most commonly used severity indices to measure the possible injury to the head in many applications, such as in vehicles and in

Table 2.2: *The values of population mean μ and standard deviation σ corresponding to different scores of Abbreviated Injury Scale (AIS)*

AIS score	μ	σ
2	6.96352	0.84664
3	7.45231	0.73998
4	7.65605	0.60580

sports [190]. HIC is defined as:

$$HIC = (t_2 - t_1)\left[\frac{1}{(t_2 - t_1)}\int_{t_1}^{t_2} a\,(t)\,dt\right]^{2.5} \tag{2.1}$$

where *a(t)* is based on the resultant acceleration of the head and measured in terms of gravity acceleration (g = 9.81 m/s^2) and $\Delta t = t_2 - t_1$ is the duration of the impact considered in calculating the resultant HIC. The two most commonly used durations to evaluate the severity of injury to the head are 36 ms and 15 ms. Because it is less restrictive, the 36 ms duration only will be used (Fig. 2.4).

The HIC standard is converted to a corresponding AIS based on the following relation [124]:

$$p\,(head\,injury) = \phi\left(\frac{\ln\,(HIC_{36}) - \mu}{\sigma}\right) \tag{2.2}$$

where ϕ is the cumulative normal distribution, and μ is the population mean, and σ is the standard deviation (Table 2.2). These values are originally specified for a test dummy head, hence, they will only be used for comparison purposes. At a particular HIC value, the probability of injury occurrence differs between each of the AIS scores (Fig. 2.3).

The 3 ms Criterion

This criterion requires that the maximum mean value over 3 ms duration of the resultant head acceleration is less than a certain threshold when there is no hard contact (Fig. 2.4). This criterion is used as part of the regulations pertaining the safety of occupants in vehicles and also used in helmet testing [172].

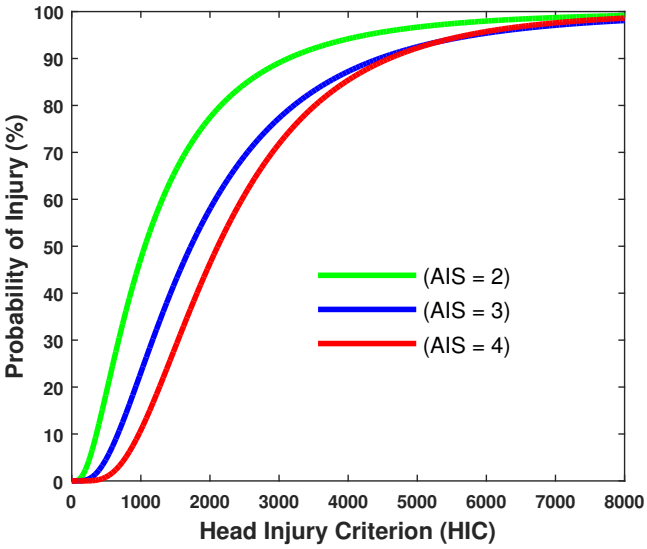

Figure 2.3: *The relationship between the Head Injury Criterion (HIC) and the probability of injury according to different Abbreviated Injury Scales (AIS) [124].*

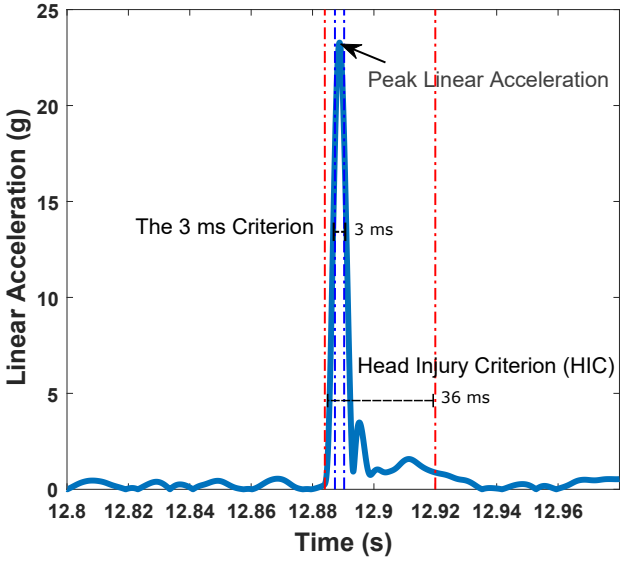

Figure 2.4: *Sample of the generated linear acceleration data demonstrating the durations of both, the Head Injury Criterion (HIC) and the 3 ms Criterion, and the instance of peak linear acceleration that were considered in the data analysis.*

The European National Car Assessment Protocol (EnuroNCAP) states that the thresholds for 3 ms criterion for a child occupant should not exceed 60 g in case of frontal impact and 60 g in case of side impact [73].

Peak Linear Acceleration

Peak linear acceleration has been used as one of the biomechanical measures for head impact to investigate its association with concussion events [87] [166]. A study investigating the head impact exposure in youth football has reported linear accelerations due to impacts anywhere in the range of 10 g to 111 g [198]. While that study did not report the occurrence of any concussions, however, it is believed that concussions could occur within that range based on the reported football-related concussions [27]. One study based on a finite element head model validated from field collisions has estimated a probability of mild TBI to be 25%, 50%, and 80% corresponding to maximum accelerations of 66 g, 82 g and 106 g, respectively [200]. One study has reported the occurrence of a concussive event at a relatively low linear acceleration value of 31.8 g [135]. Some of these studies did not report the duration of impacts while others reported impact durations of 30 ms or less.

Impact Forces

The HIC severity index is not enough for the assessment of head safety, especially for what concerns any potential damage to the skull and brain injury [191]. Contact force is another indicator to predict the fracture tolerance of the human bone structure. There have been many studies conducted on heads from cadavers to measure fracture forces of the skull. Experiments conducted were either by dropping heads from different heights or impacting the head with an impactor at various velocities.

A summary of the studies conducted on facial fracture (i.e. maxilla, zygoma, frontal bone, nasal bone, and mandible) revealed peak force tolerance anywhere in the range of 610 - 9,880 N [30]. An injury risk function with comparable consistency to facial fracture data has been proposed based on Weibull distribution to identify forces that at which facial fracture starts for and impactor with an area of 13.8 cm^2, and it is defined as [63], [30]:

$$P_{fracture}(F) = 1 - exp\left[-\left(\frac{F}{B}\right)^{\alpha}\right] \tag{2.3}$$

where α = 2.27 is the Weibull shape parameter, and B = 887.7 N is Weibull scale parameter, and F is the impact force. According to this function, a

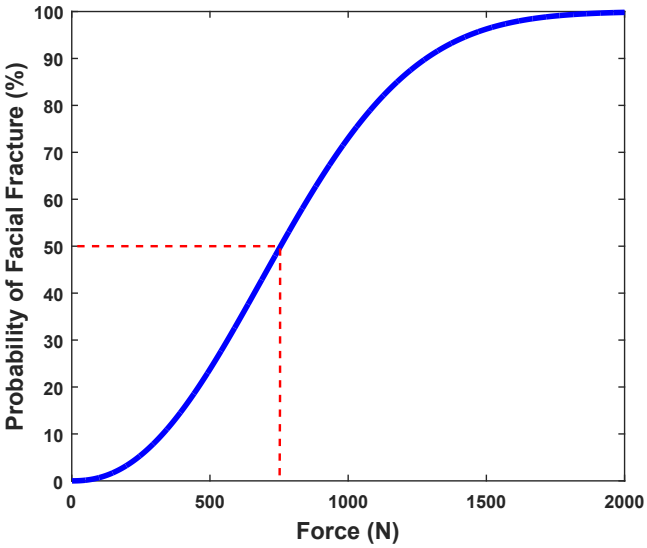

Figure 2.5: *Injury risk function for facial fractures of the face (i.e. maxilla and zygoma) [63], [30]. Dashed red line represents a facial fracture probability of 50% corresponding to a force value of 755 N.*

force of 755 N would have 50% chance of fracture risk (Fig. 2.5).

Tissue Injuries

Tissue injuries as a result of impacts with objects could take on different forms, such as skin tears, lacerations and abrasions. The magnitude and the depth of the resultant injury depends on the geometry of impactors or penetrators and pressure forces in effect [175]. Classification by depth is often used as indicator for wounds and tissue injuries [183]. According to this classification, tissue injuries could either be superficial wounds, partial-thickness, full-thickness or subcutaneous skin loss (Table 2.3). This classification will be used as a reference and indicator for the possible tissue injury in our investigation.

2.5 Taguchi Method

Experiments are usually conducted on processes and systems to understand the overall performance, to deduce the most influential parameters, and to determine the optimal settings to achieve the desired responses or overall goals [137]. Design of experiment (DOE) is an approach aimed at using

Table 2.3: *Classification of tissue injury based on depth [183]*

Classification	Affected Skin Layer	Depth
Superficial	Only the epidermis	<1 mm
Partial thickness	The epidermis and into the dermis	1 - 4 mm
Full thickness	Through the epidermis and the dermis into subcutaneous tissue	>4 mm
Subcutaneous	Extends into and beyond the subcutaneous tissue	>4 mm

the minimum amount of resources available while maximizing the amount of information obtained from a process through the selection of parameters to be investigated [137]. DOE helps in collecting different information by altering the optimal arrangement of parameters or factors to enhance product robustness [56], [95]. There are many DOE techniques available. The choice depends on the investigated problem and the aim of the experiments conducted [56]. One of such techniques is the Taguchi method.

The method was developed in 1979 and was meant to be used as an off-line quality control tool to improve manufacturing products and goods in different applications [185], [136], [97], [187]. Taguchi DOE considers two types of variables, namely controllable and noise (or uncontrollable). Control factors can be controlled in production while noise factors cannot be controlled, except experimentally. This method aims to improve the robustness of products against any variations in the noise factors by finding the optimal values of the controllable factors. Depending on the number of factors investigated, Taguchi DOE could take on different settings by considering different Orthogonal Arrays (OAs) [138] (Table 2.4). The crossed array Taguchi design that was considered provides a robust solution by understanding the interaction between the control factors and the noise factors [56]. The studies reported in Chapter 5 were conducted based on this method.

Table 2.4: *The standard $L_9(3^2)$ orthogonal array (OA).*

Run	Control factors	
	A	B
1	1	1
2	1	2
3	1	3
4	2	1
5	2	2
6	2	3
7	3	1
8	3	2
9	3	3

2.6 Activity Recognition

The research in human activity recognition relies on different sensors, technologies and wearable devices to acquire data [19], [46], [167]. Human activity recognition is being considered in the healthcare domain, for example, detecting falls among the elderly [24], [108]. Previous studies on fall detection considered wearable devices, ambient devices, and vision based devices [140]. Different sensors were used, such as accelerometers, cameras, microphones, and gyroscopes [154]. Furthermore, different classification of falls were investigated (e.g. falls from sleeping or from walking) [140]. A recent study has considered using a wearable device on a belt to detect falls [180]. The device contains an accelerometer that acquires signals at a sampling frequency of 25 Hz. Their method was able to achieve an accuracy of 99.4% using a non-linear classifier and a Kalman filter.

The detection of problematic behaviors in the population with special needs is another area in healthcare domain to consider activity recognition techniques. To facilitate the therapy for those with special needs, one study considered using accelerometers to detect problem behaviors among this population [157]. In this study, the data to develop the recognition

model were simulated by trained clinic staff. Their approach was able to achieve an accuracy of 69.7% when evaluated with realistic data. Activity recognition is also gaining attention in the area of robotics, especially when a robot operates in close proximity with humans. In robot-assisted living, one study introduced a wearable system that relies on the fusion of multi-sensors to recognize human daily activities [202]. The sensor system consisted of two nodes (i.e. on the waist and on the foot) that measure angular velocity, magnetic data, acceleration, and temperature. The system was able to produce promising results using a combination of neural networks and hidden Markov models. For more advanced and interactive applications, accelerometers were considered in robot games to model players and recognize activities [148], [147]. One study considered using a tri-axial accelerometer module embedded in the player's chest to acquire the motion data [149]. Their work showed promising results in detecting different activities with the robot, such as running, walking or dodging, and blocking the robot's path.

Different sensors and wearable devices were considered in human activity recognition research. A frequently used sensor is the accelerometer, which is a relatively low-cost sensor that is able to detect acceleration on three orthogonal directions. When associated to a gyroscope, the rotational speed can be detected along the same axis. One of the earliest works classifying different daily physical activities, such as walking and running, used five wearable small accelerometers on different body parts of 20 participants [29]. The data collected were from subjects performing a sequence of different daily tasks. The best classifier selected (i.e., a decision tree) was able to recognize the actions with an accuracy rate of 84%. Another study considered using accelerometer and sound data to recognize workshop related activities to develop a proactive system [127]. The data collected were based on tasks performed in a wood shop. The system was able to recognize different activities with an accuracy of 84.4% on continuous simulated stream of data. Nowadays, accelerometers are used in smart phones to detect a wide range of activities [64].

2.7 Chapter Summary

This chapter provided a background information about the core topics of this thesis. The chapter described autism, challenging behaviors, and social robots. Additionally, it presented the severity indices and Taguchi method. Finally, it provided the related studies to human activity recognition. This chapter established the main concepts that will be used throughout this dis-

sertation.

CHAPTER 3

Design Preference for Robot Form Factors

This chapter describes exploratory experiments between children on the spectrum interacting with different toys and two social robots. It provides the preferences among the children toward the different robotic form factors. It also highlights some key observations about their interactions.

3.1 Introduction

Social robots are emerging to become useful assistive tools to be considered in the therapy and education of children with Autism Spectrum Disorder (ASD). The nature of ASD causes its symptoms and manifestations to vary widely, resulting in a variety of robotic designs that have been developed for this application. These robots vary in structure, shape, size, color, and function. There was a significant variation in the types of form factors considered that were either small or large in size while taking the appearance of either humans, animals, toys or others. Due to the heterogeneity of ASD, the reactions of individuals with ASD toward the existing robotic designs have varied considerably, and so are their preferences.

Over the years, many social robot designs have been developed and tested for intervention sessions [47]. Those include humanoids, human-like

robots, robotic balls, mobile robots, and animaloids. In these experiments, the responses of children with ASD toward different toys and two social robot (i.e. humanoid and a robotic seal) are explored. Experiments were conducted to verify whether or not there are any effects of the different form factors on the children's interactions.

3.2 Methods

3.2.1 Participants

Ten English-speaking children aged 7 to 10 years (all were males) participated in this study. They have been diagnosed with mild to moderate autism and are attending the Step By Step Center for Special Needs in Doha, Qatar. The consent from the parents were secured by the center. The children were accompanied by either a teacher or a caregiver. The procedures for this work did not include invasive or potentially hazardous methods and were in accordance with the Code of Ethics of the World Medical Association (Declaration of Helsinki).

3.2.2 Stimuli

There were a total of 4 experiments, where different stimuli were used for each experiment. The details about the individual stimuli used are summarized below.

1. Five different toys were used. These were a rubber ball, two metal cymbals, a colourful plastic train, a small humanoid robot, and a wooden truck with wooden blocks pegged into its carrier that have alphabets and objects drawn on them (Fig. 3.1a).

2. Two interactive social robots were used (Fig. 3.1b). One was a Nao humanoid (SoftBank Robotics, Paris, France), and the other was a seal robot (PARO Robots U.S., Inc., IL, USA). The movements of Paro were autonomous and were limited to the built-in functions. The movements of Nao were initiated by the experimenter and were limited to basic activities (e.g. sit, stand up, dance).

3. Three Tank Engine toy trains were used. These included two blue trains of different sizes (Thomas train character) and one red train (James train character). These were used against a larger, multi-colored toy train (Fig. 3.1c).

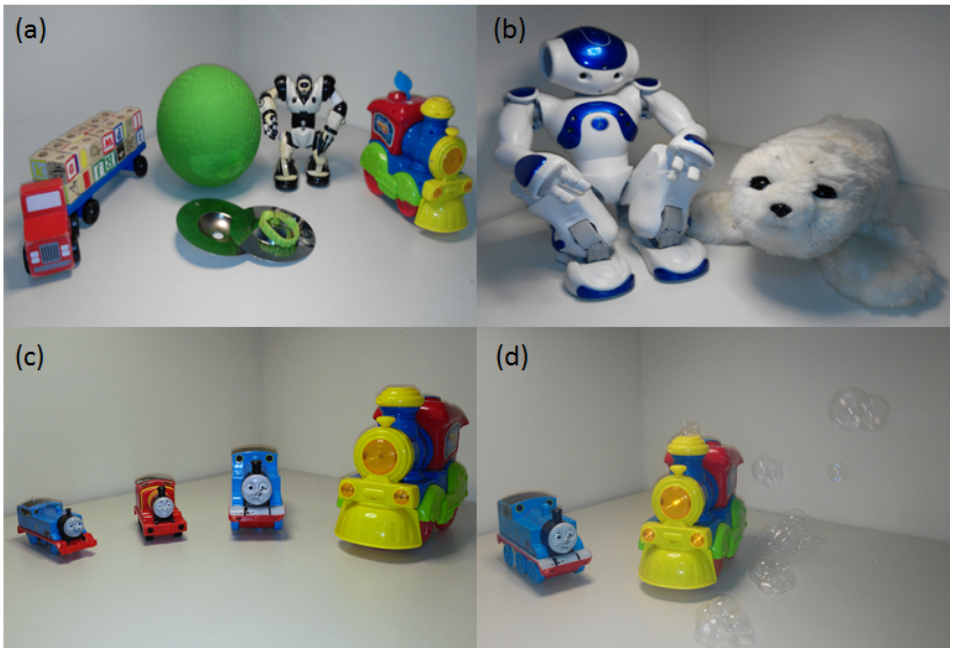

Figure 3.1: *The group of stimuli used during the experiments. (a) five different non-moving toys. (b) The social robots, Nao and Paro. (c) Thomas and Friends trains (left) and larger train (right). (d) The participant's favorite train from the previous stimuli group and bubbles train.*

4. The child's preferred train in Experiment 3 was used against a train identical to the multicolored train from Experiment 1 and Experiment 3, but emits bubbles (Fig. 3.1d).

3.2.3 Procedure

There were 4 different experiments aiming at different goals (Table 3.1). Each experiment was around 6 minutes long. Experiment 1 is an unstructured play scenario. After obtaining the results of Experiment 1, the succeeding experiments explored animating the toys and the goal was to see the effects of these in the subjects. No instructions were given to the chil-

dren, except encouragement to initiate interaction with different toys.

3.2.4 Monitoring Equipment

The children's interactions were monitored with four video cameras placed at the corners of the room. Four cameras (MyDlink DCS-931L, D-Link, Taipei, Taiwan) were mounted on four tripods. Care was taken in the setup of the equipment to ensure that it remained unobtrusive throughout the length of the experiment. The cameras were positioned to ensure that the children's activities were captured from different angles.

3.2.5 Annotation Software

An open-source video event-logging software (BORIS, version 3.12, Torino, Italy) was used to analyze the videos. The user environment of the software was prepared with all the behaviors of interest.The analysis of videos was conducted by three observers after getting well-acquainted with the software.

The measured variables were divided to either state or point. A state variable was used to calculate the duration of a specific event while a point variable is used to calculate the frequency of occurrence. The measured variables are listed as follows:

- *Experiment duration*: state variable to declare the duration of an experiment.
- *Interaction duration*: state variable to declare the durations of interaction during an experiment.
- *Preference*: experiment-dependent point variable to indicate the preference of the child based on the given stimuli for each experiment. For example in Experiment 1, Q is pressed when the preference is the small robot. The deduction of preferences were based on either direct verbal communication, longest interaction duration or most preferred.
- *Unclear*: point variable is pressed once in case the preference implied by the child is not clear. Unclear selections occur when the child either prefers, selects more than one or neither of the stimuli.

3.3 Results and Discussions

Most of the children showed continuous interaction and engaging behaviors with the experimenter. The observed reactions varied differently across

Table 3.1: *Experimental protocol and objective of each experiment*

Expt #	Protocol	Objective
1	Present 5 different non-moving toys	To determine which toy is the most preferred
2	Remove all toys from Experiment 1 and replace with interactive social robots, such as Nao and Paro.	To determine whether interactive robots, behaving autonomously, appeal to the child more than the non-moving toys from the preceding experiment, and to observe the nature of his/her interactions with them
3	Remove all toys from Experiment 2 and present the train from Experiment 1, and add different mechanical Thomas and Friends trains	To determine whether the interest in trains is limited to Thomas toys or extends to all trains
4	Remove all toys from Experiment 3 except the participant's favorite toy, and replace them with a train that automatically generates bubbles from its chimney once switched on	To determine whether bubbles can add to the appeal of a toy to verify their use as a reward mechanism

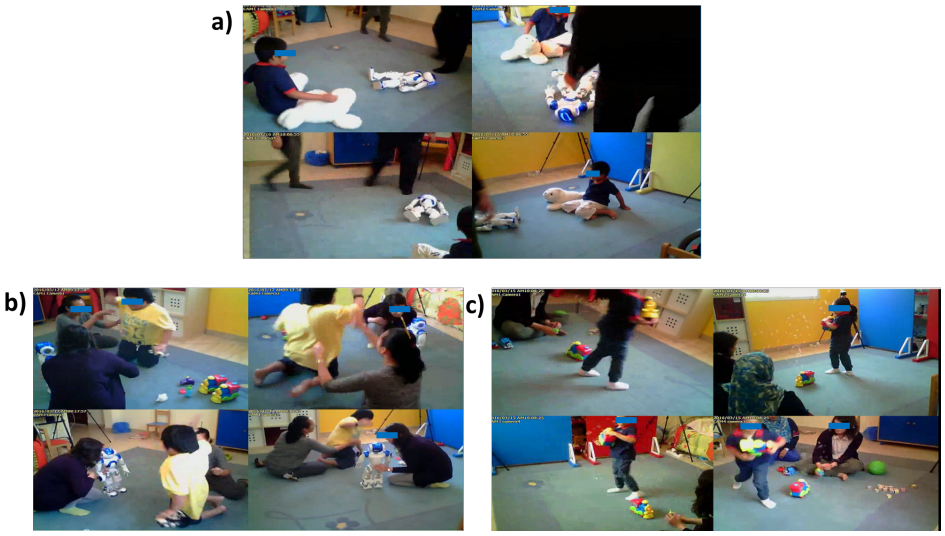

Figure 3.2: *Some of the behaviors and interactions that occurred during the experiments. (a) Nao fell after being pushed by a child. (b) A child refusing to interact with the humanoid robot while shaking the small robot with his left hand. (c) A child is getting excited about the train by shaking it around.*

all the sessions, and the participants exhibited different responsiveness to a given stimulus. Some interactions only occurred after a prompt from the experimenter or caregiver while others were instantaneous and spontaneous. Some of the children displayed some concerning behaviors during the experiments (Fig. 3.2). The preferences and the main features of interest have been observed and recorded based on post-analysis of the videos. The individual results and discussions are summarized below.

3.3.1 Experiment 1

In Experiment 1, five different toys were presented. The small robot scored the highest (30%) followed by the truck with cubes (23.3%) and the ball (16.7%) (Fig. 3.3b). The train scored 13.3% while the cymbals scored 10%. Unclear preference was around 6.7% of the participants.

Most of the interactions were limited to playing with the toys without standing up or moving around, and without showing high level of excitement. The majority of the children appeared interested to play with cubes that comes with the truck (Fig. 3.3a). They spent some time in picking

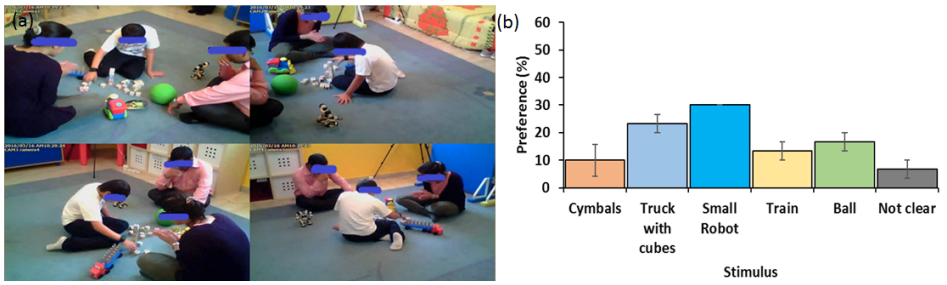

Figure 3.3: *The preferences for the toys in Experiment 1. (a) Child playing with the cubes of the truck. (b) Average rated preferences for each toy with the small robot scoring the highest.*

the cubes while trying to name the shapes and numbers on them with the experimenter. When prompted, some of the children played with the ball together with the experimenter or caregiver. The sound and reflection of the cymbals piqued the interest of two children while three liked the features on the train, such as the colors and wheels. Three participants enjoyed interacting with the small humanoid robot the most while one avoided approaching it and kept his distance. This reaction could be attributed to the human-like appearance of the small robot. One participant did not show any interest in most of the toys in this experiment and ended up ignoring the toys.

The interest in technology, especially to robots, is evident in Experiment 1. This cannot be generalized across all the participants and all individual with ASD due to varying degree in their reactions to the same stimulus (e.g. small humanoid robot) and due to the small sample involved in our experiments. Some of the features and characteristics of existing toys (e.g. cubes on the truck) seem to still get the interest of the children on the spectrum and should be considered in any new robotic designs.

3.3.2 Experiment 2

In Experiment 2, two interactive social robots were presented (Fig. 3.4a). Nao scored higher than Paro, 36.7% and 26.6%, respectively (Fig. 3.4b).

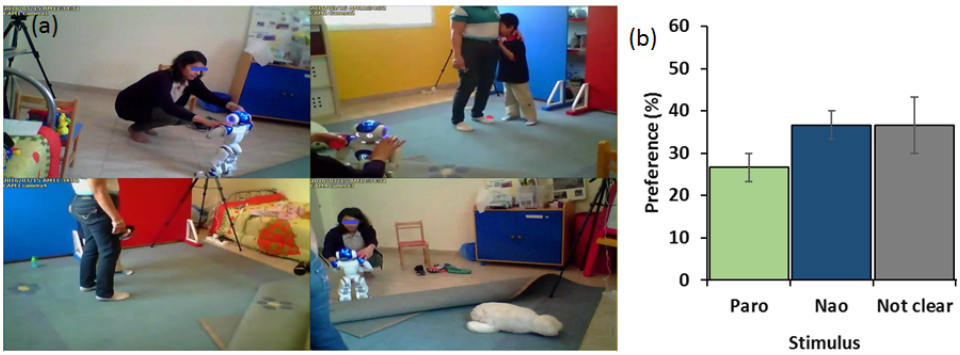

Figure 3.4: *The preferences for the social robots in Experiment 2. (a) Child crying and refusing to approach Nao. (b) Average rated preferences for each social robot. Less than half of the participants liked Nao more, while a quarter preferred Paro more. The remaining children did not like either of these robots.*

36.7% of the participants showed either refusal to interact or no definitive selection on the preference.

The observations can be divided to three groups. The first group of children interacted right away and showed positive reactions to the robots. They imitated or gave instructions to Nao and they played with Paro. The second group hesitated to interact quickly. They started by observing the movements of the robots, and they then began to approach the robots slowly to initiate the interactions. The last group refused to interact with either of the robots as they seemed afraid of interacting or even approaching the robots. Two children reacted with immediate anxiety upon the introduction of the robots and demanded the robots to be removed from the room (Fig. 3.4a).

The increased interactions and higher levels of excitement were clear in Experiment 2 among some of the participants. Part of that could be attributed to the novelty effect of the presented social robots [171]. Interestingly, the size of Nao being larger as compared to the smaller robot in Experiment 1 played an important role in altering some of the reactions negatively. This could imply that some children on the spectrum could feel more comfortable dealing with robots relatively smaller than themselves.

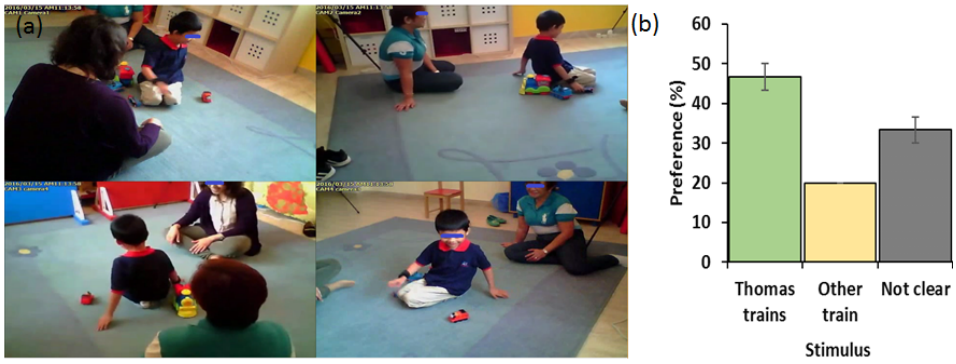

Figure 3.5: *The preferences for the trains in Experiment 3. (a) A child showing interest in the moving train. (b) Average rated preferences for the trains. The majority of children have selected Thomas and Friends trains. Around one-third of the children were not clear on their preference as they have interacted almost equally with all the trains without implying their preferences.*

Perhaps the smaller size gives them more sense of control over the presented stimuli. These negative reactions could also be attributed to lifelikeness of the presented social robots (i.e. human-like or animal-like).

3.3.3 Experiment 3

In Experiment 3, three different Thomas and Friends trains and one bigger train were presented. Around 46.7% of the participants showed interest in Thomas trains and 20% showed interest in the other train. The rest were not clear on their preferences (Fig. 3.5b).

The children were more excited in this experiment as compared to Experiment 1 and Experiment 2. Some children showed more excitement and more movements when some of the trains were powered on (Fig. 3.5a). These reactions support the idea that the implementation of simple features could serve as reward mechanisms. Some recognized Thomas Trains and started re-enacting crashing scenes while mimicking the sound of a train. One child did not seem to show the same level of interest and excitement as compared to others.

Familiarity with a presented stimuli (e.g. Thomas Trains) seems to play a role in making interactions more fluid and spontaneous. Researchers in social and educational robots could exploit this aspect in promoting their designs to achieve higher effectiveness for the intended goals and purposes.

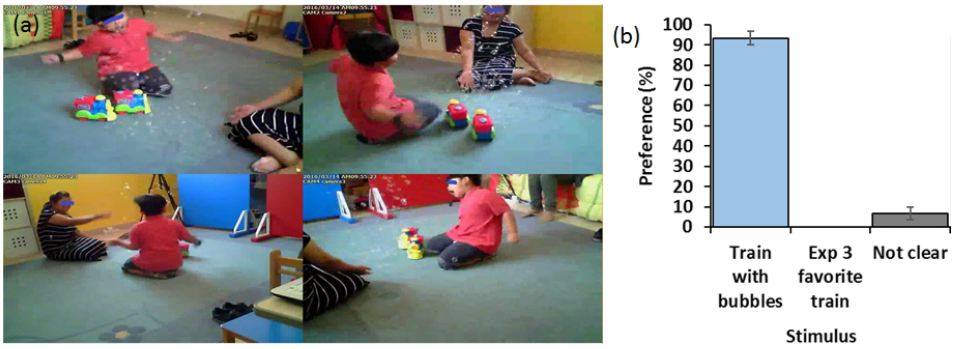

Figure 3.6: *The preferences for the trains in Experiment 4. (a) Child interacting with the bubbles generating train. (b) Average rated preferences for the trains. Almost all the children preferred the train with bubbles.*

This could be achieved by accompanying their developed robots with interactive videos and books exhibiting their robots in action. The exposure to such media prior to the presentation of the actual stimuli could help achieve better outcomes and mitigate any potential negative reactions.

3.3.4 Experiment 4

In this experiment, the bubble-generating train and the child's favorite train in Experiment 3 were presented (Fig. 3.6b). Almost all the participants showed high interest towards the train with bubbles (93.3%).

Most participants were immediately attracted to the bubbles, clapping or jumping in excitement, attempting to catch them. The interaction durations increased dramatically during this experiment. Children even showed more interactions with higher level of excitement depicted by the increased physical interactions, laughters, and movements (Fig. 3.6a). These observations support the idea of using bubbles as a reward mechanism in our proposed model. Some showed curiosity about the train and its features that they ended up carrying it while walking around. Few participants seemed to be wondering why the other big train was not generating any bubbles.

3.3.5 Limitations

The number of participants in this study was limited to ten male children. Hence, some aspects of the findings and preferences can not be generalized. The experiments were not repeated and conducted only once. Therefore, the effects of repeated exposure and continuous interaction over multiple sessions were not investigated. Finally, the influence of different features (e.g. bubbles) on different toys was not explored.

3.4 Conclusion

The results suggest diverse preferences among the participants. The most positive reactions were observed during the sessions with the train with bubbles. On the other hand, the instances where interactions were more difficult occurred during the sessions with the social robots, especially with Nao. While the humanoid robots have been reported to be a preferred candidate for imitation and eye-contact [173], the life-likeness of their appearance, relatively large sizes or sudden motions might have been a contributing negative triggers for this difficulty. There have been some instances of aggressive behaviors towards the social robots, such as pushing Nao and jumping on Paro. This could suggest that social robots that resembles the appearances of human or animal, to some degree, might not be positively perceived equally by children on the spectrum. However, repeated exposure and multiple sessions might alter these reactions overtime [161].

3.5 Chapter Summary

This chapter presented exploratory experiments for children with autism interacting with different toys and two social robots. The chapter highlighted some key obaservations and interactions between the children and the different stimuli.

CHAPTER 4

Severity Measures for Social Robots

This chapter identifies the potential harmful scenarios between a social robot and a child exhibiting some challenging behaviors toward it. Additionally, it also provides the materials and methods that were used in the experiments to quantify possible harm levels. Finally, it presents the results of the experiments and their implications concerning the potential harm.

4.1 Introduction

In the last few decades, the robotic research has witnessed a great changes in the traditional paradigm as it has shifted to cover new areas, such as entertainment, transportation, space, healthcare, and others [177]. Robots are now being considered to be used in many applications (e.g. rehabilitation and elderly care) that require direct physical human-robot interaction [177], [80].

The rapid evolution of technology has sparked a global interest in robotics and their prospective applications. The International Federation of Robotics (IFR) has predicted that the number of entertainment robots, such as toy robots, personal edutainment robots, and multi-media robots, will rise to 11 million units by 2019 [109]. This dramatic increase in the number of robots,

especially the ones with close proximity with humans, has a lot of implications on safety concerns that emphasize the need for standardization. Some of the standards that have been established are ISO 10218 [110], [111], which is concerned with safety in industrial robots; ISO/TS15066 [114], which is related to collaborative industrial robots; and the ISO 13482 [112], which is related to personal care robots. Currently, there is no safety standard pertaining social robots or toy robots.

One of the earliest work concerning safety and harm quantification with robotics introduced the human pain tolerance as an indicator for potential risks [195]. In another work, the simulation of impact tests of an industrial robot on a crash test dummy using Finite Element Method (FEM) was proposed and demonstrated as means to assess safety [146]. In later works, actual crash test dummies have been used in impact tests using industrial robotic arms [90], [92]. Various safety indices, such as for the head, chest, and neck, have been used in the evaluation of safety and potential injury levels due to impacts. Up to date, limited studies have been conducted on safety in social robotics, especially pertaining the safety of children with ASD [189], [81], [99].

The objective of this chapter is to identify potentially harmful scenarios that might occur between a child and a social robot due to the manifestation of challenging behaviors. Additionally, it is aimed to quantify the harm levels based on severity indices for one of the identified scenarios.

4.2 Robots and Potential Risks

Technology offers a lot of potential to therapeutic sessions, such as, but not limited to, independent learning, individualizing, motivation, reinforcement, social and communicative skills practice, hands-on learning, and others [71]. The advancement in several Artificial Intelligence (AI) fields has enabled robots to function independently and more naturally for effective social interactions (Fig. 4.1). Social robots differ from typical toys in many ways, such as the way they engage people at an interpersonal level to achieve positive outcomes in different domains [37]. Furthermore, social robots should be able to convey emotions, form social relationships, demonstrate personality, use natural communication cues, and to understand their social partners [98]. Child-robot interactions are characterized beyond traditional toys by the form of robot's embodiment, the interface of communication, two-ways reciprocally interaction, and the robot's adaptability to the child [78], [57].

Children interacting with social robots are prone to touching the robot.

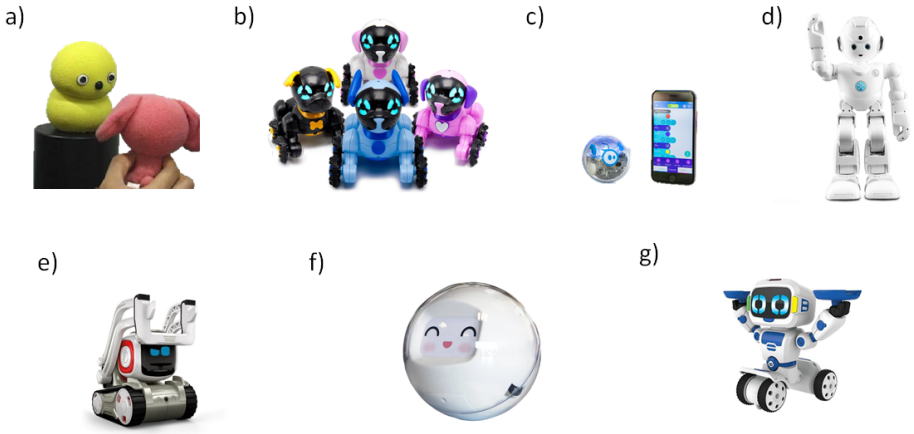

Figure 4.1: *Some of the robots that have been considered or have the potential for ASD intervention: a) Keepon, a yellow snowman-like robot [119]. b) Chippies, a pack of playful puppies (With kind permission from WowWee Group Ltd). c) SPRK+, a more than just a ball robot (With kind permission from Sphero). d) Lynx, a humanoid robot companion (With kind permission from UBTECH). e) Cozmo, an interactive tiny robot (With kind permission from Anki). f) Leka, an autonomous ball-like robot (With kind permission from Leka Inc). g) Tipster, a fun and interactive robot (With kind permission from WowWee Group Ltd).*

In some cases, they might show aggression toward the robot [13], [32], [186]. This requires that the existing design guidelines must ensure the safety of the children and the physical integrity of the robot, especially during meltdowns [47]. While some of the existing developed robots could meet many of therapy objectives, they are still not adequate enough to be used with some of the children on the spectrum that exhibit high activity and aggression levels [104]. The majority of the social robots used in the literature are just prototypes, not commercially available, and have yet to find their ways into therapy sessions or schools [103]. Hence, the exposure to such technology is still very limited worldwide, and the need to identify potential safety issues arises. The wide adoption of social companions and smart toys would introduce some concerns and ethical considerations that must be addressed early on [174], [54], [130], [57]. Furthermore, the introduction of robots to children with ASD represents a new stimulus from their environment that must be taken into account and consideration because of their potentially challenging behaviors when interacting with them.

The occurrence of challenging behaviors [131], such as kicking objects, throwing objects at others, banging on objects, and harming oneself by hitting, when a robot is present increases the chances of potentially risky scenarios (Fig. 4.2). Depending on the size of the social robot being used, the magnitude of potential risks might change accordingly. For instance, kicking a large robot will inflict an initial harm to the kicker and secondary damage on others in case of the robot falling down on them. On the other hand, kicking a small robot might impact on others and cause harm. Another challenging behavior that could inflict harm on others is throwing, especially in the case of small and light robots. The child could use the small robot involuntary as an object to be thrown on others. Self-inflicted harmful behaviors, such as banging and hitting, could be increased with the presence of a robot as it can be used by the child as an object to stimulate oneself. All the aforementioned scenarios must be accounted for when designing robots and solutions to mitigate them must be investigated.

4.3 Materials and Methods

4.3.1 Dummy Head Development

A 3D-printed head form made of polylactide was augmented with clay to reach a weight of 3.1 kg that is comparable to the weight of scaled 50th percentile 3-6 years children dummy heads [179]. A 2 mm layer of deformable soft material made of silicone (Ecoflex 00-30, Smooth-On, USA)

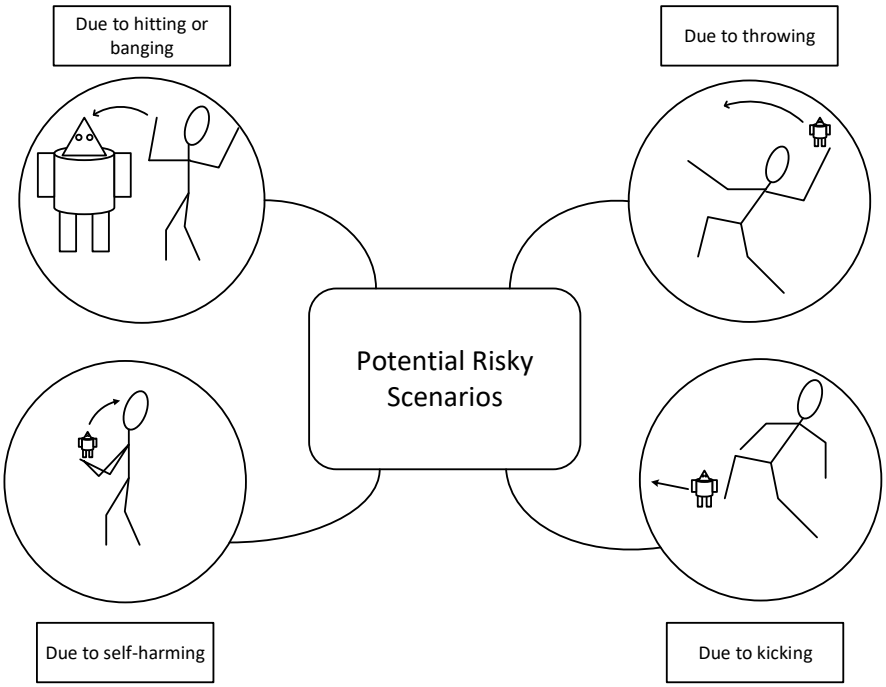

Figure 4.2: *The identified possible risky scenarios that might occur between a child and social robot due to some challenging behaviors.*

was added to the head form to add more lifelike skin [49]. This silicon layer will be used in estimating potential tissue injuries due to its close shore hardness value to that of human skin [151].

A low-cost triple-axis accelerometer (ADXL 377, SparkFun Electronics, Colorado, USA) was placed at the center of the head to measure the linear acceleration of the head. A force-sensing resistor (FlexiForce Force Sensor, Tekscan Inc, USA) was placed at the center of the forehead to measure the impact forces (Fig. 4.3). The force sensor was calibrated according to the manufacturer's guide and a small puck (i.e. disk-like force concentrator) was placed at the center of the sensing area to ensure that most of the force applied can be detected. In case the embedded sensor failed to properly register some of the impacts, digital force gauge (FGE-100X, Shimpo Instruments, USA) was used in separate experiments to measure the impact forces by attaching it to the top of the head. Thus, increasing the total weight of the head to 3.5 kg.

4.3.2 Experimental Setup

The experimental setup was based on a low-cost head model situated in a dedicated frame (Fig. 4.4). The dimensions of the frame used were (94.0 x 94.0 x 94.0 cm^3). Nylon coated wire ropes were used to situate the head at the center of the frame. Both sensors (i.e. accelerometer and force) were interfaced to a computer through a data acquisition card (PCI-6031E, National Instrument, USA). The sampling rate was 20 kHz and signals were filtered according to Channel Frequency Class 60 [58].

During the early years of a child, the muscles of the neck are not developed enough to dampen sudden and violent head's movements [102]. Furthermore, for short impact durations, the effects of the neck and body mass on the head are believed to be minimum [192]. Therefore, the developed setup focuses on the dynamics of the head only.

4.3.3 Impactor

The goal of this study is to quantify the potential harm due to the throwing action of a small robot (i.e. impactor). Hence, to represent a small social robot, a simple and small 3D model with minimum features was designed and then fabricated using a 3D printer (Replicator 5th Generation, MakerBot Industries, USA) (Fig. 4.5). The dimensions of the impactor are (18.0 x 8.0 x 17.0 cm^3) and weighs around 0.55 kg. The surface roughness of the printed robot model was limited to the resolution of the 3D printer.

While there are many large social robots, the smaller ones are more

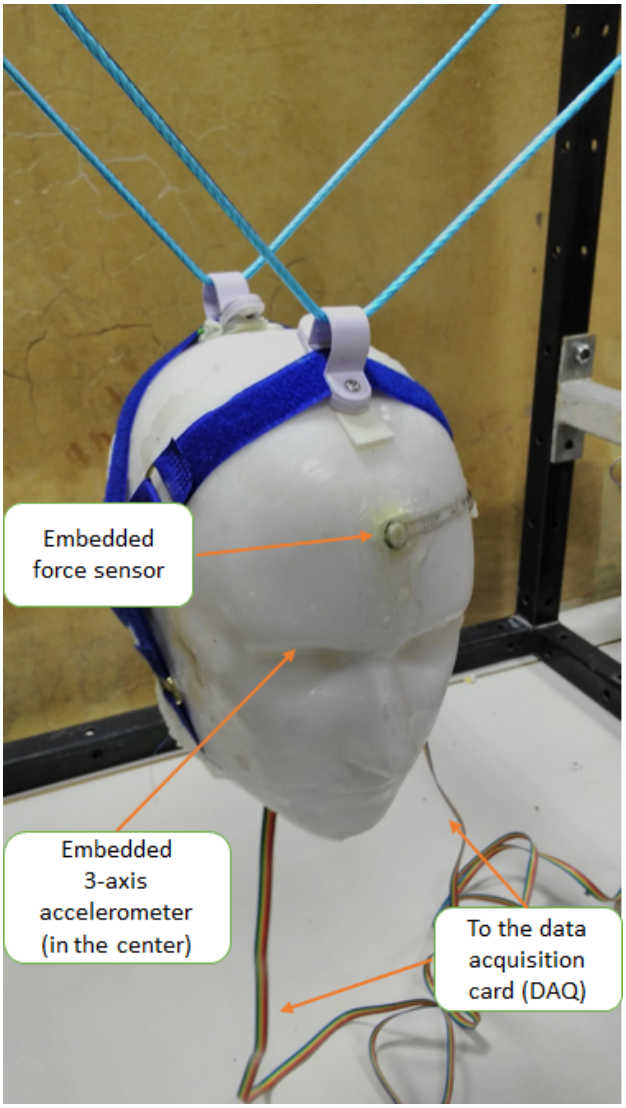

Figure 4.3: *The developed low-cost 3D printed head form with the embedded sensors.*

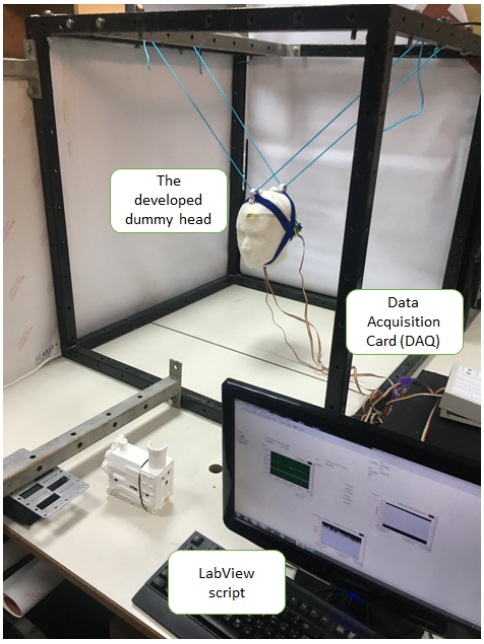

Figure 4.4: *The experimental setup used in this study.*

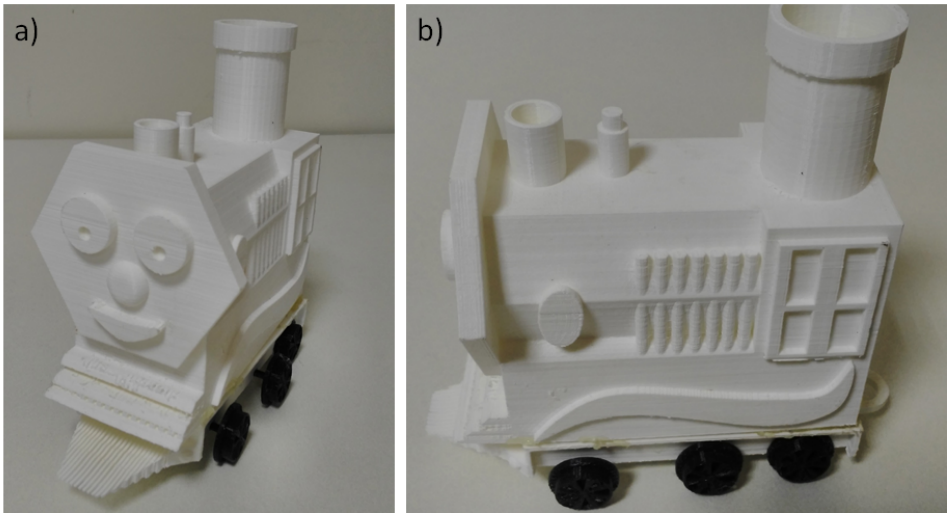

Figure 4.5: *The impactor representing a small social robot that has been used in the experiments. a) Perspective view. b) Side view.*

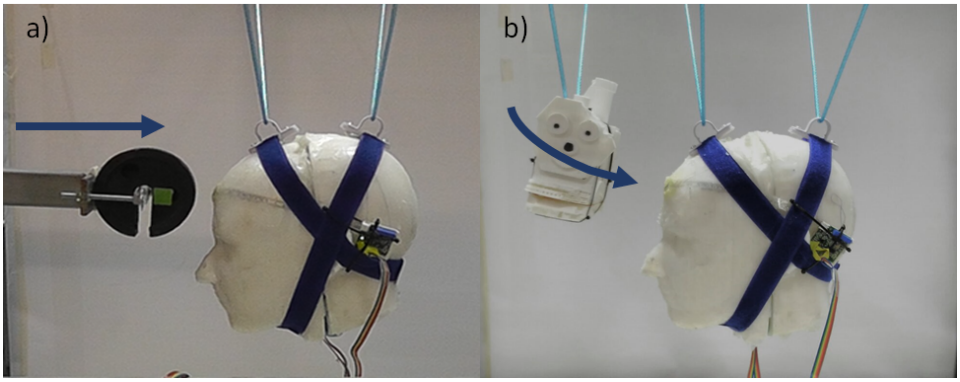

Figure 4.6: *Experiments that were conducted in this study. a) Validation experiment with the 2 kg impactor b) Harm quantification experiment with the dummy robot.*

affordable and are more suited for typical home users. The advancement in technology is allowing smaller robots to be more compact and intelligent. Hence, the size and mass of the proposed dummy robot falls according to such projections. Furthermore, the parameters of the dummy robot are within the potentially throwable range (i.e. light mass) for the targeted users (i.e. children).

4.3.4 Procedures

Setup Validation

To verify the reliability of the developed setup in reporting a comparable HIC values, six impact tests at different velocities were conducted. The impactor used was a 2 kg mass attached to a beam (Fig. 4.6a). The beam was attached to the main frame of the setup and allowed for free motion that enabled it to hit the frontal side of the head at various velocities (See supplementary material). All impact tests were recorded and the corresponding HIC, 3 ms criterion, and impact velocities were calculated.

Harm Quantification

Two different experiments of 15 trials each were conducted. Experiment 1 was in more controlled condition as the dummy robot was tied with a rope to the frame to freely allow it to swing while making its left side facing the forehead of the head (Fig. 4.6b). Experiment 2 was in a more comparable condition to the realistic scenario, and that involved the throwing of the dummy robot at various velocities from a distance of 1 m away from the head model. The velocities used in both experiments were in the range of 0.5 - 8 m/s, which was within the range of a previously reported throwing speed of tennis ball performed by children of different ages (i.e. 3 - 9 years) [168]. We believe this range is reasonable and comparable to the throwing velocities that might be exhibited by children on the spectrum.

All experiments were recorded using a video camera (FDR-X1000V, Sony, Japan) in slow-motion mode (240 fps, 720 pixels). All videos were analyzed using the open-source video analysis software Tracker (v4.10.0, Douglas Brown, Open Source Physics). A LabView (v2014, National Instrument, USA) script was used to obtain the raw data from the data acquisition card, processes it and then stores it in a worksheet file. The data were post-processed by a Matlab (v2015, MathWorks, Massachusetts, USA) script that generates the HIC and 3 ms criterion values.

4.4 Results

4.4.1 Setup Validation

To validate the head model setup, results were compared to previous studies of similar nature [91], [90], where a low-cost dummy head fixed on a frame was developed and an impactor of a mass of 1 kg was used for validation. The impact tests were conducted using robotic arms of different masses at different velocities and their results were then compared to that obtained with ATD. Their setup was able to reproduce comparable numerical HIC values.

The generated HIC values from the validation impact tests in our study were comparable to that conducted previously (Fig. 4.7). For example, impacting at a velocity of around 1 m/s has generated a HIC value in the range of 3 - 10. The trend is also similar as the values of HIC obtained have increased proportionally with the applied impacts velocities. As for the 3 ms criterion, the values at around 1 m/s were in the range of 8 - 16 (Fig. 4.8). The differences in the values obtained are attributed to the differences in the mass of the impactors used (i.e. 2 kg vs 1 kg) and the

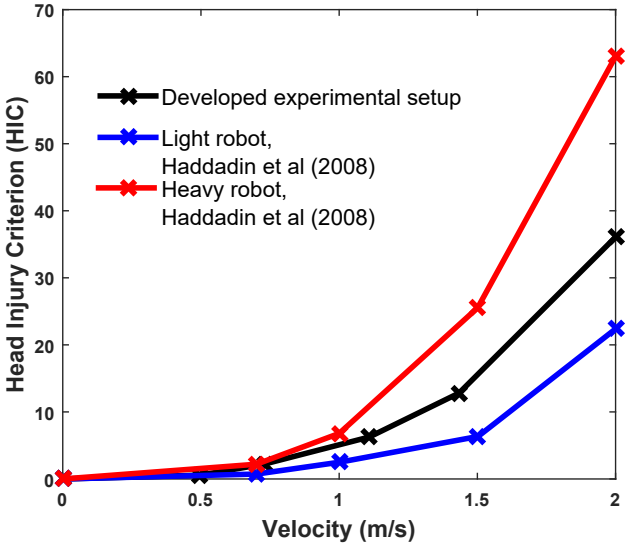

Figure 4.7: *Head Injury Criterion (HIC) values generated by the developed experimental setup due to different impact velocities with a 2 kg impactor. The results were compared with similar impacts conducted by different industrial robots.*

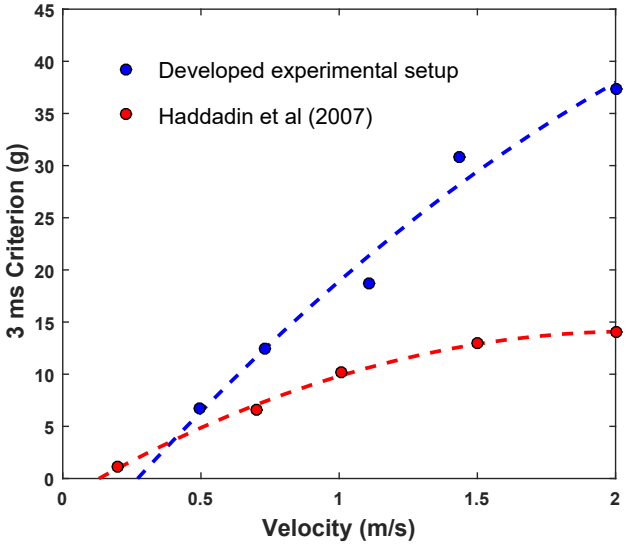

Figure 4.8: *The 3 ms criterion values generated due to different impact velocities with a 2 kg impactor. The results were compared with similar impacts conducted by an industrial robot.*

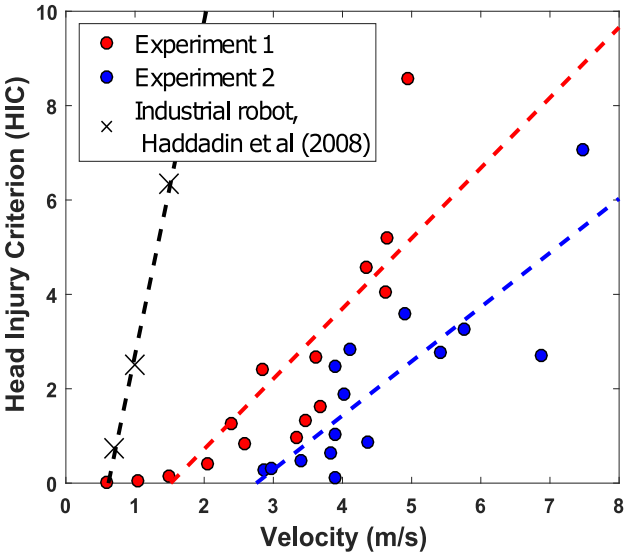

Figure 4.9: *The corresponding Head Injury Criterion (HIC) values for impact experiments conducted in Experiment 1 and 2. Experiment 1 where the dummy robot was attached to the experimental setup while Experiment 2 where the experimenter conducted the throwing of the dummy robot. The results were compared with HIC values generated by an industrial robot.*

mass of the developed dummy heads (i.e. 3.1 kg of a child vs 4.5 kg of an adult) [129], [107].

4.4.2 Harm Quantification Measures

Head Injury Criterion (HIC)

In Experiment 1, there is a more consistent trend as the velocity of impact increases the corresponding numerical HIC value increases (Fig. 4.9). The lowest recorded HIC value was 0.013 and it occurred at a velocity of 0.6 m/s while the highest recorded HIC value was 8.568 corresponding to a velocity of 5 m/s.

In Experiment 2, the overall trend is less consistent at certain velocities as compared to Experiment 1, especially around 4 m/s. However, there is an increase in the recorded HIC values as overall speed of throwing increases. The lowest HIC value obtained was 0.114 corresponding to a velocity of 3.9 m/s while the highest recorded HIC value was 7.066 at a velocity of 7.48 m/s.

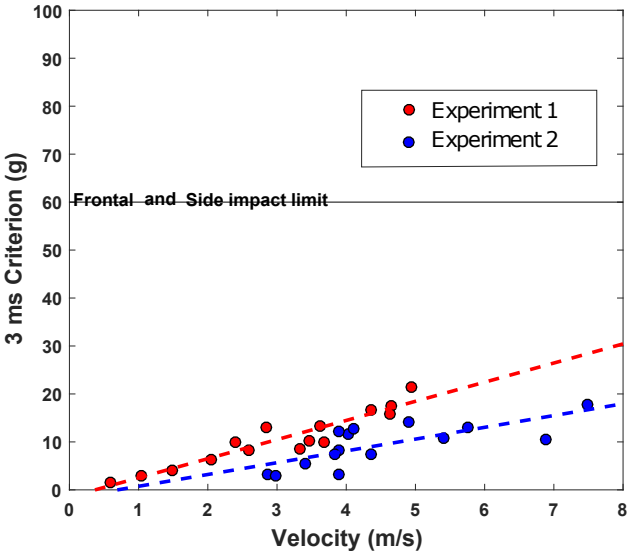

Figure 4.10: *The corresponding 3 ms criterion values for impact experiments conducted in Experiment 1 and 2. Experiment 1 where the dummy robot was attached to the experimental setup while Experiment 2 where the experimenter conducted the throwing of the dummy robot. The results were compared to the 3 ms criterion thresholds for child occupant [73].*

The 3 ms Criterion

In Experiment 1, the lowest recorded 3 ms value was 1.425 g and it occurred at a velocity of 0.6 m/s while the highest recorded 3 ms value was 21.476 g corresponding to a velocity of 5 m/s (Fig. 4.10). The trend of the 3 ms values are linearly increasing with the applied velocities.

In Experiment 2, The lowest 3 ms value obtained was 2.96 g corresponding to a velocity of 2.97 m/s while the highest recorded 3 ms value was 18 g at a velocity of 7.48 m/s (Fig. 4.10). the trend is less consistent as compared to Experiment 1 as evident around 4 m/s.

Peak Linear Acceleration

In Experiment 1, the lowest recorded peak linear acceleration value was 1.5 g and it occurred at a velocity of 0.6 m/s while the highest recorded peak value was 23 g corresponding to a velocity of 5 m/s (Fig. 4.11). The peak acceleration values are increasing linearly with throwing velocity.

In Experiment 2, the lowest peak linear acceleration value obtained was 3 g corresponding to a velocity of 2.97 m/s while the highest value was

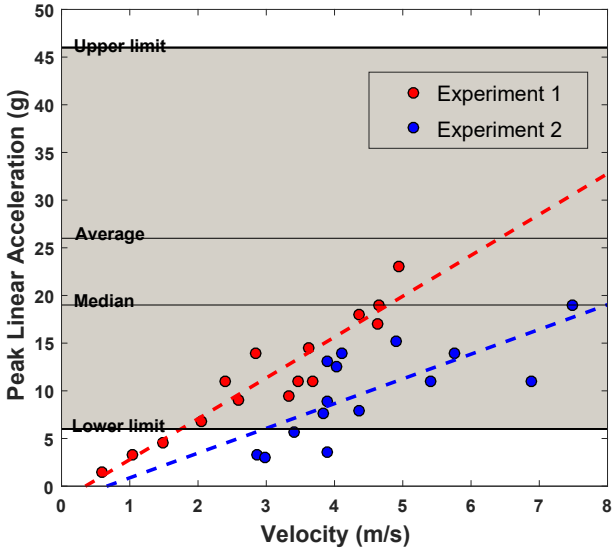

Figure 4.11: *The corresponding peak linear acceleration values for impact experiments conducted in Experiment 1 and 2. Experiment 1 where the dummy robot was attached to the experimental setup while Experiment 2 where the experimenter conducted the throwing of the dummy robot. The highlighted area represents the range of peak linear accelerations that is associated with the occurrence of subconcussive events [165].*

19 g at a velocity of 7.48 m/s (Fig. 4.10). The trend is less consistent as compared to Experiment 1, especially around 4.0 m/s.

Impact Forces

The embedded force sensor approach has failed in registering some of the impacts or maximum values due to the lack of sufficient contact between the dummy robot and the effective area of the sensor. However, the maximum force recorded in all of the experiments was 28 N at a velocity of 5.75 m/s.

In order to get a better understanding of the potential impact forces involved, four separate experiments at different velocities were conducted using a stand-alone force gauge. These experiments were conducted similar to Experiment 1 method (Fig. 4.6b). The lowest value was around 30.1 N corresponding to velocity of 0.75 m/s while the maximum value was 91.3 N at a velocity of 2.15 m/s. There is a trend and linear relationship between the applied velocities and the measured resultant peak force values (Fig. 4.12).

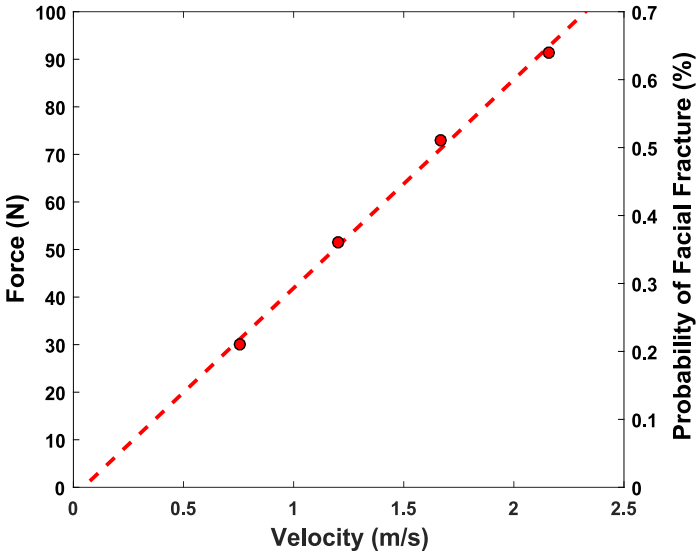

Figure 4.12: *The corresponding impact force values for impact experiments that were conducted using the stand-alone digital force gauge. The right axis represents their corresponding probabilities of causing facial fracture.*

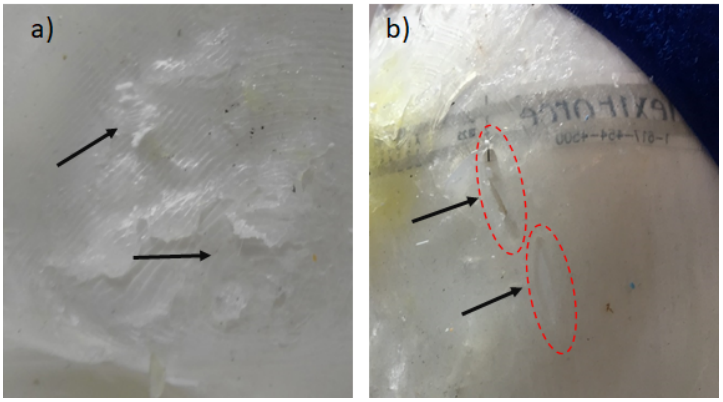

Figure 4.13: *The observed tissue damage to the artificial skin. a) Abrasions-like skin damage of depth that is less than 1 mm. b) Laceration-like skin damage of depth that is equal or greater than 2 mm.*

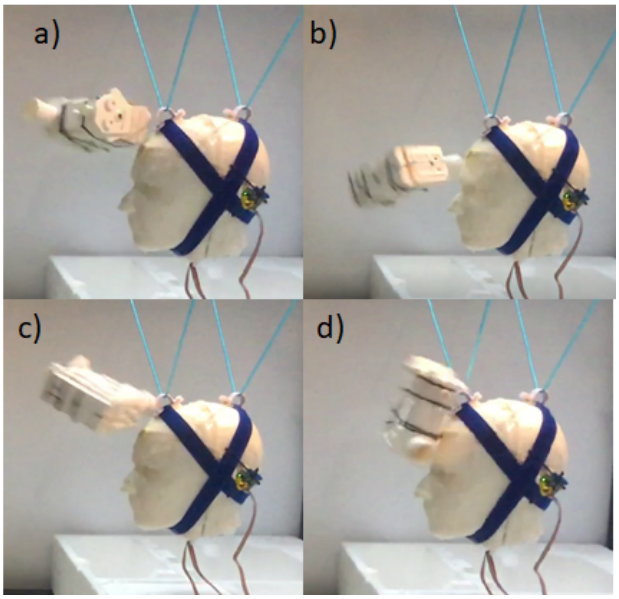

Figure 4.14: *Surface areas of the dummy robot that hit the head. a) Frontal edge. b) Chimney. c) Back. d) Side.*

Tissue Injuries

The evaluation of tissue injuries was based on the visual inspection of the artificial skin and sample measurements using vernier caliper. All observations were made after conducting Experiment 1 and Experiment 2. In terms of depth, the majority of the observed damage to the artificial skin were less than 1 mm (Fig. 4.13a). There were some instances where the depth of the observed damage was more than the thickness of the artificial skin (i.e. greater than 2 mm) and piercing the dummy head (Fig. 4.13b).

4.5 Discussion

For HIC values to be meaningful, they need to be translated to a corresponding metric for potential injury based on AIS scaling. From reported equations previously, the probabilities of injury due to all impact tests conducted in both Experiment 1 and 2 are negligible (i.e. close to 0%). Even though all the estimated potential for injuries in our experiments are low, there is still a potential for serious harm based on the reported catastrophic injuries and fatalities that occurred due to impacts with lighter objects (e.g. baseball) among children [125], [33]. While HIC severity index is significant in giving an estimation of the potential for head injury, it is insufficient

to estimate pain and assess tissue injuries.

As for the 3 ms criterion, the maximum values obtained for both sets indicate a low potential for harm. The highest value for Experiment 1 is around 36% of the 3 ms criterion impact limit (i.e. 60 g for frontal and side impacts). As for Experiment 2, the corresponding percentage for the highest 3 ms value is around 30% for the 3 ms criterion impact limit of 60 g.

The values for the peak linear accelerations for both experiments were around 20 g, which were far away from most of the reported peak accelerations (e.g. 66 - 106 g) that are associated with concussive events [200]. However, most of the obtained peak acceleration values fall within the range (i.e. 6 - 46 g) that is associated with subconcussive events (Fig. 4.11). Furthermore, two peak linear acceleration values are at or above the reported median value of 19 g that has been associated with the occurrence of subconcussive impacts, where the occurrence of which has been linked to neurocognitive deficits [165]. More research need to be done to understand the biomechanical variables and its relation to causing concussion or mild TBI among children.

For HIC, 3 ms criterion, and peak linear acceleration results, there was a noticeable disparity in Experiment 2 at a velocity of around 4 m/s. For example, HIC values range was from 0.114 to 2.834. This discrepancy can be attributed to the surface or area of the dummy robot that hit the head (e.g. chimney vs side) as observed from the analysis of the recorded videos (Fig. 4.14). This implies that at higher velocities, the harm level could even be larger depending on the contact area.

The peak force values for all the experiments were translated to percentages corresponding to the potential of causing fracture to the skull based on the previously stated relation (Fig. 2.5). All the recorded peak forces have low potential to cause real harm to any of the facial bones. For example, a peak value of 91.3 N (i.e. the maximum value obtained) corresponds to around 0.6% chance of causing fracture to the bones of the face. However, assuming the linear relation holds true for higher velocities (Fig. 4.12), the chance for facial fracture increases up to 20% at a hypothetical throwing velocity of 10 m/s for the same robot.

The depth of the observed artificial skin damage were interpreted to a corresponding tissue injuries based on the classification listed in Table 2.3. Most of the damage caused by the impacts conducted in this study falls into superficial category that affects the epidermis layer, and they were in the form of abrasions. There were few lacerations that are classified as partial-thickness skin loss that would require medical care. No instances of

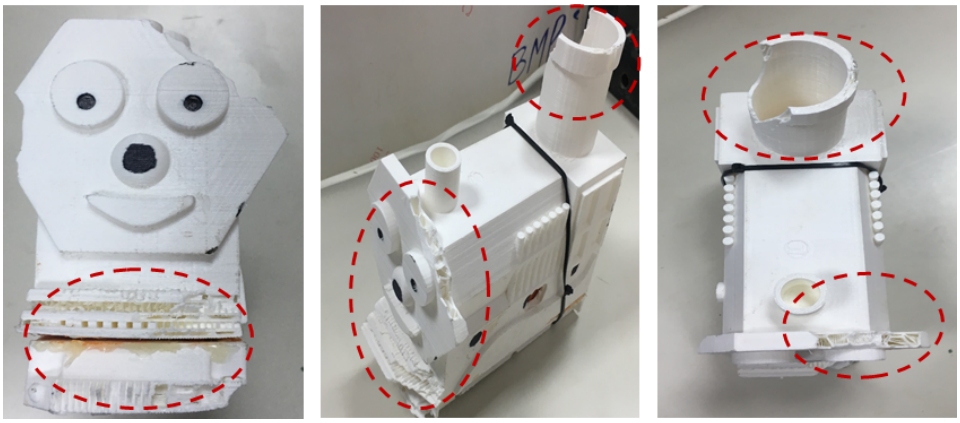

Figure 4.15: *The sustained damage on the small robot after finishing all of the experiments.*

full-thickness (i.e. depth greater than 4 mm) skin loss were observed.

The dummy robot has sustained a considerable damage (Fig. 4.15). The damage was more apparent after performing Experiment 2 (i.e. mimicking real throwing scenario). Some of the lacerations on the artificial skin of the head could have resulted from the newly formed sharp edges on the robot due to the sustained damage from some of the initial impacts. This implies that any robotic design should remain robust and safe, especially after being subjected to similar impacts and conditions. Superficial injury as an indicator for potential harm could serve better than some of the typical severity indices. Similar conclusion has been reached in studies investigating the potential harm due industrial robots [90], [89].

The safety investigations conduced in this study were limited to one potential scenario that may happen between a child and a social robot, which is harm to the head due to throwing. The developed experimental setup was limited to the head, but to better understand the overall dynamics involved due to impacts, a child dummy model should have been used. Quantifying harm was limited to the head, however, the actual harm could potentially affect other areas, such as the neck or the chest. The impact scenario considered was limited to one and did not account for any impact boundaries,

such as against a wall. Measurements of harm to the head was limited to the existing severity indices and to the closest available data. Thus, some aspects can not be measured, such as pain levels. The tissue injury investigations were limited to artificial skin and not a live skin. Thus, actual depth of lacerations on an actual live skin might differ. Finally, the study was limited to small form factor impactor representing a small social robot, hence, the obtained results are only applicable to closely comparable robots in terms of mass, design, material and size.

4.6 Conclusion

The motivation of this study is to investigate the potential for harm due to the interaction between social robots and children with ASD, especially during the manifestation of challenging behaviors. Throwing, kicking, hitting, and self-harming are some of the challenging behaviors that during the exhibition of which, especially in the presence of a social robot, could inflict some harm to the children themselves and those around them. Our investigation of harm due to throwing of a small social robot revealed that it could potentially cause tissue injuries, subconcussive or concussive event in extreme cases.

4.7 Chapter Summary

This chapter identified the potential harmful scenarios that could occur between a child with autism and a social robot. The chapter presented the experimental setup and methods that were used to quantify the potential for harm due to throwing based on the severity indices. Finally, the chapter presented the results for the impact experiments and discussed their implications on the potential harm.

CHAPTER 5

Parametric Design of Small Robots

This chapter investigates different design parameters of small robots to reduce the potential harm by conducting two different studies. The first section provides a brief introduction about the problem and motivation. The methods and materials are then presented in this chapter. The last two sections of this chapter provide the details about the two studies and their outcomes.

5.1 Introduction

The interest in robots is increasing globally as estimated by the International Federation of Robotics (IFR) [109]. The application of robots is extending to new areas, such as that in healthcare. Most notably is the application of social robots in therapy sessions with children with autism, which has been reported to improve the overall outcomes [47]. However, such children exhibit a multitude of challenging behaviors that could raise some safety concerns when a robot is present in their vicinity [3]. The occurrence rates of challenging behaviors are high (e.g. 49% up to 69% [25], [34], [116]), and that have many consequences on the services and treatments provided to them [106].

Unlike typical toys, social robots have the ability to demonstrate emotions, establish social connections, display of personalities, using cues, and engage with partners at an interpersonal level [178], [52], [193]. The introduction of robots to children with ASD represents new challenge that must be taken into account. Some studies reported that children interacting with social robots might show some aggression [13], [45], [94]. Furthermore, robots are meant to elicit behaviors [66], [53]. Hence, the introduction of such technology to children with ASD could represent a potential harm during the manifestation of unwanted behaviors (e.g. kicking, throwing, and banging [131]). For instance, a thrown small robot that hits the head might cause subconcussion or superficial injuries [3]. There is a need to evaluate social robots to achieve safe physical human-robot interaction during such scenarios.

When the head is subjected to bumps or blows and impacts with objects, a traumatic brain injury (TBI) might occur. In serious cases, TBI could lead to a disability or, in extreme cases, it could cause death. The occurrence of TBI among children could cause challenges, such as disabilities and impairment in daily skills [17], [159]. In 2013 alone, 2.8 million cases of TBI have been reported in the United States [188]. The cases of TBI among children were occurred due to getting struck by or against an object. A study analyzing mild brain injuries among children in Sweden for the years 1998 and 1999 has found that 47% of the cases occurred at home and during playtime or leisure activity and due to childcare products, which includes toys [69]. These figures have many implications on the design of robotic toys pertaining to the safety of the head. There is a need for further safety considerations and user-focused design to take into account the characteristics of special needs users, such as children with ASD [3], [13]. The work in social robotics safety is still limited [99], [67], especially in relation to improving design aspects of small robots [189], [100], [41], [48].

The establishment of safety standards in different fields of robotics is making notable advances. However, the progress in establishing safety standards in relation to social robots and robotic toys is still lacking [99], [67]. Some of the existing safety standards in toys can be readily imported to cover some fundamental design and safety aspects. For example, the ISO 8124 standard [113]. Safety aspects of the mechanical and physical properties of toys are covered in part one of this standard while part two and three covers flammability and migration of certain elements, respectively. More rigorous design considerations are needed that consider the unwanted behaviors exhibited by children with autism. For example, considering a scenario where the robotic toy is thrown to the head.

In this chapter, two studies based on Taguchi method to investigate the influence of different design parameters on a selected severity index are presented. The first study investigates two design factors (i.e. mass and shape) of a small robot that is subjected to different throwing velocities (i.e. noise factor) and understand their effects on the acceleration of a dummy's head. Furthermore, the first study identifies the conditions of the design factors at which the response is minimized. The second study investigates a way to reduce the harm to the head by studying the influence of two control factors (i.e. storage modulus of soft material and its thickness) and one noise factor (i.e. throwing velocity) of a small form factor toy on the resultant head's acceleration. Furthermore, the optimal levels of the investigated control factors that help in reducing the response are identified.

5.2 Materials and Methods

5.2.1 Impact Setup

The impact setup was used to conduct the experiments that contained a 3D-printed head that was mounted on a frame (Fig. 4.4). The mass of the dummy head was made close to that of children's dummy heads [179]. To measure the linear acceleration of the head, an accelerometer was placed inside the head. The data was acquired at 20 kHz. The impact setup has been shown to give similar results to that of related studies. More in-depth details about the experimental setup and validation can be found in Chapter 4 or in our earlier studies [11], [3], [12], [7].

5.2.2 Impactors

Study One

The goal of this study is to understand the influence of the mass and shape of a small robot on the resultant peak linear head acceleration due to an impact. Hence, 3D models of three basic shapes were considered (Fig. 5.1). The shapes were constructed using a 3D printer (Replicator 5^{th} Generation, MakerBot Industries, USA). A clay material was used to adjust the mass of each shape according to the mass levels in Table 5.1. The center of mass was made sure to be balanced for all the objects.

Study Two

A 3D printed cylindrical object was used as an impactor in the second study investigating the influence of adding soft materials to the robotic design.

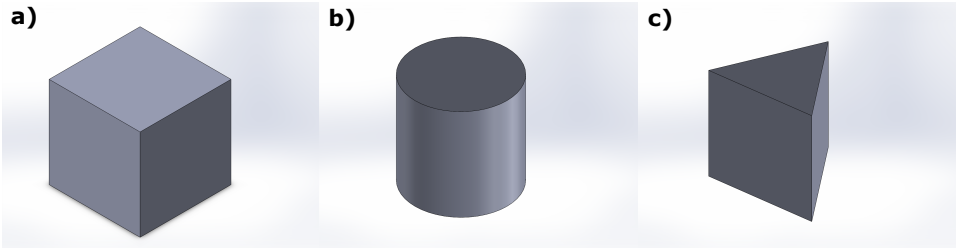

Figure 5.1: *The three basic 3D designs of the impactors that have been considered in the study. a) Cube (*$10 \times 10 \times 10\ cm^3$*, length, width and height). b) Cylinder (*$10 \times 10\ cm^2$*, diameter and height). c) Wedge (*$10 \times 10\ cm^2$*, length and height). For simplicity, the three basic featureless shapes were considered to isolate the contribution of the shape on the response.*

The dimensions of the impactor were ($10 \times 10\ cm^2$, height and diameter). The 3D printer was used to build the object. Clay was used to fill the impactor to reach 0.4 kg. The soft materials (Ecoflex OO-30 & Dragon skin FX-Pro, Smooth-On, USA) were prepared according to manufacturer's instructions. The soft materials were prepared in molds of different thicknesses and then rectangular ($5 \times 8\ cm^2$) samples of each were attached to the impactor covering the area of impacts (Fig. 5.2).

5.2.3 Procedures

Impact Experiments

All experiments were performed according to the $L_9(3^2)$ orthogonal array (OA) (Table 2.4). For each noise level, 9 experiments were conducted that have covered all possible combinations of the control factors (Data available in [8], [6]). The objects were tied to the frame which provided a controlled condition in the execution of the experiments (Fig. 5.3). Furthermore, it has provided more consistent impact velocities by adjusting the drop height of an object. Three different drop locations generated three different noise levels. The impact velocities were based on the video analysis of the experiments.

The impact velocities were estimated based on the slow-motion record-

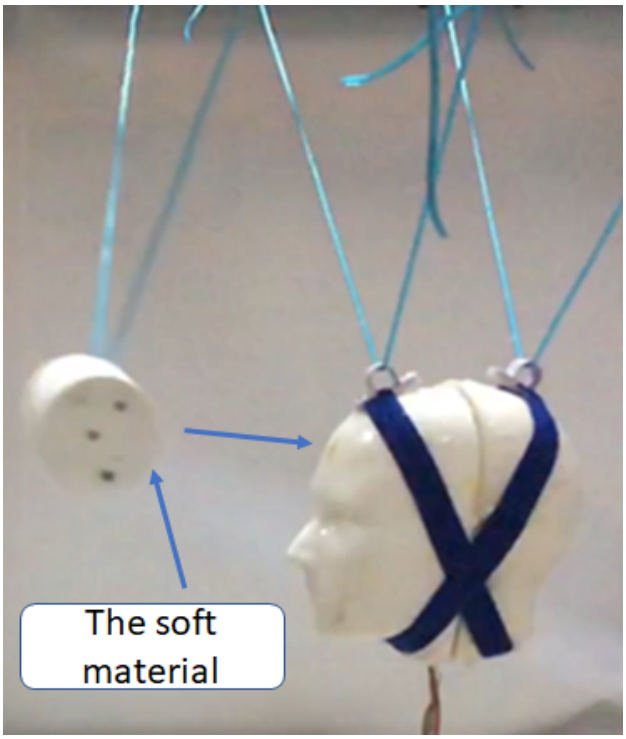

Figure 5.2: *Sample of the experiments conducted for the second study.*

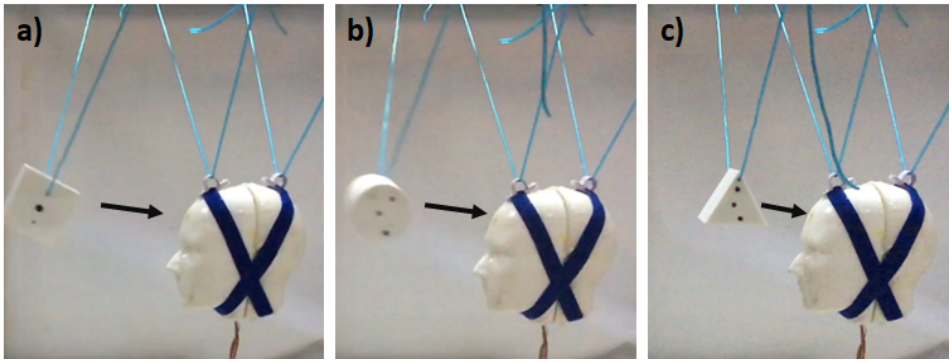

Figure 5.3: *Samples of the experiments that were conducted in the first study [10]. a) For the cube. b) For the cylinder. c) For the wedge.*

ings of the experiments using a video analysis software (Tracker v5.0.7 [38]). The raw readings were obtained from the data acquisition card and then stored using a LabView script. Finally, the peak head acceleration for each experiment was calculated based on a MATLAB script. More detailed procedures can be found in our earlier studies [11], [3], [12], [7].

Dynamic Mechanical Analysis

For the second study, the properties of the soft materials were studied using a dynamic mechanical analyzer (RSA-G2, TA instruments, USA ; Fig. 5.4). The dynamic mechanical analysis (DMA) is a common test to measure the properties (i.e. elastic and viscous) of a material. The properties were studied by applying a stress (e.g. sinusoidal) and measuring the resultant strain and the phase difference between the input and output. A frequency sweep tests were conducted to study the storage modulus. In these tests, the frequency was varied from 0.1 Hz to 100 Hz while the strain and temperature kept constant. The storage modulus readings for each material were generated (Fig. 5.5). The values of storage modulus at 1 Hz for each material were considered in the analysis. This frequency is believed to be at which the high rate of challenging behaviors might occur [157].

5.2.4 Head Severity Index

Several head severity indices were used in the literature to study the potential harm to the head, such as Head Injury Criterion, 3 ms criterion, and peak head linear acceleration. Previous studies have considered the peak linear acceleration of the head to investigate concussive events due to impacts [166] [198]. Among hockey players, an earlier study has reported the possibility of the occurrence of a concussion at 31.8 g [135]. Another study investigating football impacts identified the occurance of subconcussive events at 26 ± 20 g [165]. Dummies that report the head acceleration were also considered to evaluate the potential injuries to the head (e.g. in industrial robots and in sports [91], [196], [150]). Similarly, the experimental setup in this study will use the peak linear head acceleration to conduct the impact experiments.

5.2.5 Data Analysis

ANOVA

To study the significance of each factor on the head's acceleration, three-way analysis of variance (ANOVA) test was conduced on the responses of

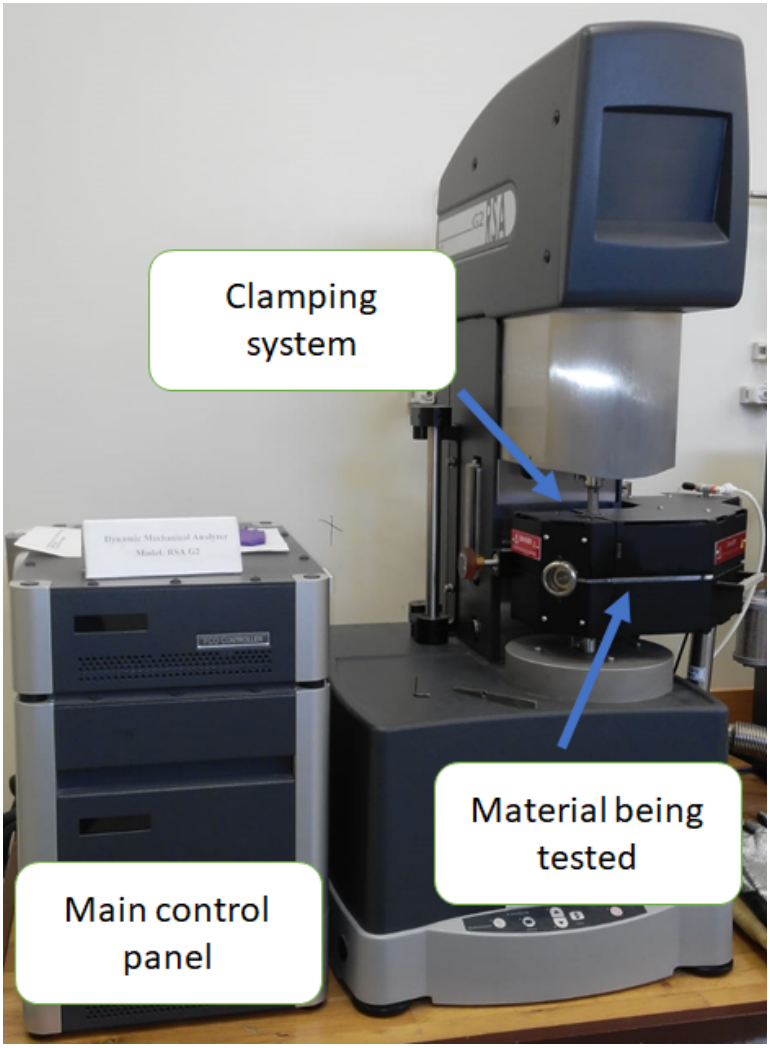

Figure 5.4: *The Dynamic Mechanical Analyzer device that was used to analyze the soft materials.*

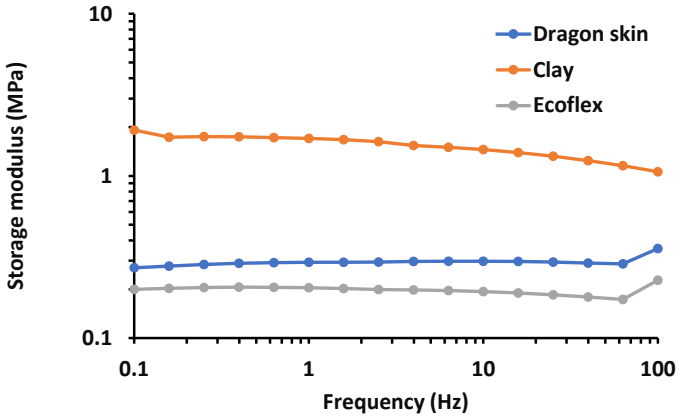

Figure 5.5: *The storage modulus results for the dynamic mechanical analysis (DMA) tests that were performed on the three materials.*

all the investigated factors. The level for statistical significance was set to $p < 0.05$. All analyses were performed using Minitab (v18.1, Minitab Inc., USA).

Signal to Noise Ratio

The optimization technique considered the signal-to-noise (S/N) ratio. The aim of this study is reduce the head's acceleration. Hence, the appropriate S/N ratio was selected, and it is defined as [56]:

$$S/N = -10log_{10}E\left[y_i^2\right] \tag{5.1}$$

where E is the expectation and y_i^2 is the head's acceleration (i.e. the response).

5.3 Shape and Mass of Small Robotic Design

5.3.1 Experimental Factors

The goal is to investigate whether the shape or the mass play any role in affecting the response. Hence, two control factors are considered in this investigation for their possible influence in attenuating the peak acceleration of the head. Twenty seven (i.e. 9×3) experiments must be conducted to

Table 5.1: *The experimental factors and their descriptions. The impact velocity levels are represented by the mean and the standard deviation.*

Type	Factor	Code	Level 1	Level 2	Level 3
Control	Mass	A	0.3 kg	0.4 kg	0.5 kg
Control	Shape	B	Cube	Cylinder	Wedge
Noise	Impact velociy (m/s)	X	Low (1.14 ± 0.10)	Medium (1.72 ± 0.12)	High (2.7 ± 0.10)
Response	Peak linear head acceleration (g)				

cover all the possible combination of all the factors based on the $L_9(3^2)$ OA (Table 2.4). The considered control and noise factors are independent.

All levels of all factors have been defined (Table 5.1). The range for the mass is comparable to that of small robotic toys. For the sake of simplicity, the selection of the overall shapes of the form factor were limited to three basic 3D geometric shapes while ignoring any other features. For consistency, the noise levels were limited to low velocities divided into levels (i.e. < 3 m/s) [139].

5.3.2 Results

Orthogonal Array

The Taguchi L_9 orthogonal array was completed by finding the average response, the standard deviation, and the respective S/N ratio for each combination of the investigated factors (Table 5.2). The range for the linear acceleration values was 2.72 to 13.03 g. The lowest response value was at a mass of 0.3 kg, wedge shape, and Level 1 impact velocity (i.e. A1-B3-X1). As for the highest response, it occurred at a mass of 0.5 kg, cylinder shape, and at an impact velocity Level 3 (i.e. A3-B2-X3). The lowest overall av-

Table 5.2: *The complete Taguchi orthogonal array along with columns showing the average response, standard deviation (SD), and the signal to noise ratio (S/N) for each row.*

	Inner control factors array		Outer noise factor array			Average response	Standard deviation	Signal-to-noise ratio
RUN	A	B	X1	X2	X3	Mean	SD	S/N
1	1	1	3.75	5.74	6.58	5.36	1.45	-14.79
2	1	2	3.25	7.28	9.24	6.59	3.05	-16.96
3	1	3	2.72	5.81	7.18	5.24	2.28	-14.90
4	2	1	4.18	7.56	8.96	6.90	2.46	-17.13
5	2	2	4.20	9.04	10.96	8.07	3.48	-18.64
6	2	3	3.72	7.04	9.04	6.60	2.69	-16.85
7	3	1	4.93	9.14	10.94	8.34	3.08	-18.80
8	3	2	4.42	9.50	13.03	8.98	4.33	-19.69
9	3	3	4.41	8.84	11.40	8.22	3.54	-18.80

erage response across all factors was 3.95 g with a S/N ratio of -12.05 and was due to Level 1 velocity (Table 5.3 and Table 5.4). On the other hand, Level 3 velocity scored the highest average response (ie. 9.70 g) with a S/N ratio of -19.91.

ANOVA

The statistical significance of each factor on the average response due to varying their levels was investigated based on three-way ANOVA test. The inverse transformation of the response was considered in this test. A post-hoc pairwise Tukey test was also conducted.

To understand the contribution of the mass on the head's acceleration, a three-way ANOVA was conducted (Table 5.5). The test revealed a statistical significance due to altering the conditions of the mass on the response

Table 5.3: *The average response at every level of each factor.*

	A	B	X
Level	Mean (SD)	Mean (SD)	Mean (SD)
1	5.73 (0.75)	6.86 (1.49)	3.95 (0.67)
2	7.19 (0.77)	7.88 (1.21)	7.77 (1.43)
3	8.51 (0.41)	6.69 (1.49)	9.70 (2.07)

Table 5.4: *The average signal-to-noise (S/N) ratios at every level of each factor.*

	A	B	X
Level	S/N	S/N	S/N
1	-15.55	-16.90	-12.05
2	-17.54	-18.43	-17.94
3	-19.10	-16.85	-19.91

Table 5.5: *Summary of the three-way ANOVA test on the three factors.*

Source	df	Sum of squares	Mean square	F-Value	P-Value
A	2	0.02	0.01	46.97	0.00
B	2	0.00	0.00	7.03	0.02
X	2	0.12	0.06	289.24	0.00
A*B	4	0.00	0.00	1.22	0.374
A*X	4	0.00	0.00	2.70	0.11
B*X	4	0.00	0.00	3.91	0.05
Error	8	0.00	0.00		
Total	26	0.15			

(F(2,8) = 46.97, p = 0.00) at the $p< 0.05$. A post-hoc Tukey test showed that Level 1 mass (M = 5.73, SD = 0.75), Level 2 mass (M = 7.19, SD = 0.77), and Level 3 mass (M = 8.51, SD = 0.41) were statistically different at $p< 0.05$.

To investigate the effects of the shape on the response, a three-way ANOVA test was conducted (Table 5.5). There was a significant difference due to the alteration of the shape on the response (F(2,8) = 7.03, p = 0.02) at $p< 0.05$. A post-hoc Tukey test showed that Level 2 shape (M = 7.88, SD = 1.21) differed significantly from Level 3 shape (M = 6.69, SD = 1.49).

To understand the contribution of the impact velocity, a three-way ANOVA was performed (Table 5.5). A significant difference was reported due to altering the conditions of the impact velocity on the head acceleration (F(2,8) = 289.24, p = 0.00) at $p< 0.05$. A post-hoc Tukey test showed that Level 1 impact velocity (M = 3.95, SD = 0.67), Level 2 impact velocity (M = 7.77, SD = 1.43), and Level 3 impact velocity (M = 9.70, SD = 2.07) were statistically different at $p< 0.05$.

There was no significant interaction between the mass and the shape (i.e. A and B) on the response (F(4,8) = 1.22, p = 0.37) at $p< 0.05$. There was no significant interaction between the mass and the impact velocity (i.e. A and X) on the response (F(4,8) = 2.70, at p = 0.11) at $p< 0.05$. There was no significant interaction between the shape and the impact velocity (i.e. B and X) on the response (F(4,8) = 3.91, at p = 0.05) at $p< 0.05$.

5.3.3 Discussion

The responses of the 27 experiments conducted suggest that the control factors and noise factor have influenced the response. A trend between Factor A (i.e. the mass) and the response can be observed by observing the columns of the OA (Table 5.2). For instance, observing the average response values in the noise factor columns (i.e. X1, X2, and X3), the registered head acceleration value appear to increase as the mass level increases (i.e. from row 1 to 9). No consistent trend can be observed for Factor B. However, the second shape B2 (i.e. cylinder) appears to score higher responses compared to the other two shapes as observed in the average response column. Observing the noise columns shows that the head's acceleration has increased with the impact velocity. The relatively large values of the standard deviation also support that the noise factor affects the resultant head acceleration significantly. The velocity and mass of the impactors have been reported to affect the magnitude of the peak linear

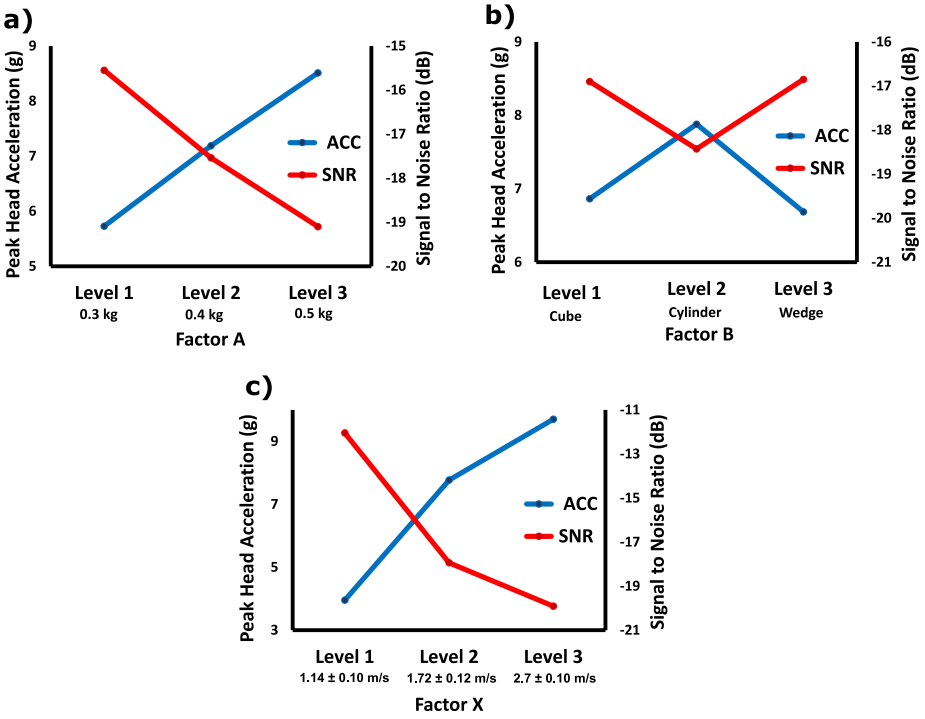

Figure 5.6: *The average response values and signal-to-noise (S/N) ratios for the factors investigated in this study. a) For Factor A, the mass. b) For Factor B, the shape. c) For Factor X, the impact velocity.*

head acceleration [107], [91]. The average responses and the results of the ANOVA test were in accordance with these findings (Table 5.3 and Table 5.5). As for the shape factor, it appears to affect the response the least (Table 5.3). The response for the cylinder shape reported higher average response compared to the other shapes.

Optimization

The goal of Taguchi design in this study was to optimize the control factors in order to reduce the head linear acceleration. The optimization was accomplished by inspecting the average response and the corresponding average S/N ratio at every level of the control factors (Table 5.3 and Table 5.4; Fig. 5.6). The ideal case in this study is producing a lower response and higher S/N ratio, hence, the focus is on the factor conditions that satisfies this criterion.

The optimal conditions for the mass and shape were found (Fig. 5.6). The mass of 0.3 kg achieved the lowest response. As for control factor of the shape, cube (i.e. Level 1) and wedge (i.e. Level 3) scored comparably the best. For the noise factor, Level 1 (i.e. 1.14 ± 0.10 m/s) achieved the lowest response.

The identified conditions were 0.3 kg for the mass factor and cube or wedge for the shape (i.e. A1-B1 and A1-B3, respectively). Compared to other combinations, the identified optimal conditions generated relatively lower responses, for example, the individual responses at noise Level 2 and Level 3 (i.e. X2 and X3) for runs 1 and 3 (Table 5.2).

Confirmation Runs

The confirmation runs are needed to validate the optimal conditions that were obtained in the previous section. To achieve that, 18 experiments were conducted. For each of the identified conditions in the previous section, 3 runs were performed (Table 5.6). The confirmation runs showed that the average response values were comparable to respective ones obtained in the complete OA (Table 5.2), hence, confirming the optimal identified conditions for the control factors.

Limitations of the Study

The investigation conducted in this study was limited to three factors conducted in a laboratory developed experimental setup with controlled conditions that might differ from an actual and more dynamic scenario (e.g. potential for secondary impacts). The values of the object mass that were

Table 5.6: *The responses, the average, and standard deviation for the confirmation runs. The conditions selected achieved relatively better responses in comparison to the other conditions in the main experiments.*

Combination	X1	X2	X3
	3.32	5.48	7.57
A1-B1	3.78	5.64	6.51
	4.04	6.17	6.46
Mean (SD)	3.71 (0.36)	5.76 (0.36)	6.85 (0.63)
	2.57	5.31	7.97
A1-B3	2.68	5.28	6.63
	3.25	6.18	7.76
Mean (SD)	2.83 (0.37)	5.59 (0.51)	7.45 (0.72)

tested were limited to the range of 0.3 - 0.5 kg. In reality, lighter or heavier robotic toys could exist. Studying the effect of shape was limited to three basic featureless shapes. However, actual robotic forms could have other unusual shapes with a lot of detailed features. Due to the way the experimental setup was designed, the impact area for each shape was limited to achieve consistency between the experiments. The effects of different impact areas and their interactions with different shapes and surface's features were not investigated in the current work. The noise levels that were tested were limited to low velocity impacts. Hence, the generated head's accelerations from our experiments were limited to a small range (i.e. $<$ 10 g), which is unlikely to cause any potential harm. However, in an actual scenario, the toy robot could be subjected to higher velocities generating higher head's accelerations. Finally, the investigated severity index was limited to the head acceleration. Other severity indices (e.g. tissue injuries) could be considered to investigate different effects due to different design parameters.

5.3.4 Conclusion

In this study, the Taguchi parameter design method was used to identify the optimal design parameters for small form factor robotic toy in order to reduce the peak linear head acceleration due to impacts on the head. The investigated control factors were the mass and the shape. The impact velocity was the noise factor. Based on $L_9(3^2)$ orthogonal array, a total number of 27 experiments were conducted covering the possible combinations of the control factors and the noise factor. The optimal levels of the shape and mass that minimize the peak head linear acceleration were found based on the S/N ratio. The three-way ANOVA test revealed statistical significance for the control factors and the noise factor in influencing the head's acceleration. The optimal levels for the control factors were as 0.3 kg for the mass and cube or wedge for the shape. The confirmation runs at the optimal conditions for the control factors provided the best responses as compared to others.

5.4 Thickness and Storage Modulus of Soft Materials

5.4.1 Experimental Factors

In this study, the thickness and the storage modulus (i.e. two control factors) of three different soft materials are investigated for their potential in reducing the linear acceleration of the head. Experiments are conducted based on an $L_9(3^2)$ Taguchi OA (Table 2.4). A total of 27 (i.e. 9×3) experiments have to be conducted that consider the three levels of the control and noise factors. The considered control factors can be adjusted at the product design level while the noise factor is dependent on the real life scenario (e.g. throwing). Finally, the selected factors are independent while the measured output (i.e. head's acceleration) is dependent.

The levels of the two control factors (i.e. material thickness and storage modulus) and noise factor (i.e. impact velocity) have been defined (Table 5.7). To achieve consistency, the mass and the shape of the impactor were kept the same throughout the experiments. The mass of the impactor was kept at 0.4 kg, which is within the expected range of the targeted applications (i.e. small robotic toys). The shape of the impactor was cylindrical without any features on the surface. Finally, the impact velocities used were limited to low velocities to achieve more consistency in terms of the noise levels.

Table 5.7: *The experimental factors and their descriptions. The impact velocity levels are represented by the mean and the standard deviation.*

Type	Parameter	Code	Level 1	Level 2	Level 3
Control	Thickness	A	1 mm	3 mm	5 mm
Control	Storage modulus	B	0.2 MPa	0.3 MPa	1.7 MPa
Noise	Impact velocity (m/s)	X	Low (1.1 ± 0.04)	Medium (1.81 ± 0.07)	High (2.75 ± 0.10)
Response	Peak linear head acceleration (g)				

5.4.2 Results

Orthogonal Array

A total of 27 responses of the peak linear head acceleration were recorded and the corresponding average value, standard deviation, and S/N ratio for each combination were calculated to complete the Taguchi L_9 orthogonal array (Table 5.8). The obtained linear acceleration values were in the range from 2.42 to 10.75 g due to different levels of control and noise factors. The lowest linear acceleration value obtained corresponds to a thickness of 3 mm, Ecoflex, and Level 1 impact velocity (i.e. A2-B1-X1) while the highest linear acceleration value corresponds to a thickness of 1 mm, Ecoflex, and Level 3 impact velocity (i.e. A1-B1-X3). The average response and the S/N ratio due to varying the level of each factor were tabulated (Table 5.9 and Table 5.10). The lowest average linear head acceleration was 3.18 g with S/N ratio of -10.10 occurred at Level 1 impact velocity while the highest average linear head acceleration was 10.10 g with S/N ratio of -20.09 due to Level 3 impact velocity.

ANOVA

Three-way ANOVA test was conducted to understand if there is a significant difference due to varying the conditions on the resultant average peak linear head acceleration. In case the ANOVA test reported a significant difference, a post-hoc Tukey test was conducted.

A three-way ANOVA was conducted to compare the effect of varying the three conditions of the thickness on the response (Table 5.11). The test revealed that there was no significant difference due to varying the thickness on the resultant average linear head acceleration for the three conditions ($F(2,8) = 2.62$, $p = 0.13$) at the $p < 0.05$.

A three-way ANOVA was conducted to study the effects of the storage modulus on the head peak acceleration (Table 5.11). The test revealed that there was no significant difference due to changing the storage modulus on the resultant average linear head acceleration for the three conditions ($F(2,8) = 1.30$, $p = 0.33$) at $p < 0.05$.

A three-way ANOVA was conducted to compare the effect of the three different levels of the impact velocity on the head peak acceleration (Table 5.11). The test revealed that there was a significant difference due to varying the impact velocity on the resultant average linear head acceleration for the three conditions ($F(2,8) = 697.74$, $p = 0.00$) at the $p < 0.05$. A post-hoc Tukey test showed that velocity Level 1 (M = 3.18, SD = 0.42), velocity

Table 5.8: *The complete Taguchi orthogonal array along with columns showing the average response, standard deviation (SD), and the signal to noise ratio (S/N) for each row.*

	Inner control factors array		Outer noise factor array			Average response	Standard deviation	Signal-to-noise ratio
RUN	A	B	X1	X2	X3	Mean	SD	S/N
1	1	1	2.90	6.56	10.75	6.74	3.92	-17.45
2	1	2	3.98	6.04	10.23	6.75	3.18	-17.19
3	1	3	3.41	6.35	10.26	6.67	3.43	-17.19
4	2	1	2.42	5.65	9.99	6.02	3.80	-16.61
5	2	2	3.24	6.01	10.29	6.51	3.55	-17.06
6	2	3	3.13	6.06	10.18	6.46	3.54	-16.99
7	3	1	3.03	6.15	10.03	6.40	3.50	-16.92
8	3	2	3.38	6.14	10.53	6.68	3.60	-17.27
9	3	3	3.08	6.50	8.59	6.06	2.78	-16.21

Table 5.9: *The average response at every level of each factor.*

	A	B	X
Level	Mean (SD)	Mean (SD)	Mean (SD)
1	6.72 (0.04)	6.39 (0.36)	3.18 (0.42)
2	6.33 (0.27)	6.65 (0.12)	6.16 (0.28)
3	6.38 (0.31)	6.40 (0.31)	10.10 (0.61)

Table 5.10: *The average signal-to-noise (S/N) ratios at every level of each factor.*

	A	B	X
Level	S/N	S/N	S/N
1	-17.28	-16.99	-10.10
2	-16.89	-17.17	-15.80
3	-16.8	-16.80	-20.09

Table 5.11: *Summary of the three-way ANOVA test on the three factors.*

Source	df	Sum of squares	Mean square	F-Value	P-Value
A	2	0.82	0.41	2.62	0.13
B	2	0.40	0.20	1.30	0.33
X	2	216.63	108.31	697.74	0.00
A*B	4	0.64	0.16	1.03	0.45
A*X	4	0.62	0.16	1.00	0.46
B*X	4	1.33	0.33	2.14	0.17
Error	8	1.24	0.16		
Total	26	221.67			

Level 2 (M = 6.16, SD = 0.28), and velocity Level 3 (M = 10.10, SD = 0.61) were different significantly at $p< 0.05$.

There was no significant interaction between the thickness and the storage modulus (i.e. A and B) on the response (F(4,8) = 1.03, p = 0.45) at $p< 0.05$. There was no significant interaction between the thickness and the impact velocity (i.e. A and X) on the response (F(4,8) = 1.00, at p = 0.46) at $p< 0.05$. There was no significant interaction between the storage modulus and the impact velocity (i.e. B and X) on the response (F(4,8) = 2.14, at p = 0.17) at $p< 0.05$.

5.4.3 Discussion

The alteration of the control factors and noise factor levels have an effect on the resultant head accelerations (Table 5.8). No definite trend can be observed between the thickness (i.e. Factor A) and the resultant response by visually investigating the orthogonal array. For example, looking at the response values in the noise factor columns X1 - X3 from row 1 to 9, the registered head acceleration value appear to remain consistent. Similar observation can be made for Factor B. One the other hand, the noise factor levels seem to affect the response significantly. For example, examining columns X1, X2, and X3 reveals that the response increases proportionally with the applied impact velocity (i.e. noise factor) as supported by the relatively large standard deviations across each row.

The peak linear head acceleration has been reported to be influenced by the impact velocity of an impactor [107], [91]. The increasing average values of the response at each level of the impact velocity supports these findings (Table 5.9). Furthermore, ANOVA test results and post-hoc Tukey findings showed that the impact velocity has a significant effect on the resultant peak head acceleration. On the other hand, no similar conclusion can be made for the control factors. For example, the reported ANOVA results for the effect of the material's thickness revealed that there was no statistical significance. This could be attributed to the relatively small selected thickness range and to the small difference between each level.

Optimization

The second goal of this study is to find the optimal values that reduces the response. This is achieved by investigating the mean value of the resultant head acceleration and the corresponding mean S/N ratio for each factor (Table 5.9 and Table 5.10). The plots were generated for the mean response at each factor level and the corresponding mean S/N ratios for a better visual

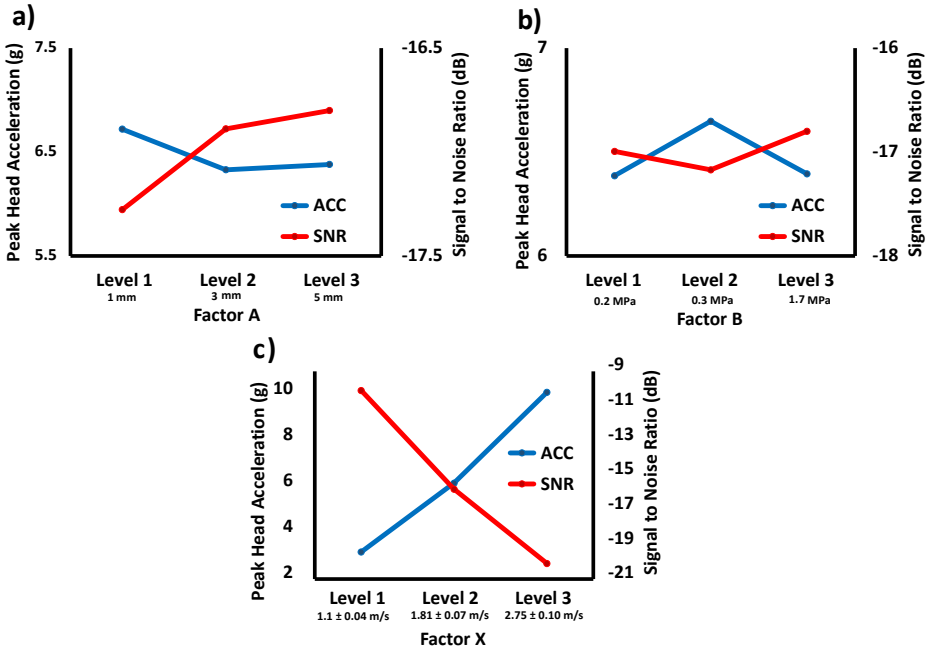

Figure 5.7: *The average response values and signal-to-noise (S/N) ratios for the factors investigated in this study. a) For Factor A, the material thickness. b) For Factor B, the storage modulus. c) For Factor X, the impact velocity.*

comparison (Fig. 5.7). The criterion for selecting the optimal conditions is based on finding the levels that produce the lowest response and highest S/N ratio.

The best conditions for the thickness and storage modulus were identified based on the lowest generated head linear acceleration and highest S/N ratio (Fig. 5.6). For the control factor of material's thickness (i.e. Factor A), 3 mm (i.e. Level 2) and 5 mm (i.e. Level 3) achieved closely the best results. As for control factor of material's storage modulus (i.e. Factor B), ecoflex (i.e. Level 1) and clay (i.e. Level 3) scored closely the best results. Even though ANOVA tests on both of the control factors reported no significance in affecting the peak head acceleration, the identified levels for each factor provided the lowest responses and highest S/N ratios as compared to other conditions. Hence, these conditions were selected as the optimal values. As for the noise factor, 1 - 1.2 m/s impact velocities (i.e Level 1) scored the best results. The optimized conditions for the control

factors investigated were 3 mm or 5 mm for the material's thickness factor and ecoflex or clay for the material's storage modulus (i.e. A2-B1, A2-B3, A3-B1, and A3-B3). Interestingly, the selected optimal control factors' levels produced relatively lower average peak head accelerations compared to other conditions at even higher noise levels (Table 5.8).

Confirmation Runs

After finding the optimal levels for each control factor, the last stage of Taguchi design is to perform the confirmation runs. The goal of this study is to minimize the peak head acceleration due to an object being thrown at the head by investigating the effect of two control factors, namely the material's thickness and its storage modulus. Hence, the optimal levels obtained in the previous section should produce relatively smaller head accelerations as compared to other conditions. Confirmation runs are needed to confirm these findings. To ensure that the optimal levels are robust and applicable to different noise scenarios, two confirmation runs will be conducted at every noise level.

A total of 24 confirmation runs were conducted at the optimal control factors' levels. For each control and noise factors combination, 2 runs were conducted and the corresponding mean values for each were calculated (Table 5.12). Comparing the results of the confirmation runs to that obtained from the main experiments, the average values were very close to respective ones obtained in the complete Taguchi orthogonal array (Table 5.8). Hence, the confirmation runs confirmed that the selected optimal levels produced the lowest peak head accelerations.

Limitations of the Study

This study considered only the application of three soft materials while there are many other candidates that could be considered. The effects of the added mass of the soft materials were ignored (e.g Less than 0.05 kg). However, this added mass might influence the results significantly, especially when larger area is covered (e.g. covering the whole object with a soft material) or larger thickness is considered (i.e. greater than 5 mm). For consistency, the shape of the object was limited to one shape while the velocity of impacts was limited to low range. However, different shapes of robotic toys exist and higher impact velocities might occur in realistic scenarios. Other severity indices could have been considered to measure different potential harm. For example, measuring the soft tissue injuries and quantify the potential of soft materials in mitigating it.

Table 5.12: *The responses, the average, and standard deviation for the confirmation runs. The conditions selected achieved relatively better responses in comparison to the other conditions in the main experiments.*

Combination	X1	X2	X3
	2.17	5.11	10.18
A2-B1	3.17	6.74	9.45
	2.68	5.60	9.69
Mean (SD)	2.67 (0.50)	5.81 (0.83)	9.78 (0.37)
	2.12	5.04	9.18
A2-B3	3.43	6.59	10.60
	3.37	5.06	10.25
Mean (SD)	2.97 (0.74)	5.56 (0.89)	10.01 (0.74)
	3.06	6.27	10.25
A3-B1	2.27	6.13	9.71
	2.87	6.27	9.82
Mean (SD)	2.74 (0.41)	6.22 (0.08)	9.93 (0.28)
	3.34	7.08	8.54
A3-B3	2.99	6.38	8.76
	3.32	6.4	8.60
Mean (SD)	3.22 (0.20)	6.62 (0.40)	8.63 (0.11)

5.4.4 Conclusion

In this study, the influence of an added soft material to an object on the linear acceleration of the head upon impact has been investigated. The Taguchi $L_9(3^2)$ orthogonal array design has been used to plan the 27 main experiments that were conducted. The control factors were the thickness and the storage modulus of three different soft materials. The noise factor was the impact velocity. The significance of each factor has been identified based on three-way ANOVA test while the optimal levels for the control factors were identified based on the analysis of S/N ratio. ANOVA test showed that the control factors were not statistically significant in influencing the linear acceleration of the head. On the other hand, ANOVA test of the noise factor revealed that it was statistically significant. Material thickness of 3 mm and 5 mm achieved the best results. This implies that the application of a higher thickness of soft material will attenuate the head's acceleration better. Ecoflex and clay have achieved better response as compared to dragon skin. Confirmation runs at the optimal identified conditions achieved better responses as compared to other conditions.

5.5 Chapter Summary

This chapter presented the investigation of different design parameters (i.e. control factors) of small robotic toys in their influence on one severity index of the head (i.e. linear acceleration of the head). This chapter presented two studies designed based on Taguchi method that was then used to design the experiments and to optimize the design factors. The first study in this chapter investigated the effects of the mass and shape of small objects on the selected severity index while the second study investigated the influence of the thickness and storage modulus of three different soft materials on the same severity index. The results showed that some of the control factors are significant in affecting the response. The confirmation runs revealed that the identified optimal conditions for the control factors achieved relatively better results.

CHAPTER 6

Adaptive Robot Intelligence during Unwanted Interactions

This chapter presents two studies aimed at making a robot adaptive toward unwanted interactions. The first study explores the possibility of embedding the knowledge of unwanted physical interactions into a small robotic toy. It highlights the feasibility of recognizing six different possible interactions between a child and a small robotic toy based on an embedded tri-axial accelerometer. The second study investigates the influence of reaction time in the emotional response of a robot on the interactions between a child and a robot.

6.1 Introduction

The recent advances in robotics accelerated the integration of robots to new areas, such as in healthcare. More specifically, social robots or rehabilitation robots are being developed to monitor and improve health, to assist with difficult tasks, and to prevent the declining of one's health [163]. Assisting in therapy is an application of robots in healthcare that has shown a promising potential. For example, social robots were found to be effective

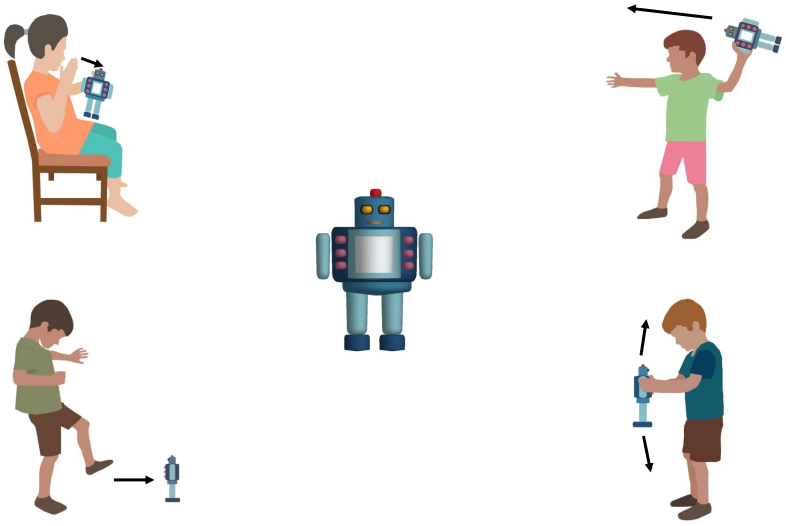

Figure 6.1: *Some of the unwanted and aggressive interactions that might be exhibited by children toward a companion robotic toy [5].*

in improving the outcomes of therapy sessions, especially among children with autism [47], [178].

Aggression is a behavior that is done by a living agent, such as a human or an animal, that causes harm and violates the rights of others [59]. The American Psychological Association (APA) defines aggression as a behavior that is aimed at hurting others either physically or psychologically [15]. APA categorizes aggression as hostile aggression, which is intended to cause harm; instrumental aggression, which is not intended to cause harm; and affective aggression, which is emotionally motivated toward the source of distress. The frequency of physical aggression among children was reported to peak during the years before school [144]. Kicking, biting, and hitting are examples of the physical aggressive behaviors that might occur during the early years of childhood [14]. Aggression among children is considered as one of the most common reasons for the mental health referrals [181]. The occurrence of aggression or disruptive behavior was reported to be higher among children with psychiatric disorders. For example, the prevalence rates of such behaviors was reported to reach 62.3% among children with anxiety disorders, while it could reach 45.8% among those with mood disorders [145].

Social robots represent new stimuli that are meant to elicit behaviors and initiate interactions, and that might trigger unwanted ones. Previous studies showed that children might exhibit some aggression toward the

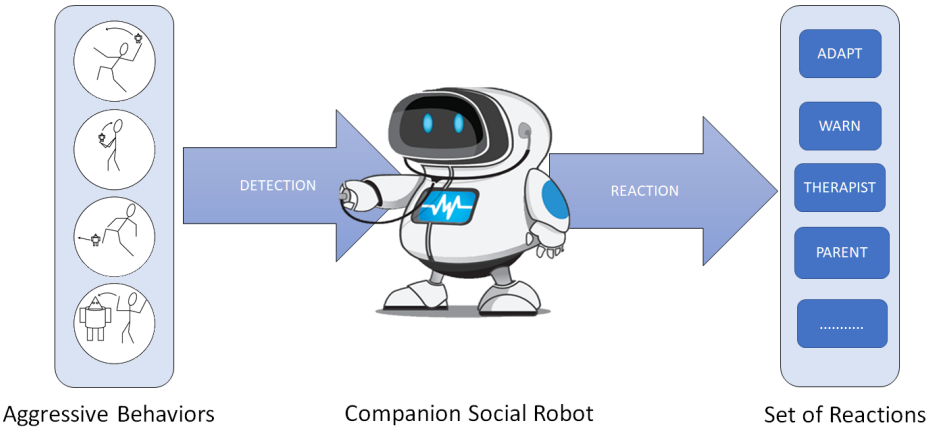

Figure 6.2: *Overview of the proposed model to detect unwanted physical interactions between a child and a small social robot.*

robots [13], [32], [45]. In case of small robots, children might carry the robot and mishandle it (Fig. 6.1). To date, the studies to characterize the unwanted and aggressive interactions are limited [169], [32], [126]. Additionally, limited work has been done to investigate the proper reactions once such behaviors are detected. The ability of a robot to detect and respond to unwanted interactions will provide many benefits, such as the prevention of potential harm, monitoring, promoting safety culture, and as a therapeutic and teaching tool. Furthermore, it can be used by the robot to help the child to stop the unwanted behavior and to prevent any progression [45]. For example, a child shaking or hitting a robot could be a precursor for a meltdown episode.

In this chapter, two studies aimed at adding adaptive capabilities to a small robotic toy are presented. The first study investigates the potential of using an artificial neural network to develop a model that is capable of classifying the unwanted physical interactions between a child and a small robotic toy (Fig. 6.2). This study considers six different interaction behaviors, namely, hitting, shaking, dropping, throwing, picking up, and being idle (i.e. no active interaction). The second study investigates the effects of reaction time and sound modality employed in robotic toys on the perceived perception by children interacting with the robots. A recognition architecture based on Long Short-term Memory Cell (LSTM) was adopted to classify the behaviors based on the acceleration data received. Different reactions with different timings were produced once a pickup, a shake, a drop or a throw was detected.

6.2 Recognition of Aggressive Interactions

6.2.1 Overview

For social robots that interact with children with ASD, there have been some studies conducted to characterize the interactions [74], [32]. An earlier study used a ball-like mobile robot (i.e. Roball [169]) embedded with sensors to detect the direct interaction instances with the robot. The study considered four interaction cases with the robot, namely robot being alone, robot receiving an interaction, robot being carried, and robot being spun. The study demonstrated the possibility of using the sensor data to make the robot more adaptable. Another study considered different interactions with a smaller ball-like robot (i.e. Sphero), such as holding, kicking, and picking up [126]. Adult participants were asked to perform the behaviors. A set of features were extracted from the data of the embedded tri-axis accelerometer and gyroscope and then tested with different supervised learning algorithms. The best classifier (i.e. random forest algorithm) trained on data obtained from the adult participants achieved an accuracy of around 49% when evaluated with data generated from children participants.

This study explores the possibility of embedding the knowledge of unwanted physical interactions into a small robotic toy based on an embedded tri-axial accelerometer. The study aims to recognize six different possible interactions between a child and a small robotic toy, namely, hitting, shaking, dropping, throwing, picking up, and being idle (i.e. no active interaction).

6.2.2 Materials and Methods

Experimental Setup

Robot System Design The progress in technology is enabling smaller robots to be more intelligent and more compact. Furthermore, smaller social robots are considered to be more affordable and suitable to be used by average home users. Hence, the toys considered in this study were selected accordingly. Three different forms of toys were used, namely a stuffed robot (LATTJO soft toy, IKEA, Netherlands), a stuffed panda (KRAMIG Soft toy, IKEA, Netherlands), and a toy excavator (Fig. 6.3). The dimensions of the toys (i.e. less than (38.0 x 29.0 x 9.0 cm^3)) and their masses (i.e. less than 0.75 kg) were of the range that enable ease of interactions (e.g. carrying) for children. The differences in sizes, in shapes, and in materials of the selected toys should cover any variations among different small robotic toys. Additionally, the selected toys varied in terms of their softness. For

Figure 6.3: *The toys that have been considered as dummy robotic forms. From left to right, a stuffed panda, a soft toy robot, and a toy excavator.*

example, the stuffed robot is considered the softest while the excavator toy is considered the least soft. Both of the stuffed toys (i.e. the robot and the panda) were modified with zippered pockets to allow the insertion of the data acquisition system.

Data Collection System The recognition device used was a small computing device (Raspberry Pi 3 Model B+, Raspberry Pi Foundation, UK). This device is powered by a 1.4 GHz quad-core processor and supports wireless, Bluetooth, and Ethernet communication. The availability of such communication channels make it easier to access, to program, and to configure with other devices. Furthermore, it contains many peripherals that make it possible to augment it with other devices. The official operating system (Raspbian v4.19, Debian Project) was installed on a micro SD card (16 GB, Edge, Sanddisk). The selected storage should provide more than enough space for the operating system, trained recognition mode, collected data, and for any needed packages. A remote access software (TeamViewer Host for Raspberry Pi, US) was installed to allow ease of access to the device and more flexibility for debugging and testing. The kernel, the firmware, and the packages were all upgraded to their latest versions.

The standard Raspberry Pi does not contain any on board sensors, how-

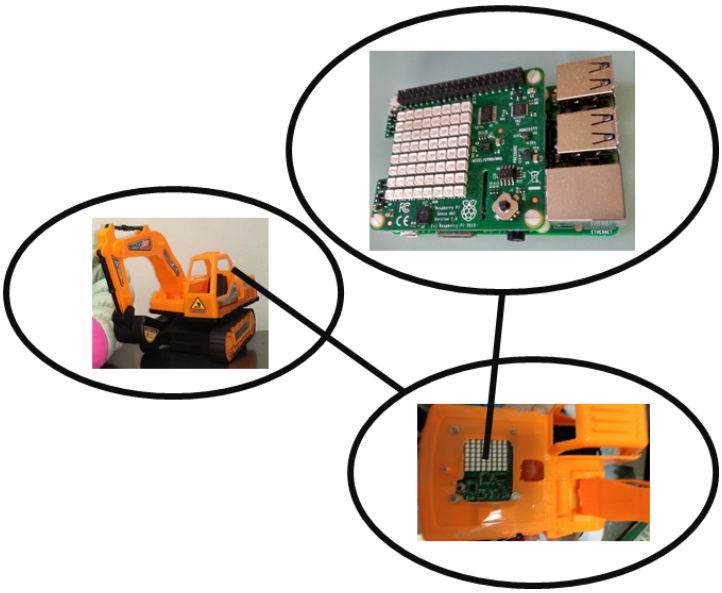

Figure 6.4: *The data collection system that was based on a SenseHat board mounted on a Raspberry Pi board.*

ever, the 40-pin can support different boards with different functionalities. A Sense Hat board (Raspberry Pi Foundation, UK), which contains different sensors and a display, was mounted on the Raspberry pi. The built-in accelerometer (LSM9DS1, STMicroelectronics, Switzerland) was used in the recognition model to acquire the raw acceleration data at a rate of around 30 Hz and up to 16 g. This rate and magnitude were shown to be adequate enough for the recognition of human activities [36], [117]. The entire device was placed in a dedicated enclosure with a small fan mounted on the side for cooling (Fig. 6.4). For the experiments, the devices were embedded inside the toys and each was powered with a dedicated power bank (Slim 2, 5000 mAh, POWERADD).

Procedures

Acquiring sufficient data from adults is relatively easier than from children [126], [157]. Hence, the development of the model was based on the data acquired from adult participants. The participants who took part in this study were asked to perform five different behaviors with each robot. The participants were given the freedom in performing the required behaviors and to take breaks between experiments. No instructions were given to the participants, especially about how a particular behavior should be per-

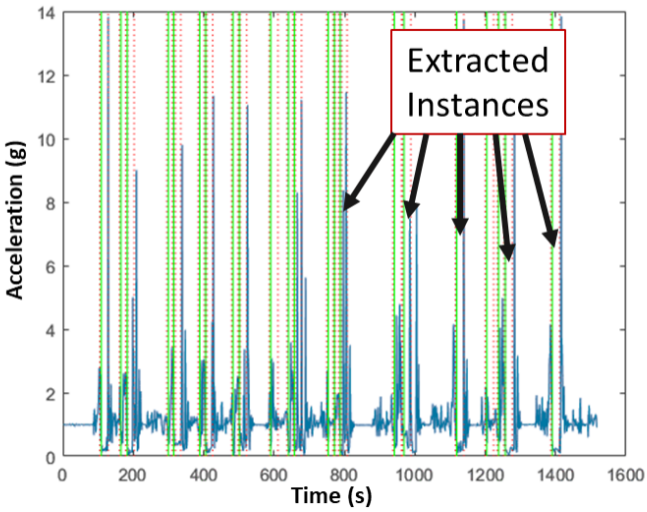

Figure 6.5: *A sample of the extracted features for the acceleration signal.*

formed (e.g. the way to hit or shake the robot). The only instructions were given to let the participants know the start and the end of each experiment. A MATLAB script (v2018, MathWorks, Massachusetts, USA) was used to analyze the data and then extract the instances of each behavior based on the thresholds (Fig. 6.5). This data was then used in the training, testing, and development of the neural network model.

The data to validate the model was acquired from neurotypical children. Imaginative scenarios were told to the children to make them perform the behaviors of interest. For example, to acquire pickup and shake behaviors, they were told that "*The robot is asleep and you need to pick it up and then shake it to wake it up*" (Fig. 6.6). The interaction durations were around 5 mins each. We believe that the characteristics of behaviors (e.g. hitting) considered in this study are similar and comparable between neurotypical children and those with autism. Hence, this data will be used as an indicator for the applicability of the developed model to the targeted end-users.

Participants

Five healthy adults (one female and four males) aged 24 to 31 years old participated in this study. Their data was used to train and test the model. Additionally, the study acquired data from four neurotypical children (one female and three males) aged 4 to 9 years old. The children's data were used to validate the developed model. The procedures for this work did not

Figure 6.6: *Samples from the sessions with the children.*

include invasive or potentially hazardous methods and were in accordance with the Code of Ethics of the World Medical Association (Declaration of Helsinki).

Algorithm

The development of the classification algorithm was based on Scikit-learn, a Python-based machine learning library [153]. This library includes many supervised and unsupervised learning algorithms along with other evaluation tools. Furthermore, it uses high-level language that makes the implementation convenient and flexible. The classification algorithm in this study was based on a supervised learning algorithm, the Multi-layer Perceptron (MLP). To investigate the potential of the adopted methods in producing promising results, the testing of the classification algorithms was limited to MLP. Future work might consider other algorithms.

MLP is one of the most widely used form of neural networks. The simplest configuration of this network consists of an *input* and an *output layer* while a more complex configuration consists of a *hidden layer* or several *hidden layers* between the *input* and the *output* layers. Connections between layers follow a consecutive order starting from the *input layer* and

terminating at the *output layer*. All connections have assigned values called *weights* that are learned during the training of the network. Each *neuron* has an *activation function* (e.g. sigmoid) that generates an output based on the product of the inputs of the preceding layer and the weights of their connections. More detailed mathematical description of MLP can be found in [123].

The neurons of the *input layer* of the classification algorithm take the resultant acceleration values as an input vector. In human recognition applications, there is a trade off between recognition performance, recognition speed, and computational complexity [39]. A robot's reaction to unwanted interactions should be quick and comparable to that of a human. Hence, a smaller window size (i.e. 25 samples) was selected, which is enough to capture most of the behavioral characteristics (Fig. 6.7). This size should provide a fast recognition speed while maintaining a sufficient accuracy [28]. Furthermore, minimizing the window size should reduce the overall delay in the recognition system.

The magnitude of the resultant acceleration was based on the square root of the sum of the squares of the individual accelerations. The relation is represented as follows:

$$|A| = \sqrt{A_x^2 + A_y^2 + A_z^2} \tag{6.1}$$

where A_x is the magnitude of acceleration in the *X* direction, A_y is the magnitude of acceleration in the *Y* direction, and A_z is the magnitude of acceleration in the *Z* direction. The classification algorithm trains to map the resultant acceleration values into labeled outputs corresponding to different behaviors.

The goal is to detect the behaviors of interest regardless of the orientation changes of the toy and the placement of the accelerometer within. Hence, the magnitude of the acceleration has been considered because it is insensitive to such changes [182]. Future work might consider the direction of the accelerations to add more insights about the orientation of the toy in relation to the behavior being exhibited.

Evaluation Metrics

Several metrics were used to evaluate the developed model, such as the accuracy, classification report, and confusion matrix. Accuracy reported the percentage of correct predictions in relation to the overall predictions performed by the model as in (6.2). Classification report provided the precision, recall, and F1- Score, and support for the model. Precision provided

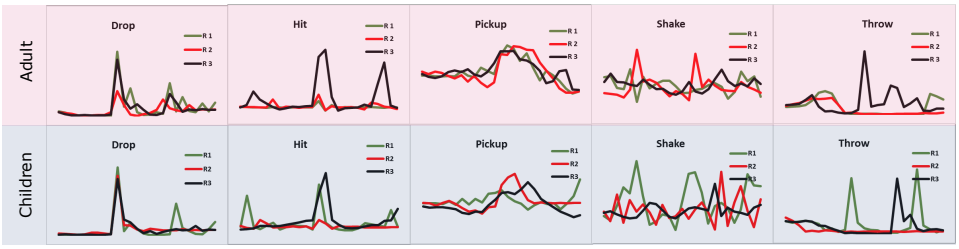

Figure 6.7: *Samples of the extracted behaviors from the accelerometer signals for adults and children. The different colors represent different robots where R 1 (i.e in green) stands for the excavator toy, R 2 (i.e. in red) for the panda toy, and R 3 (i.e. in black) for the soft robot toy.*

the percentage of true positives in relation to the total predicted positive as in (6.3). Recall indicated the number of true positives in relation to the total number of actual positive as in (6.4). F1 - score provided the harmonic mean of precision and recall as in (6.5). The confusion matrix provided a breakdown for all the predictions (i.e. correct and incorrect) by each class.

$$Accuracy = \frac{Correct\ Predictions}{Total\ Predictions} \tag{6.2}$$

$$Precision = \frac{True\ Positive}{True\ Positive + False\ Positive} \tag{6.3}$$

$$Recall = \frac{True\ Positive}{True\ Positive + False\ Negative} \tag{6.4}$$

$$F1 = 2 \times \frac{Precision * Recall}{Precision + Recall} \tag{6.5}$$

6.2.3 Results and Discussion

All participants have performed the requested behaviors differently. For example, different intensities were demonstrated when shaking or hitting the robots. The data of the behaviors were post-processed and the features were extracted (Fig. 6.7). The selected window size was sufficient enough to

capture the most important features of each behavior. The features of some of the behaviors performed by the participants with the robots appeared to have some similarities in their characteristics. For example, drop behavior was characterized by low acceleration values followed by a large spike and then oscillations. A hit behavior was characterized by a large spike of a short duration. Pickup has some resemblance to hit, but the spikes were longer in duration and smaller in amplitude. Shake behavior was characterized by continuous oscillations at different amplitudes and frequencies. Throw was characterized by a wave of low amplitude (i.e. start of throwing) followed by decline in acceleration and then ending with a large spike (i.e. upon impact).

Model Development

The extracted instances of behaviors were labeled and organized as a dataset to be used in the model training. A total of 1,000 instances for each behavior covering all robots and participants were extracted. For the idle case, 1,000 instances were added, hence, making the total instances to be 6,000. Augmentation (i.e roll by a factor of 25) on the data was performed that should provide more robustness to the model in terms of predicting new data. Additionally, it should help in avoiding the learning of any specific pattern in the data. A standard scaler was used to standardize the features by scaling (i.e. to unit variance) and removing the mean. The data was randomly split into 70% for training and 30% for validation. Different network configurations were tested and evaluated. The configurations for the best trained model (i.e. accuracy of 92%) were hidden layer settings of (300,150), Rectifier Linear unit (i.e. *ReLu*) as the activation function, *alpha = 0.0001* for the regularization penalty term, and Limited-memory Broyden Fletcher Goldfarb Shanno method (i.e. *lbfgs*) as the weight optimization solver. The performance of the model improved proportionally with the number of iterations (Fig. 6.8a). The losses of the training and validation were decreasing over iterations and converging closely (Fig. 6.8b). This indicated a comparable performance and a good fit for the model. Finally, the entire dataset was then used to train the finalized model.

An accuracy of 88% was achieved when testing the finalized model with unseen adult data. The confusion matrix and classification report for the model were generated for further analysis (Fig. 6.9 and Table 6.1). Excluding the idle case, the confusion matrix reported the highest for the throw case while the lowest recognition for pickup and hit behaviors. The model has identified incorrectly some pickup instances mainly as hit or as shake instances. Similar observation for the incorrect identification of some in-

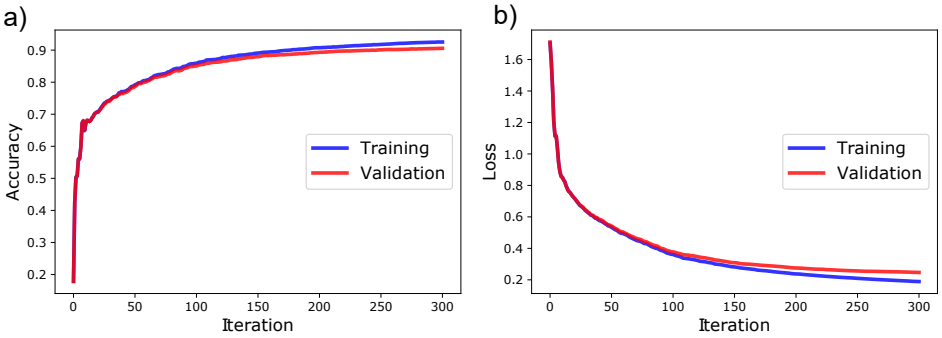

Figure 6.8: *The training and validation over iterations plots for the developed model a) Accuracy plot. b) Loss plot.*

Figure 6.9: *The confusion matrix for the unseen adult's dataset.*

Table 6.1: *The classification report for the evaluated unseen adult's dataset*

Behavior	Precision	Recall	F1 - score	Support
Drop	0.91	0.90	0.90	265
Hit	0.84	0.84	0.84	797
Idle	1.00	1.00	1.00	131
Pickup	0.80	0.84	0.82	747
Shake	0.91	0.86	0.88	776
Throw	0.94	0.94	0.94	614
Avg/ Total	0.88	0.88	0.88	3330

stances can be made for shake and hit behaviors. Throw behavior instances were mainly identified incorrectly as drop behavior. These incorrect identification could be attributed to some similarities in the features of these behaviors. Regardless, the overall evaluation metrics of the model were promising. For example, the model has achieved an average precision of 88%, a recall of 88%, and an F1- score of 88%. Precision shows the ability of the model not to identify an incorrect instance as correct, while recall shows the ability of the model to find all correct instances. Finally, the F1 score takes the average of recall and precision into consideration.

Model Evaluation with Children's Data

The main objective of this study is to develop a model that can characterize the interactions between a child and a small companion robot. Hence, evaluating the developed model with children's data is necessary to investigate the model's feasibility and applicability to children. There are some similarities between the acceleration characteristics of behaviors that were exhibited by the children and the adult participants, for example, in case of hit, drop, and shake behaviors (Fig. 6.7). Visual differences in performing some of the behaviors were evident in pickup and throw.

The developed model has achieved an overall accuracy of 80% when evaluated with the children's dataset. The confusion matrix showed that the model was able to identify drop and shake behaviors with the best results (i.e. accuracy $>$ 90%) followed by hit and throw behaviors (i.e. 67%)

Figure 6.10: *The confusion matrix for the evaluated children's dataset.*

(Fig. 6.10). Pickup instances were the lowest to be identified correctly with an accuracy of 52%. One quarter of pickup instances were identified as shake behavior. The majority for the incorrectly classified throw behaviors were identified as either drop or shake. As for hit, they were incorrectly identified as pickup or shake. These misclassifications could be attributed to the differences in the behaviors' intensities as exhibited by different age groups that confuses the classifier. For example, a child's pickup behavior is more gentle and slower as compared to that of an adult, hence, it was identified as a shake behavior. The overall precision, recall, and F1 - score of the model were all promising (i.e. 80%; Table 6.2).

The results showed the possibility of using adult-based generated data to develop a model that can classify some of the children's unwanted interactions with a small robotic toy. Furthermore, it showed the capabilities of using multi-layer perceptron (MLP) in such applications as compared to other algorithms (e.g. support vector machines and random forests).

The detection capabilities of the proposed model is limited to during the exhibition of an unwanted behavior or after. The advantage of this approach is that it helps in teaching the children the causation between their interactions and the robot's responses. This work was limited to the detection of negative or unwanted interactions. However, future work might consider the positive or desirable interactions. This work did not account for the vibrations that are usually produced by a social companion robot due to its functionalities. However, the idle class can be updated to account for such vibrations to make a proper distinction. Alternatively, a rule that checks

Table 6.2: *The classification report for the evaluated children's dataset*

Behavior	Precision	Recall	F1 - score	Support
Drop	0.72	0.98	0.83	49
Hit	0.81	0.67	0.73	195
Pickup	0.44	0.52	0.48	56
Shake	0.87	0.91	0.89	377
Throw	0.78	0.67	0.72	70
Avg/ Total	0.80	0.80	0.80	747

the magnitudes of the acceleration could be implemented to discriminate between a shake and the natural vibrations of the robot.

6.2.4 Conclusion

In this study, a Multi-layer Perceptron (MLP) based neural network was developed and validated for its potential in classifying behaviors between a child and a small robot. The physical interactions considered were hit, shake, throw, drop, and pickup. These behaviors could potentially be used to identify any unwanted interaction between a child and a robot, which could then act to prevent the occurrence of aggressive behaviors that might lead to harm. The data to develop the model was based on adult participants performing the behaviors while the data used to validate the developed the model was based on the children's interactions. The developed model was able to achieve a high recognition accuracy (i.e. $> 80\%$) when tested with children's data. Furthermore, the classification report and the confusion matrix showed promising results (Fig. 6.10 and Table 6.2).

6.3 Influence of Reaction Time

6.3.1 Overview

Species in nature offer a lot of biologically-inspired concepts and ideas to roboticists. One of these mechanisms is the reflex system that can be adopted in the design and developments of robots [2]. Reflexes are meant to ensure the survival of the living organism externally while ensuring the

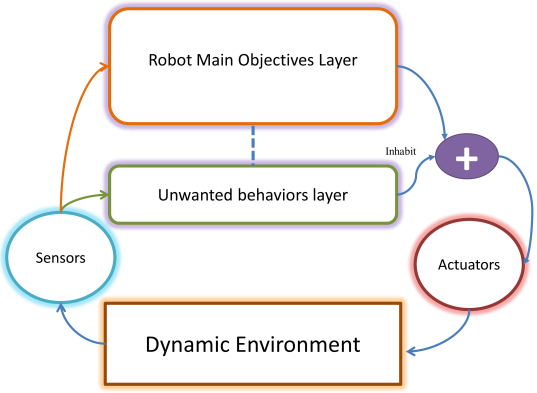

Figure 6.11: *The proposed reflex model to respond to unwanted interactions. A layer to detect the unwanted interactions will temporarily inhibit the system to produce a proper response.*

balance of operations internally. Reaction to a stimulus is usually carried out by the reflex arc that consists of several stages, namely, arrival of stimulus, activation of sensory neuron, information process, motor neuron activation, and peripheral effector response. The implementation of reflexes in a robotic system should operate without affecting the main objectives of the robot (Fig. 6.11). Once an unwanted interaction is detected, the robot may respond with the appropriate reaction to deliver the corresponding message to the user [45]. The timing of the reaction and its modality should be felt as natural to provide a clear implication about the interaction. Few robots were developed that demonstrate some reactions to a human interactions. PARO is one of the commercially available robots that reacts to physical interactions [176]. PARO is a seal-looking interactive therapeutic toy that is covered with white fur and emits voices similar to that of a baby seal. Different embedded sensors enable PARO to interact with its environment. The light sensor enables it to recognize dark and light. The audio sensor gives PARO the ability to recognize the direction of voice. The tactile sensor gives PARO the ability to feel any stroke or pressure. PARO interacts with people by making sounds and moving some parts of its structure, such as the head, paddle and eyelid.

Roball is another robot that was developed to react to certain physical interactions [169]. The robot is shaped like a ball with a diameter of 0.27 m and weighs around 2 kgs. It is equipped with accelerometers and tilt sensors that allows it to interact and navigate in its environment. Based on the sensors readings, several interaction modes are possible, such as being

alone, general interaction, being carried, and being spun.

Teo is a mobile, soft robot, which was developed to interact with children with ASD [35]. It can sense distance and touch, and can distinguish different dynamic interactions, like hug, push, punch, getting close, among others. Based on the interpretation of sensors, the robot can react with sounds, words, movements, and coloured lights.

This study investigates the influence of reaction time in the emotional response of a robot on the interactions between a child and a robot. The study considers three different interactions, namely, pickup, shake, and drop or throw; and considers three reaction times, namely, 0.5 s, 1.0 s, and 1.5 s.

6.3.2 Materials and Methods

The Model

Recognition Architecture The recognition network that was adopted in our work was proposed by an earlier study that relied on Long Short-term Memory network (LSTM) in combination with bidirectional and residual connections [201]. In their proposed model, the network was able to produce improved results (i.e. 93.5%) on the public domain (i.e. UCI Machine Learning Repository) dataset on human activity recognition as compared to other configurations [18]. The recognition problem in this study would benefit from this network due to the similarity in the characteristics of the activities that needs to be recognized. In this section, a brief description about this recognition network is provided.

LSTM network is a special structure based on a Recurrent Neural Network (RNN) that is used to process a data stream. In RNN, the prediction depends on the history information that is maintained within the internal memory of the network. A typical RNN consists of three layers, namely, an input layer x, a hidden layer h, and an output layer y. The relations among these layers are defined as follows:

$$h(t) = f(Ux(t) + Wh(t-1)) \tag{6.6}$$

$$y(t) = g(Vh(h)) \tag{6.7}$$

where U is the connection weights matrix from the input layer to the hidden layer, W is the connection weights matrix within the hidden layers, and V is the connection weights matrix between the last hidden layer and the output. Furthermore, f and g represent the activation functions.

Compared to standard RNN structure, LSTM showed stability and powerful performance in the modeling of long sequences (e.g. [184]). The

structure of LSTM is unique due to a memory cell c_t that accumulates the state information [194]. Furthermore, this structure allows one to deal with the vanishing gradients problem [101]. The LSTM cell contains three controlling gates, namely, input gate, forget gate, and output gate (Fig. 6.12). These gates control what information that should be kept, updated, or forgotten. More complex structures can be formed by combining multiple LSTM cells. The internal parameters of an LSTM cell are defined as follows [84]:

$$i_t = \sigma\left(W_{xi}x_t + W_{hi}h_{t-1} + W_{ci}c_{t-1} + b_i\right) \tag{6.8}$$

$$f_t = \sigma\left(W_{xf}x_t + W_{hf}h_{t-1} + W_{cf}c_{t-1} + b_f\right) \tag{6.9}$$

$$c_t = f_t c_{t-1} + i_t tanh\left(W_{xc}x_t + W_{hc}h_{t-1} + b_c\right) \tag{6.10}$$

$$o_t = \sigma\left(W_{xo}x_t + W_{ho}h_{t-1} + W_{co}c_t + b_o\right) \tag{6.11}$$

$$h_t = o_t\ tanh\left(c_t\right) \tag{6.12}$$

where *i* is the input gate, *f* is the forget gate, *o* is the output gate, σ is the logistic sigmoid function, and *c* is the cell activation vectors.

The recognition network also made use of bidirectional LSTM due to its advantages over standard LSTM. For example, the output of bidirectional LSTM is related to previous and subsequent information, hence, a better overall performance. The output of the proposed algorithm is determined by concatenating the results of the forward and backward sequences through a hidden layer that reduces the number of features [201]. Finally, the algorithm uses a residual network that provide different advantages, such as efficient training and easier optimization.

Data Format The data that were used in training and testing the recognition model were acquired from an earlier study [4]. The data for the acceleration were in the form of the resultant acceleration computed as the square root of the sum of the squares of the individual accelerations. The relation is defined as in (B.2).

The training data were acquired from adult participants performing the behaviors of interest while the test data were acquired from children participants. To create a temporal data stream from these discrete data samples, artificial sequences were created from the data samples randomly (Fig. 6.13). The sequences were selected based on the likelihood of their occurrence in realistic interaction scenarios. This approach will support the creation of more variability in data and decrease subject-dependent learning. For example, a sequence could contain samples from any of the participants and from any of the robotic toys used. This procedure was applied to both the training and testing data.

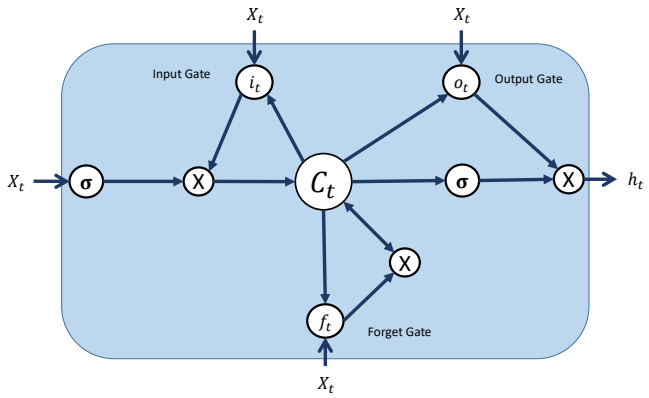

Figure 6.12: *A graphical representation of the Long Short-term Memory (LSTM) cell. The LSTM cell consists of three gates, namely, the input gate i, the output gate o, and the forget gate f. These gates control the information within the cell.*

Model Evaluation Several models were trained and the best one was considered. The configuration of the selected model included a *bias mean* of 0.3, *weights SD* of 0.3, and 28 hidden neurons per layer. The configuration of the architecture was 2×2, where there are 2 hidden layers that contains 2 bidirectional layers each. More details about the architecture can be found in [201]. The model achieved promising results that considered precision, recall, and f1-score metrics (Table 6.3). The confusion matrix revealed that the model might confuse some of the behaviors (Fig. 6.14). For example, it might confuse *hit* as *pickup*. For the purpose of this study, the focus is on detecting *pickup*, *shake*, and *throw* or *drop*. Once these behaviors are detected, the robot will produce the corresponding responses. All other interactions will be ignored and will not produce any response once they are detected.

Experimental Setup

Three different toys embedded with recognition devices were considered. The toys were a stuffed panda (KRAMIG Soft toy, IKEA, Sweden), a stuffed toy robot (LATTJO soft toy, IKEA, Sweden), and an excavator toy (Fig. 6.3). The mass and dimensions of the selected toys were in the range that allowed the ease of carrying and manipulation for the targeted users. The toys were equipped with the recognition device that was based on Raspberry Pi. The same toys and the device were previously used in the earlier study to collect the data that was then used to train the recognition model [4].

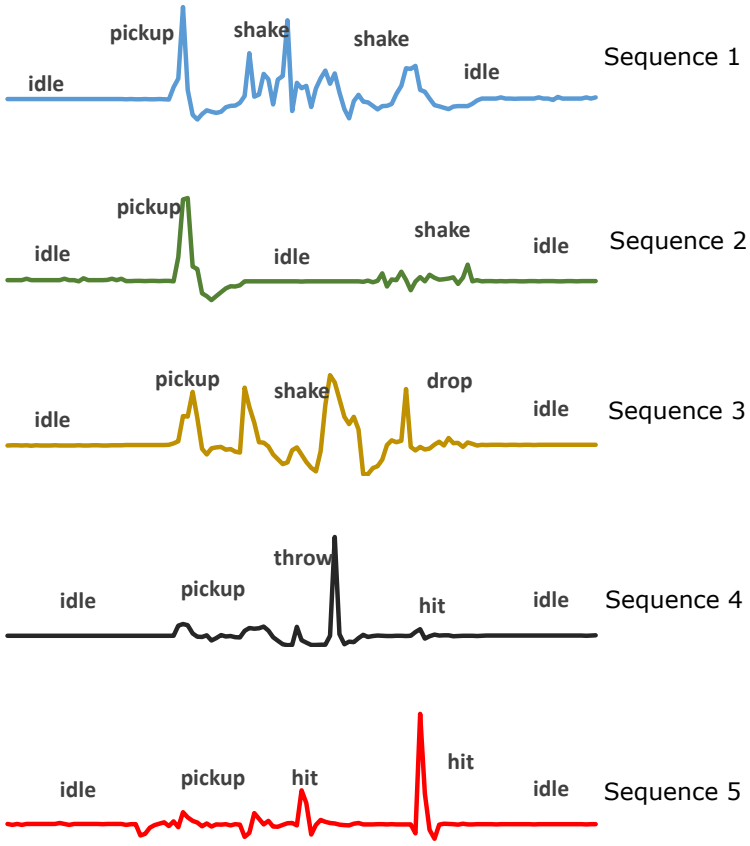

Figure 6.13: *Five samples of the artificially created sequences from the data samples obtained from an earlier study [4]. The sequences were selected based on their likelihood of occurring in realistic scenarios. The behaviors in the sequences were obtained randomly from the available pool of samples from each participant.*

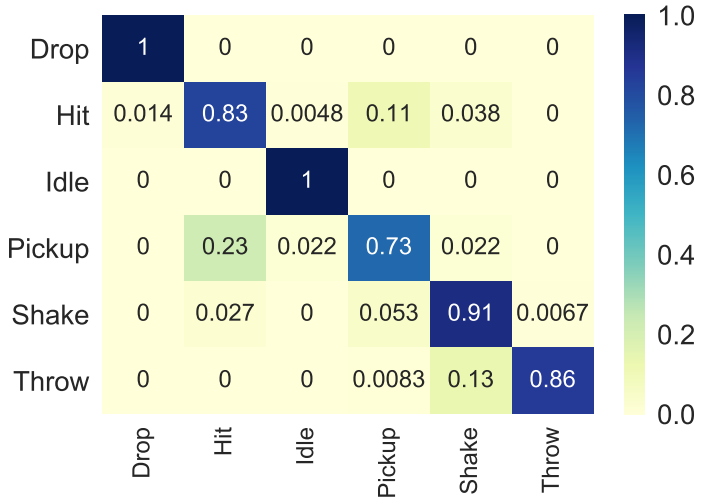

Figure 6.14: *The confusion matrix for the recognition algorithm when tested with the children data. The recognition performance of the model is higher than 90% for drop, idle, and shake. The recognition performance is less than 90% for hit, pickup, and throw.*

Table 6.3: *The classification report for the recognition algorithm when tested with the children's data.*

	precision	recall	f1-score	support
drop	0.98	1.00	0.99	120
hit	0.72	0.83	0.77	210
idle	0.98	1.00	0.99	390
pickup	0.86	0.73	0.79	270
shake	0.82	0.91	0.86	150
throw	0.99	0.86	0.92	120
avg / total	0.89	0.89	0.89	1260

Robot Reactions

The robotic toys showed reactions when manipulated by the user. For example, a robot would display discomfort when shaken. The reactions were implemented as different short sounds. The samples were obtained from *https://freesound.org* and were modified for the experiments. The sound samples were cut and shortened to less than one second and were saved as *wav* files. For the behaviors considered in the experiments, 6 different sound samples for each behavior were selected, to provide variety. For example, when a *pickup* is detected, one sound sample is randomly selected from the pool of the available samples for *pickup* and then played (See supplementary material). A Bluetooth speaker (AQL Sparkle, Cellularline, Italy) was used to produce the sound samples for the behaviors, activated by the system embedded in the robot. The actions triggering reactions were limited to *pickup*, *shake*, and *drop* or *throw*.

To investigate the effects of response time on the interactions, three different timings were considered to generate a reaction, namely, 0.5 s, 1 s, and 1.5 s. A scheduled task that periodically checks the detected behaviors was used to control the tested reaction times. This task generates a reaction based on the detected manipulation with a delay equal to the selected time. However, a condition has been implemented that prevents the generation of two consecutive responses in less than one second. This was designed to make the toy more natural in terms of response rate and more pleasant to interact with.

Participants

The experiments conducted in this study were focused on the evaluation of the appropriateness of the reactions implemented in the robots, in particular on the reaction timing. Subjects (9 females and 21 males) volunteering in the experiments were students aged 8 to 13 years old (10.26 ± 1.48 years old). The consent from the parents was secured by their school and the children were accompanied by their teachers to the experiment site. The children were introduced in the experimental room one at a time. In the room, one researcher and one assistant were present. The procedures for these experiment did not include any invasive or potentially hazardous methods and were in accordance with the Code of Ethics of the World Medical Association (Declaration of Helsinki).

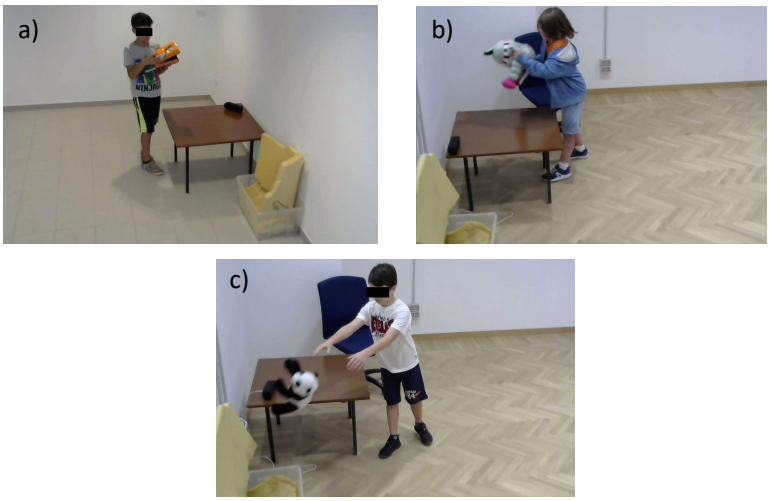

Figure 6.15: *Samples of the conducted experiments. a) A child exploring the toy. b) A child shaking the toy. c) A child throwing the toy.*

Reaction Evaluation

Robotic toys or social companion robots should provide a timely feedback, a reaction, to the user performing an interactive act. A late and less frequent response might render the interaction slow and uninteresting while a very fast and more frequent response might be felt as eerie and unnatural. The frequency and the speed of response should be natural and comfortable to the user. To evaluate the effects of these, a set of experiments were performed with a group of children individually. The three robotic toys were configured with reactions at different timing, namely, 0.5 s, 1 s, and 1.5 s. The participants were divided into three groups accordingly. A robotic toy was placed on a small table and a child was encouraged to interact with it. The evaluated behaviors were limited to pickup, shaking, and throwing or dropping (Fig. 6.15). All tasks were requested in the form of an imaginative scenario that the the children need to perform with the robotic toys (Table 6.4). After each session, a simple questionnaire containing five simple questions was given to the child (Table 6.5). The questions were related to the interactions and the possible answers were in Likert scale showing five different levels of agreement (from total agreement to total disagreement). All sessions were recorded with a webcam (C310 HD, Logitech, Switzerland) and then annotated with an open-source software (BORIS,

Table 6.4: *The experimental protocol for the experiments conducted in this study*

Number	Reaction evaluation
Task 1	Pick up the robot up and explore it
Task 2	The robot is sleeping and in order to wake it up you need to shake it
Task 3	The robot would like to be to a specific place, toss it there

Table 6.5: *The questions stated in the questionnaire*

Number	Questionnaire statement
Q1	The robot reacted to my interaction
Q2	The robot reacted quickly to my interaction
Q3	The robot liked it when I picked it up
Q4	The robot liked it when I shook it
Q5	The robot liked it when I threw it

version 3.12, Torino, Italy).

Data analysis

The data collected from the participants were based on questionnaires containing five different questions. To visualize the collected responses, histogram plots were generated for each question to check for the peaks, spread, and symmetry. Furthermore, Kruskal-Wallis tests were performed on each question to check for any statistically significant differences between the medians of the three groups at $p < 0.05$. Furthermore, the test was performed to check for effect due to gender differences.

6.3.3 Results

In this section, a summary of all the responses for each question are presented as histogram plots for the different groups. Then, statistical analysis is provided for the effect of gender and the response time.

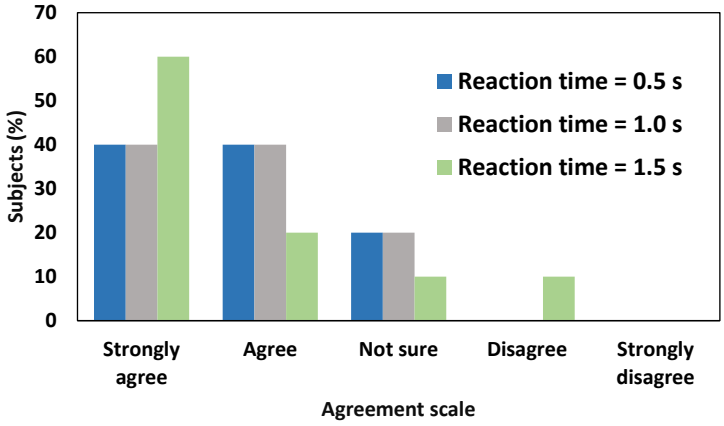

Figure 6.16: *A histogram summarizing the responses for the first question of the questionnaire: "The robot reacted to my interaction."*

Summary of the questionnaire

The first statement in the questionnaire was: *"The robot reacted to my interaction."* The frequency of answers for each group were presented as a histogram plot in Figure 6.16. The majority (i.e. 80%) of the responses for each group fall into the agreement region. This clustering of the responses created a right-skewed symmetry for all the groups. The peak of the data was at the *strongly agree* response for group 3 (i.e. reaction time of 1.5 s). There was only one subject's response in the disagreement region for group 3. This could be due to the slow reaction time compared to other groups (i.e. 1.5 s vs 1.0 s or 0.5 s) that gave the wrong impression of the robot's responses to the subject. Alternatively, this could have been simply an outlier.

The distribution of the responses have changed when the subjects were asked about the second statement of the questionnaire, which was: *"The robot reacted quickly to my interaction."* Similar to Q1, the majority of participants have answered in agreement to the statement, with group 2 being the highest (i.e. 80% of the subjects) and group 3 the lowest (i.e. 60% of the subjects)(Fig. 6.17). The data for each group appear to be skewed to the right. There were three peaks for each group at the strongly agree and agree scales. More responses were in the disagreement region as compared to the previous question. Group 3 contained the highest number (i.e.

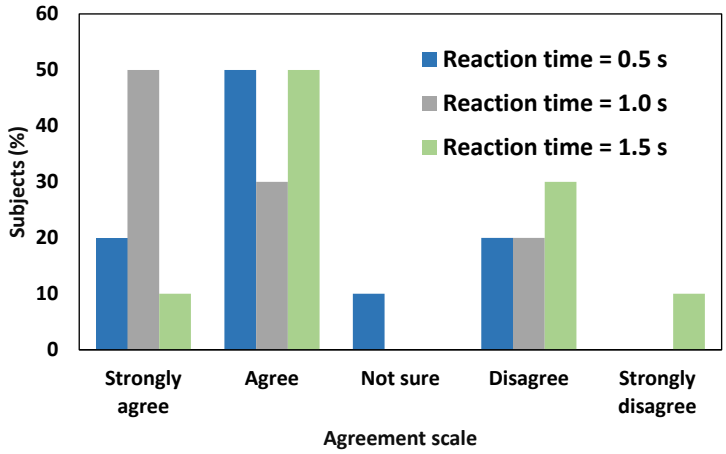

Figure 6.17: *A histogram summarizing the responses for the second question of the questionnaire: "The robot reacted quickly to my interaction."*

40% of the subjects) of responses in the disagreement scales. This could be attributed to the relatively late response of the robot for this group as compared to the other groups.

The distributions for the third question (i.e. *"The robot liked it when I picked it up"*) showed different spread for each group (Fig. 6.18). The responses for group 2 (i.e., reaction time of 1.0 s) appears to be right-skewed with 60% of the responses in the agreement region. Group 3 (i.e. reaction time of 1.5 s) also appears to be right-skewed, but with 50% of the subjects in agreement with the statement. The peak for group 2 was at *Strongly agree* selection while for group 3 the peak was at the *Agree* selection. As for group 1 with a reaction time of 0.5 s, the overall responses appear to be scattered in the agreement region (i.e. 50% of the subjects), however, the peak is at the *Not sure* scale. There were some responses in the disagreement region mainly for reaction time of 1.0 s and 1.5 s (i.e. 20%). The discrepancy in the responses could be attributed to the perceived understanding of the robot's reactions due to the subjects' interaction. The robot voice reaction to being picked up was similar to that of being surprised, but in a joyful manner. This could have confused some of the participants which made more responses leaning toward the *Not sure* scale or even into the disagreement region.

The fourth question was *"The robot liked it when I shook it."* For this

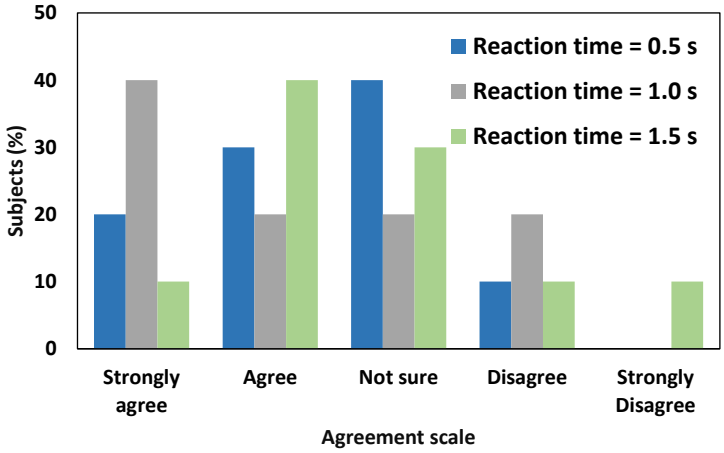

Figure 6.18: *A histogram summarizing the responses for the third question of the questionnaire:"The robot liked it when I picked it up."*

case, the robot produced a voice that indicated being annoyed to being shook. Hence, the responses are expected to be mostly in the disagreement zone. More than 70% of the responses for group 1 and group 2 fall into the disagreement region (Fig. 6.19). Group 1 and group 2 (i.e. reaction time of 0.5 s and 1.0 s) appear to be left-skewed with two peaks occurred at the *Strongly disagree* scale. The majority of the participants of group 3 (i.e. reaction time of 1.5 s) have voted in agreement (i.e. 70% of the subjects) to the fact that the robots have liked being shook. These results could be due to the relatively late response time for this group that made the robot produce delayed or incorrect reactions for the current interaction being made. For example, the robot is making the reaction for pickup while it should produce the one for shake. Clearly, a reaction time greater than one second could alter the perceived perception of a robot's response.

The fifth question was related to the perceived understanding of the robots' response after being thrown. The robot produced a sound indicating the feeling of pain after being thrown. The majority of the responses appear to be clustered in the disagreement region when the participants were asked *"The robot liked it when I threw it."* The highest peak was for group 1 (i.e. reaction time of 0.5 s) at the *Strongly Disagree* scale followed by group 2 (i.e. reaction time of 1.0 s) at the *Disagree* scale (Fig. 6.20). Group 3 with a reaction time of 1.5 s achieved the highest number of responses (i.e. 40%

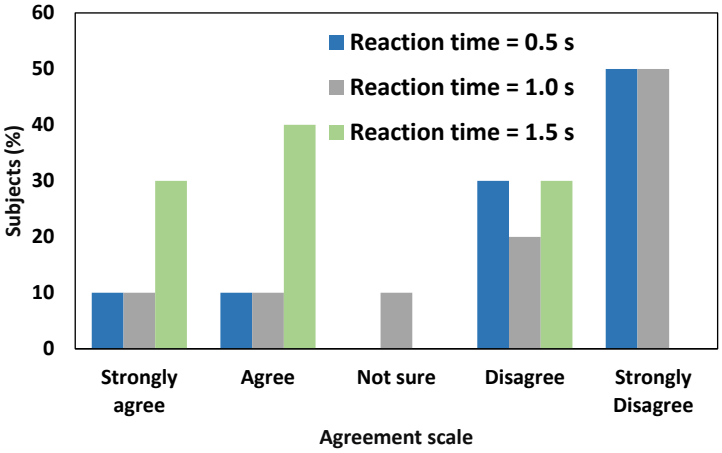

Figure 6.19: *A histogram summarizing the responses for the fourth question of the questionnaire:"The robot liked it when I shook it."*

of the subjects) in the agreement region followed by group 1 (i.e. 30% of the subjects).

Statistical Analysis - Gender Effect

As a secondary objective, it is interesting to find if there is an effect of gender on the responses for the different groups. For this analysis, only group 1 and group 2 were considered because of the close number of participants' genders (i.e., total of 8 females vs 12 males). A Mann-Whitney U test was run on 20 participants to determine if there were differences in the responses between males and females. The median response score for males (3.5) and females (4.0) was not statistically significantly different, $p = 0.948$. These results were expected as the human perception of a response should be similar regardless of the gender.

Statistical Analysis - Response Time Effect

A Kruskal-Wallis test for each item in the questionnaire was conducted to check for any significant difference between the three groups.

For the first question, the median values for group 1 (4.0), group 2 (4.0), and group 3 (5.0) were not statistically significantly different, $p = 0.827$ (Table 6.6).

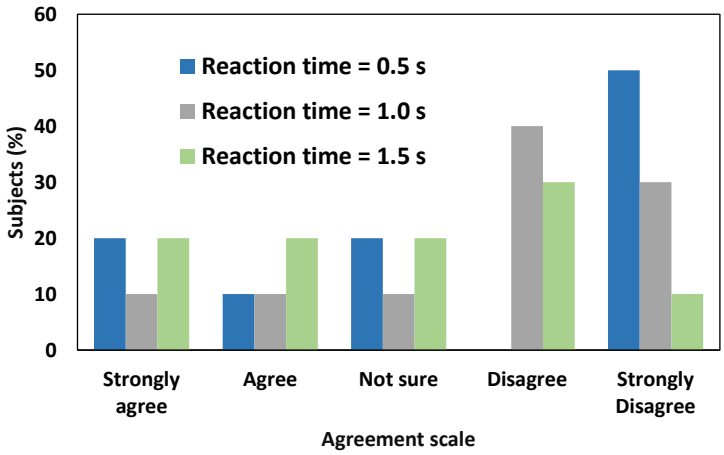

Figure 6.20: *A histogram summarizing the responses for the fifth question of the questionnaire: "The robot liked it when I threw it."*

Table 6.6: *Kruskal-Wallis test for the first question of the questionnaire for the three groups*

Group	N	Median	Ave Rank	Z	P-value
1	10	4.00	14.8	-0.31	0.827
2	10	4.00	14.8	-0.31	
3	10	5.00	16.9	0.62	
Overall	30		15.5		

Table 6.7: *Kruskal-Wallis test for the second question of the questionnaire for the three groups*

Group	N	Median	Ave Rank	Z	P-value
1	10	4.00	15.2	-0.13	0.223
2	10	4.50	19.1	1.56	
3	10	4.00	12.3	-1.43	
Overall	30		15.5		

Table 6.8: *Kruskal-Wallis test for the third question of the questionnaire for the three groups*

Group	N	Median	Ave Rank	Z	P-value
1	10	3.50	15.4	-0.02	0.666
2	10	4.00	17.3	0.79	
3	10	3.50	13.8	-0.77	
Overall	30		15.5		

The median values for the second questions of group 1 (4.0), group 2 (4.5), and group 3 (4.0) were not statistically significantly different, p = 0.223 (Table 6.7).

As for the third question, the differences between the median values of group 1 (3.5), group 2 (4.0), and group 3 (3.5) were not statistically significant, p = 0.666 (Table 6.8).

The median values for the fourth question of group 1 (1.5), group 2 (1.5), and group 3 (4.0) had statistically significant differences, p = 0.023 (Table 6.9). The average rank and median values showed that group 3 was different compared to the other groups. Group 3 was the one with the longest reaction time (i.e. 1.5 s) and that could explain the statistical difference.

As for the fifth question, the differences in the median values of group 1 (2.0), group 2 (2.0), and group 3 (3.0) were not statistically significant, p = 0.415 (Table 6.10). However, the average rank for group 3 (18.5) is higher than that of group 1 (14.3) and group 2 (13.8).

Table 6.9: *Kruskal-Wallis test for the fourth question of the questionnaire for the three groups*

Group	N	Median	Ave Rank	Z	P-value
1	10	1.50	12.2	-1.47	0.023
2	10	1.50	12.6	-1.28	
3	10	4.00	21.8	2.75	
Overall	30		15.5		

Table 6.10: *Kruskal-Wallis test for the fifth question of the questionnaire for the three groups*

Group	N	Median	Ave Rank	Z	P-value
1	10	2.00	14.3	-0.55	0.415
2	10	2.00	13.8	-0.77	
3	10	3.00	18.5	1.32	
Overall	30		15.5		

6.3.4 Discussion

The participants displayed different reactions while performing the tasks with the robotic toys. The first task was to pick up the robot and explore it, and the robot would respond with sounds implying a joyful reaction. For this task, many showed curiosity and laughter about the sounds that the robots were emitting. Some of the children showed surprised expressions and stopped temporarily to explore the robots then looked at the experimenters. The second task was to shake the robot, and the robot would respond with sounds implying annoyance. For this task, many were surprised, stopped shaking the robot, and then placed it back after hearing the robots' reactions. A few resumed shaking after stopping temporarily. The last task was to throw the robot at a specific target, and the robot would emit a sound, which implied pain. Many showed surprised expressions about the responses while some of them gazed at the experimenter with astonished looks.

The results of the questionnaire implied that there is an effect for the reaction timings on the perceived understanding of the robots' responses. Group 3 (i.e. reaction time of 1.5 s) scored more incorrect responses across most of the questions as compared to other groups. This was very evident in the responses for the fourth item in the questionnaire (Fig. 6.19). The delay in producing a reaction to an interaction might have given the wrong impression about the causation effect, hence, making it difficult to understand the aim or goal behind a robot's response. In other words, the longer the duration to make a reaction, the more likely it will deliver an incorrect message to the user for the intended interaction. Producing a response within one second from detecting a stimuli should produce more favorable results. The Kruskal-Wallis test results for the fourth question supports these findings.

Another dimension that might have influenced the responses is the modality of the response itself. The sounds for the responses were considered to indicate three different expressions, namely, joyful surprise, being annoyed, and feeling pain. These responses were selected by adults to target children as the primary users. Some of the incorrect responses to the questions could be attributed to a possible confusion about the intended message behind each sound (i.e. response). This implies the need for more commonly-accepted responses that could be easily understood regardless of age, culture, or geographical region.

The experiments in this study were limited to three different responses corresponding to three different interactions. However, more responses

could exist to imply different emotions and reactions. Sound was the only modality that was considered to convey the robot's responses. Different modalities could be considered and integrated to provide clearer responses. Children were the only participants in our experiments because of the targeted end-users of this study. However, adults participants could be considered to obtain more comprehensive and more in-depth feedback about the experiments. Finally, the recognition model could be improved to increase its capabilities in recognizing more behaviors accurately and quickly.

6.3.5 Conclusion

An approach to detect and respond to three types of manipulation of robotic toys was presented. The interactions with the toys considered were being picked up, being shaken, and being thrown. Furthermore, the study evaluated the perception of the reaction provided at different timing through the emission of sounds. The results showed that the reaction time affect the understanding of a robot's response to an interaction. Ideally, the response to an action for robotic toys should occur not more than one second after the detection of an aggressive behavior or an unwanted interaction. Furthermore, sound as a modality to a robot's response provided a sufficient message to be understood by the majority of the participants.

6.4 Chapter Summary

This chapter presented the finding of two studies aimed at making a robot more adaptive once an unwanted interaction is detected. The first study showed the possibility of recognizing unwanted physical interactions based on the data received from an embedded tri-axial accelerometer. The second study investigated the influence of reaction time in the emotional response of a robot on the perceived message during interactions. This study showed the importance of producing a timely response to an unwanted interaction to deliver the right message to the user.

CHAPTER 7

Conclusions and Recommendations

7.1 Conclusions

Social robots have gained a lot of attention in health care generally, and specifically in therapy, due to the increased number of studies reporting the efficacy of using such technology. Among children with ASD, social robots have been reported to effectively help in the elicitation of some positive behaviors. This has been attributed to the fact that social robots are simpler than humans, and could exhibit more coherent behaviors. The advancement in technology has enabled robots to be more autonomous and intelligent. In particular, it is possible to develop smaller social robots exhibiting a high level of interaction with many capabilities. While larger social robots can be used in therapeutic settings, especially for training, the smaller form of social robots are more affordable and suitable options to be considered at home for continuous support. The introduction of a new device, such as a social robot, that is meant to evoke behaviors to the surrounding of such children could pose as new source of harm to themselves or others, especially during the manifestation of challenging behaviors.

Children on the spectrum lack the ability to properly communicate their needs and the case of harm due to impacts might be problematic, especially

during therapy sessions. Generalization of skills is usually done with other children. Hence, being subjected to pain due to impacts might affect any positive outcomes, and potentially cause more challenging behaviors. With children generally, and those with ASD especially, any source of potential harm, pain or even annoyance must be kept to a minimum or eliminated altogether.

As for the parametric studies conducted in Chapter 5, some of the control factors investigated provided a reduction in the overall head's acceleration. For example, reducing the mass of a thrown object appear to reduce the head acceleration considerably. This was more evident at higher impact speed. This finding combined with the application of soft materials could provide a better overall reduction of the potential harm.

Optimization of a robot's design can benefit from the techniques provided by Taguchi methods, as it gives an efficient and convenient way to assess and optimize the safe design of small social robots. Moreover, such benefits are magnified for two reasons. On one hand, the safety requirements of the target users, such as children with special needs who may have a tendency for meltdowns, are addressed. On the other hand, the manufacturers have done their due diligence in optimizing their design for minimizing the chances of harm to the users and avoid lawsuits or product recall later on.

Many children show aggression toward others and animals [75], [20]. Social companion robots could be used to mitigate aggression. Being able to detect unwanted interactions while providing timely reactions, will enable the robot to train the children about the culture of safety. By selecting an appropriate response to their negative action, the robot could be used to display that the current behavior is undesirable and unacceptable.

Companion robots would benefit from having the capability of detecting and reacting to aggressive interactions. This layer to detect undesired interactions would operate independently from the robot's main objectives. Having such capabilities to detect undesired behaviors could be used to make children experiment with the consequences of their actions on others. For example, a robot displaying sad emotion after being hit can influence a child to believe that this behavior is not appropriate in social interactions. Furthermore, this also has the potential to be extended to target aggression among neurotypical and neurodivergent children.

The need for a quick response implies the need for fast recognition algorithms that must provide a quick prediction about an interaction. The modality of a response should be clear enough to provide the right message intended from an interaction. Multiple modalities could be fused together

to provide a stronger response and clearer message to the user. Hence, it would reduce the likelihood of a user's misinterpreting the intended message behind a response.

7.2 Recommendations

More research needs to be done to investigate the potential for harm due to different robotic shapes, and to identify means to mitigate it through both hardware and software approaches. For small social robots, regulations from standards that are concerned with the safety of toys can readily be adopted. For example, ISO 8124-1:2014 [113], which is related to mechanical and physical properties safety aspects of toys. Another direction for safer social robots is the adoption of some of the techniques and advances in soft robotics. New social robotic safety standards targeting and tailored for special end-users, such as children with ASD, must be established to ensure their safety and to take into consideration their needs.

The designers of small social robots or robotic toys for children with special needs, or even for neuro-typical children, should try to minimize the mass of their products as much as possible while adding an external layer of a suitable soft material. Additionally, they need to investigate different soft materials to find suitable materials that provide robustness and ease of application to their products while improving the safety aspects. In addition to the optimization efforts at the design level, the manufacturers should include special warning labels for their products that are meant to be used by users with special needs, especially those that exhibit challenging behaviors.

The studies presented in Chapter 6 open the possibilities for future work on continuous online recognition that is embedded within a robotic toy with appropriate responses. These findings provide a contribution toward improved therapy sessions by anticipating some unwanted interactions and then preventing the occurrence or progression of challenging behaviors by the intervention of a human therapist or the social robot itself. Future studies can investigate sounds along with other modalities in the emotional response of a robot. Moreover, further improvements on the recognition algorithm should be considered to ensure smoother interactions, which should reach a much higher performance to become acceptable as a product in the mass market.

Bibliography

[1] Ahmad Yaser Alhaddad, Sami Emad AlKhatib, Rahib Ahmed Khan, Salman Mohammad Ismail, Al-Sendibad Said Shehadeh, Abdellatif Mohammad Sadeq, and John-John Cabibihan. Toward 3D printed prosthetic hands that can satisfy psychosocial needs: Grasping force comparisons between a prosthetic hand and human hands. In Abderrahmane Kheddar, Eiichi Yoshida, Shuzhi Sam Ge, Kenji Suzuki, John-John Cabibihan, Friederike Eyssel, and Hongsheng He, editors, *Social Robotics*, pages 304–313, Cham, 2017. Springer International Publishing.

[2] Ahmad Yaser Alhaddad and John-John Cabibihan. Reflex system for intelligent robotics. In *Qatar Foundation Annual Research Conference Proceedings Volume 2016 Issue 1*, volume 2016, page HBSP2914. Hamad bin Khalifa University Press (HBKU Press), 2016.

[3] Ahmad Yaser Alhaddad, John-John Cabibihan, and Andrea Bonarini. Head impact severity measures for small social robots thrown during meltdown in autism. *International Journal of Social Robotics*, nov 2018.

[4] Ahmad Yaser Alhaddad, John-John Cabibihan, and Andrea Bonarini. Recognition of aggressive interactions of children toward robotic toys. In *2019 28th IEEE International Conference on Robot and Human Interactive Communication (RO-MAN)*, pages 1–8. IEEE, 2019.

[5] Ahmad Yaser Alhaddad, John-John Cabibihan, and Andrea Bonarini. Influence of reaction time in the emotional response of a companion robot to a child's aggressive interaction. *International Journal of Social Robotics*, pages 1–13, 2020.

[6] Ahmad Yaser Alhaddad, John-John Cabibihan, Ahmad Hayek, and Andrea Bonarini. The impact of different shaped objects of different masses at different impact velocities on a dummy head (dataset). 2018.

[7] Ahmad Yaser Alhaddad, John-John Cabibihan, Ahmad Hayek, and Andrea Bonarini. Data on the impact of an object with different thicknesses of different soft materials at different impact velocities on a dummy head. *Data in Brief*, page 103885, April 2019.

[8] Ahmad Yaser Alhaddad, John-John Cabibihan, Ahmad Hayek, and Andrea Bonarini. Data on the impact of objects with different shapes, masses, and impact velocities on a dummy head. *Data in Brief*, 22:344–348, feb 2019.

[9] Ahmad Yaser Alhaddad, John-John Cabibihan, Ahmad Hayek, and Andrea Bonarini. The impact of an object with different thicknesses of different soft materials at different impact velocities on a dummy head (dataset). 2019.

[10] Ahmad Yaser Alhaddad, John-John Cabibihan, Ahmad Hayek, and Andrea Bonarini. Influence of the shape and mass of a small robot when thrown to a dummy human head. *SN Applied Sciences*, 1(11):1468, 2019.

[11] Ahmad Yaser Alhaddad, John-John Cabibihan, Ahmad Hayek, and Andrea Bonarini. A low-cost test rig for impact experiments on a dummy head. *HardwareX*, page e00068, 2019.

[12] Ahmad Yaser Alhaddad, John-John Cabibihan, Ahmad Hayek, and Andrea Bonarini. Safety experiments for small robots investigating the potential of soft materials in mitigating the harm to the head due to impacts. *SN Applied Sciences*, 1(5):476, 2019.

[13] Ahmad Yaser Alhaddad, Hifza Javed, Olcay Connor, Bilikis Banire, Dena Al Thani, and John-John Cabibihan. Robotic trains as an educational and therapeutic tool for autism spectrum disorder intervention. In Wilfried Lepuschitz, Munir Merdan, Gottfried Koppensteiner, Richard Balogh, and David Obdržálek, editors, *Robotics in Education*, pages 249–262, Cham, 2019. Springer International Publishing.

[14] Lenneke RA Alink, Judi Mesman, Jantien Van Zeijl, Mirjam N Stolk, Femmie Juffer, Hans M Koot, Marian J Bakermans-Kranenburg, and Marinus H Van IJzendoorn. The early childhood aggression curve: Development of physical aggression in 10-to 50-month-old children. *Child development*, 77(4):954–966, 2006.

[15] American Psychological Association. APA Dictionary of Psychology. *URL: https://dictionary.apa.org/aggression*, 2018. (Date last accessed 26-Aug-2018).

[16] Vicki Anderson and Cressida Moore. Age at injury as a predictor of outcome following pediatric head injury: A longitudinal perspective. *Child Neuropsychology*, 1(3):187–202, 1995.

[17] Vicki A Anderson, Cathy Catroppa, Paul Dudgeon, Sue A Morse, Flora Haritou, and Jeffrey V Rosenfeld. Understanding predictors of functional recovery and outcome 30 months following early childhood head injury. *Neuropsychology*, 20(1):42, 2006.

[18] Davide Anguita, Alessandro Ghio, Luca Oneto, Xavier Parra, and Jorge Luis Reyes-Ortiz. A public domain dataset for human activity recognition using smartphones. In *Esann*, 2013.

[19] Ong Chin Ann and Lau Bee Theng. Human activity recognition: a review. In *Control System, Computing and Engineering (ICCSCE), 2014 IEEE International Conference on*, pages 389–393. IEEE, 2014.

[20] Frank R Ascione. Children who are cruel to animals: A review of research and implications for developmental psychopathology. *Anthrozoös*, 6(4):226–247, 1993.

[21] Jill Ashburner, Jenny Ziviani, and Sylvia Rodger. Surviving in the mainstream: Capacity of children with autism spectrum disorders to perform academically and regulate their emotions and behavior at school. *Research in Autism Spectrum Disorders*, 4(1):18–27, 2010.

[22] American Psychiatric Association et al. *Diagnostic and statistical manual of mental disorders (DSM-5®)*. American Psychiatric Pub, 2013.

[23] Richard Auger. Autism spectrum disorders: A research review for school counselors. *Professional school counseling*, 16(4):256–268, 2013.

[24] Fabio Bagala, Clemens Becker, Angelo Cappello, Lorenzo Chiari, Kamiar Aminian, Jeffrey M Hausdorff, Wiebren Zijlstra, and Jochen Klenk. Evaluation of accelerometer-based fall detection algorithms on real-world falls. *PloS one*, 7(5):e37062, 2012.

[25] A Baghdadli, C Pascal, S Grisi, and C Aussilloux. Risk factors for self-injurious behaviours among 222 young children with autistic disorders. *Journal of Intellectual Disability Research*, 47(8):622–627, 2003.

[26] Jon Baio. Prevalence of autism spectrum disorders: Autism and developmental disabilities monitoring network, 14 sites, united states, 2008. morbidity and mortality weekly report. surveillance summaries. volume 61, number 3. *Centers for Disease Control and Prevention*, 2012.

[27] Lisa L Bakhos, Gregory R Lockhart, Richard Myers, and James G Linakis. Emergency department visits for concussion in young child athletes. *Pediatrics*, 126(3):e550–e556, 2010.

[28] Oresti Banos, Juan-Manuel Galvez, Miguel Damas, Hector Pomares, and Ignacio Rojas. Window size impact in human activity recognition. *Sensors*, 14(4):6474–6499, apr 2014.

[29] Ling Bao and Stephen S Intille. Activity recognition from user-annotated acceleration data. In *International Conference on Pervasive Computing*, pages 1–17. Springer, 2004.

[30] Cameron R Bass and Narayan Yoganandan. Skull and facial bone injury biomechanics. In *Accidental Injury*, pages 203–220. Springer, 2015.

[31] Momotaz Begum, Richard W Serna, and Holly A Yanco. Are robots ready to deliver autism interventions? a comprehensive review. *International Journal of Social Robotics*, 8(2):157–181, 2016.

[32] Laura Boccanfuso, Erin Barney, Claire Foster, Yeojin Amy Ahn, Katarzyna Chawarska, Brian Scassellati, and Frederick Shic. Emotional robot to examine differences in play patterns and affective response of children with and without asd. In *The Eleventh ACM/IEEE International Conference on Human Robot Interaction*, pages 19–26. IEEE Press, 2016.

[33] Barry P Boden, Robin Tacchetti, and Fred O Mueller. Catastrophic injuries in high school and college baseball players. *The American journal of sports medicine*, 32(5):1189–1196, 2004.

[34] James W Bodfish, Frank J Symons, Dawn E Parker, and Mark H Lewis. Varieties of repetitive behavior in autism: Comparisons to mental retardation. *Journal of autism and developmental disorders*, 30(3):237–243, 2000.

[35] Andrea Bonarini, Franca Garzotto, Mirko Gelsomini, Maximiliano Romero, Francesco Clasadonte, and Ayşe Naciye Çelebi Yilmaz. A huggable, mobile robot for developmental disorder interventions in a multi-modal interaction space. In *Robot and Human Interactive Communication (RO-MAN), 2016 25th IEEE International Symposium on*, pages 823–830. IEEE, 2016.

[36] Carlijn VC Bouten, Karel TM Koekkoek, Maarten Verduin, Rens Kodde, and Jan D Janssen. A triaxial accelerometer and portable data processing unit for the assessment of daily physical activity. *IEEE transactions on biomedical engineering*, 44(3):136–147, 1997.

[37] Cynthia Breazeal, Kerstin Dautenhahn, and Takayuki Kanda. Social robotics. In *Springer handbook of robotics*, pages 1935–1972. Springer, 2016.

[38] Douglas Brown. Tracker 5.0.7. (Date last accessed 22-Mar-2019).

[39] Andreas Bulling, Ulf Blanke, and Bernt Schiele. A tutorial on human activity recognition using body-worn inertial sensors. *ACM Computing Surveys (CSUR)*, 46(3):33, 2014.

[40] J-J Cabibihan, Stéphane Pattofatto, Moez Jomâa, Ahmed Benallal, Maria Chiara Carrozza, and Paolo Dario. The conformance test for robotic/prosthetic fingertip skins. In *The First IEEE/RAS-EMBS International Conference on Biomedical Robotics and Biomechatronics, 2006. BioRob 2006.*, pages 561–566. IEEE, 2006.

[41] JJ Cabibihan, H Javed, KK Sadasivuni, and AY Al Haddad. Smart robotic therapeutic learning toy. *WIPO Patent WO2018033857, World Intellectual Property Organization*, 2018.

[42] John-John Cabibihan, M Khaleel Abubasha, and Nitish Thakor. A method for 3-d printing patient-specific prosthetic arms with high accuracy shape and size. *IEEE Access*, 6:25029–25039, 2018.

[43] John-John Cabibihan, Maria Chiara Carrozza, Paolo Dario, Stephane Pattofatto, Moez Jomaa, and Ahmed Benallal. The uncanny valley and the search for human skin-like materials for a prosthetic fingertip. In *2006 6th IEEE-RAS International Conference on Humanoid Robots*, pages 474–477. IEEE, 2006.

[44] John-John Cabibihan, Sushil Singh Chauhan, and Shruthi Suresh. Effects of the artificial skin's thickness on the subsurface pressure profiles of flat, curved, and braille surfaces. *IEEE Sensors Journal*, 14(7):2118–2128, 2014.

[45] John-John Cabibihan, Ryad Chellali, Catherine Wing Chee So, Mohammad Aldosari, Olcay Connor, Ahmad Yaser Alhaddad, and Hifza Javed. Social robots and wearable sensors for mitigating meltdowns in autism - a pilot test. In Shuzhi Sam Ge, John-John Cabibihan, Miguel A. Salichs, Elizabeth Broadbent, Hongsheng He, Alan R. Wagner, and Álvaro Castro-González, editors, *Social Robotics*, pages 103–114, Cham, 2018. Springer International Publishing.

[46] John-John Cabibihan, Hifza Javed, Mohammed Aldosari, Thomas W. Frazier, and Haitham Elbashir. Sensing technologies for autism spectrum disorder screening and intervention. *Sensors*, 17(1), 2017.

[47] John-John Cabibihan, Hifza Javed, Marcelo Ang Jr, and Sharifah Mariam Aljunied. Why robots? a survey on the roles and benefits of social robots in the therapy of children with autism. *International journal of social robotics*, 5(4):593–618, 2013.

[48] John-john Cabibihan, Hifza Javed, Kishor Kumar Sadasivuni, and Ahmed Yaser Alhaddad. Smart robotic therapeutic learning toy, June 20 2019. US Patent App. 16/326,169.

[49] John-John Cabibihan, Deepak Joshi, Yeshwin Mysore Srinivasa, Mark Aaron Chan, and Arrchana Muruganantham. Illusory sense of human touch from a warm and soft artificial hand. *IEEE Transactions on Neural Systems and Rehabilitation Engineering*, 23(3):517–527, 2015.

[50] John-John Cabibihan, Raditya Pradipta, Yun Zhi Chew, and Shuzhi Sam Ge. Towards humanlike social touch for prosthetics and sociable robotics: Handshake experiments and finger phalange indentations. In *FIRA RoboWorld Congress*, pages 73–79. Springer, 2009.

[51] John-John Cabibihan, Kishor Kumar Sadasivuni, and Ahmad Yaser Alhaddad. Biometric liveness detection through biocompatible capacitive sensor, February 14 2019. US Patent App. 16/058,453.

[52] John-John Cabibihan, Wing Chee So, Medi Nazar, and Shuzhi Sam Ge. Pointing gestures for a robot mediated communication interface. In *International Conference on Intelligent Robotics and Applications*, pages 67–77. Springer, Berlin, Heidelberg, 2009.

[53] John-John Cabibihan, Wing-Chee So, Sujin Saj, and Zhengchen Zhang. Telerobotic pointing gestures shape human spatial cognition. *International Journal of Social Robotics*, 4(3):263–272, 2012.

[54] Dympna Casey, Heike Felzmann, Geoff Pegman, Christos Kouroupetroglou, Kathy Murphy, Adamantios Koumpis, and Sally Whelan. What people with dementia want: designing mario an acceptable robot companion. In *International Conference on Computers Helping People with Special Needs*, pages 318–325. Springer, 2016.

[55] Andrew Cashin and Philip Barker. The triad of impairment in autism revisited. *Journal of Child and Adolescent Psychiatric Nursing*, 22(4):189–193, 2009.

[56] Marco Cavazzuti. *Optimization methods: from theory to design scientific and technological aspects in mechanics*. Springer Science & Business Media, 2012.

[57] S Chaudron, R Di Gioia, M Gemo, D Holloway, J Marsh, G Mascheroni, J Peter, and D Yamada-Rice. Kaleidoscope on the internet of toys-safety, security, privacy and societal insights, 2017.

[58] Safety Test Instrumentation Stds Comm. Instrumentation for impact test-part 1-electronic instrumentation (j211/1). *Warrendale, PA: Society of Automotive Engineers*, 2003.

[59] Daniel F Connor. *Aggression and antisocial behavior in children and adolescents: Research and treatment*. Guilford Press, 2012.

[60] Cristina Alén Cordero, Giuseppe Carbone, Marco Ceccarelli, Javier Echávarri, and José Luis Muñoz. Experimental tests in human–robot collision evaluation and characterization of a new safety index for robot operation. *Mechanism and machine theory*, 80:184–199, 2014.

[61] Albert J Cotugno. Social competence and social skills training and intervention for children with autism spectrum disorders. *Journal of autism and developmental disorders*, 39(9):1268–1277, 2009.

[62] Kerstin Dautenhahn, Chrystopher L Nehaniv, Michael L Walters, Ben Robins, Hatice Kose-Bagci, N Assif Mirza, and Mike Blow. Kaspar–a minimally expressive humanoid robot for human–robot interaction research. *Applied Bionics and Biomechanics*, 6(3-4):369–397, 2009.

[63] Martin B Davis. *Facial fracture and eye injury tolerance from night vision Goggle loading*. PhD thesis, University of Virginia, 2004.

[64] Michael del Rosario, Stephen Redmond, and Nigel Lovell. Tracking the evolution of smartphone sensing for monitoring human movement. *Sensors*, 15(8):18901–18933, 2015.

[65] Lorenzo Desideri, Marco Negrini, Massimiliano Malavasi, Daniela Tanzini, Aziz Rouame, Maria Cristina Cutrone, Paola Bonifacci, and Evert-Jan Hoogerwerf. Using a humanoid robot as a complement to interventions for children with autism spectrum disorder: a pilot study. *Advances in Neurodevelopmental Disorders*, pages 1–13, 2018.

[66] Joshua J Diehl, Lauren M Schmitt, Michael Villano, and Charles R Crowell. The clinical use of robots for individuals with autism spectrum disorders: A critical review. *Research in autism spectrum disorders*, 6(1):249–262, 2012.

[67] Lucy Diep, John-John Cabibihan, and Gregor Wolbring. Social robotics through an anticipatory governance lens. In *International Conference on Social Robotics*, pages 115–124. Springer, Cham, 2014.

[68] Lucy Diep, John-John Cabibihan, and Gregor Wolbring. Social robots: Views of special education teachers. In *Proceedings of the 3rd 2015 Workshop on ICTs for improving Patients Rehabilitation Research Techniques*, pages 160–163. ACM, 2015.

[69] I Emanuelson. How safe are childcare products, toys and playground equipment? a swedish analysis of mild brain injuries at home and during leisure time 1998-1999. *Injury control and safety promotion*, 10(3):139–144, 2003.

[70] Demetria Loryn Ennis-Cole. Strategies for supporting students with asd. In *Technology for Learners with Autism Spectrum Disorders*, pages 15–27. Springer, 2015.

[71] Demetria Loryn Ennis-Cole. *Technology for learners with autism spectrum disorders*. Springer, 2015.

[72] Annette Estes, Jeffrey Munson, Geraldine Dawson, Elizabeth Koehler, Xiao-Hua Zhou, and Robert Abbott. Parenting stress and psychological functioning among mothers of preschool children with autism and developmental delay. *Autism*, 13(4):375–387, 2009.

[73] Euro, NCAP. Assessment protocol-child occupant protection, 2017.

[74] David Feil-Seifer and Maja J Matarić. Automated detection and classification of positive vs. negative robot interactions with children with autism using distance-based features. In *Human-Robot Interaction (HRI), 2011 6th ACM/IEEE International Conference on*, pages 323–330. IEEE, 2011.

[75] Alan R Felthous. Aggression against cats, dogs and people. *Child Psychiatry and Human Development*, 10(3):169–177, 1980.

[76] Gabriel P Fife, David M O'sullivan, Willy Pieter, David P Cook, and Thomas W Kaminski. Effects of olympic-style taekwondo kicks on an instrumented head-form and resultant injury measures. *Br J Sports Med*, pages bjsports–2012, 2012.

[77] Jill C Fodstad, Johannes Rojahn, and Johnny L Matson. The emergence of challenging behaviors in at-risk toddlers with and without autism spectrum disorder: A cross-sectional study. *Journal of Developmental and Physical Disabilities*, 24(3):217–234, 2012.

[78] Terrence Fong, Illah Nourbakhsh, and Kerstin Dautenhahn. A survey of socially interactive robots. *Robotics and autonomous systems*, 42(3-4):143–166, 2003.

[79] Centers for Disease Control, Prevention, et al. Report to congress on mild traumatic brain injury in the united states: Steps to prevent a serious public health problem. *Atlanta, GA: Centers for Disease Control and Prevention*, 45, 2003.

[80] Shuzhi Sam Ge, John-John Cabibihan, Zhengchen Zhang, Yanan Li, Cai Meng, Hongsheng He, MR Safizadeh, YB Li, and J Yang. Design and development of nancy, a social robot. In *Ubiquitous Robots and Ambient Intelligence (URAI), 2011 8th International Conference on*, pages 568–573. IEEE, 2011.

[81] Manuel Giuliani, Claus Lenz, Thomas Müller, Markus Rickert, and Alois Knoll. Design principles for safety in human-robot interaction. *International Journal of Social Robotics*, 2(3):253–274, 2010.

[82] Nicole Giullian, Daniel Ricks, Alan Atherton, Mark Colton, Michael Goodrich, and Bonnie Brinton. Detailed requirements for robots in autism therapy. In *2010 IEEE International Conference on Systems, Man and Cybernetics*, pages 2595–2602. IEEE, 2010.

[83] Ofer Golan, Emma Ashwin, Yael Granader, Suzy McClintock, Kate Day, Victoria Leggett, and Simon Baron-Cohen. Enhancing emotion recognition in children with autism spectrum conditions: An intervention using animated vehicles with real emotional faces. *Journal of autism and developmental disorders*, 40(3):269–279, 2010.

[84] Alex Graves, Navdeep Jaitly, and Abdel-rahman Mohamed. Hybrid speech recognition with deep bidirectional lstm. In *2013 IEEE workshop on automatic speech recognition and understanding*, pages 273–278. IEEE, 2013.

[85] Hazel Green, Áine McGinnity, Howard Meltzer, Tamsin Ford, Robert Goodman, et al. Mental health of children and young people in great britain, 2004, 2005.

[86] Lorne Greenspan, Barry A McLellan, and Helen Greig. Abbreviated injury scale and injury severity score: a scoring chart. *Journal of Trauma and Acute Care Surgery*, 25(1):60–64, 1985.

[87] Richard M Greenwald, Joseph T Gwin, Jeffrey J Chu, and Joseph J Crisco. Head impact severity measures for evaluating mild traumatic brain injury risk exposure. *Neurosurgery*, 62(4):789–798, 2008.

[88] James G Gurney, Melissa L McPheeters, and Matthew M Davis. Parental report of health conditions and health care use among children with and without autism: National survey of children's health. *Archives of pediatrics & adolescent medicine*, 160(8):825–830, 2006.

[89] Sami Haddadin, Alin Albu-Schaffer, Fahed Haddadin, Jurgen Rosmann, and Gerd Hirzinger. Study on soft-tissue injury in robotics. *IEEE Robotics & Automation Magazine*, 18(4):20–34, 2011.

[90] Sami Haddadin, Alin Albu-Schäffer, and Gerd Hirzinger. Safety evaluation of physical human-robot interaction via crash-testing. In *Robotics: Science and Systems*, volume 3, pages 217–224, 2007.

[91] Sami Haddadin, Alin Albu-Schaffer, and Gerd Hirzinger. The role of the robot mass and velocity in physical human-robot interaction-part i: Non-constrained blunt impacts. In *Robotics and Automation, 2008. ICRA 2008. IEEE International Conference on*, pages 1331–1338. IEEE, 2008.

[92] Sami Haddadin, Alin Albu-Schäffer, and Gerd Hirzinger. Requirements for safe robots: Measurements, analysis and new insights. *The International Journal of Robotics Research*, 28(11-12):1507–1527, 2009.

[93] Jaap Ham, Raymond H Cuijpers, and John-John Cabibihan. Combining robotic persuasive strategies: the persuasive power of a storytelling robot that uses gazing and gestures. *International Journal of Social Robotics*, 7(4):479–487, 2015.

[94] Jaap Ham, Mirjam van Esch, Yvonne Limpens, Jente de Pee, John-John Cabibihan, and Shuzhi Sam Ge. The automaticity of social behavior towards robots: the influence of cognitive load on interpersonal distance to approachable versus less approachable robots. In *International Conference on Social Robotics*, pages 15–25. Springer, 2012.

[95] Michael Hamada. Reliability improvement via taguchi's robust design. *Quality and Reliability Engineering International*, 9(1):7–13, jan 1993.

[96] Mary Hart. Autism/excel study. In *Proceedings of the 7th international ACM SIGACCESS conference on Computers and accessibility*, pages 136–141. ACM, 2005.

[97] Ajit M. Hebbale, Anikethan Bekal, and M. S. Srinath. Wear studies of composite microwave clad on martensitic stainless steel. *SN Applied Sciences*, 1(3), feb 2019.

[98] Frank Hegel, Claudia Muhl, Britta Wrede, Martina Hielscher-Fastabend, and Gerhard Sagerer. Understanding social robots. In *Advances in Computer-Human Interactions, 2009. ACHI'09. Second International Conferences on*, pages 169–174. IEEE, 2009.

[99] Guido Herrmann and Chris Melhuish. Towards safety in human robot interaction. *International Journal of Social Robotics*, 2(3):217–219, 2010.

[100] Truong Dien Hoa and John-John Cabibihan. Cute and soft: baby steps in designing robots for children with autism. In *Proceedings of the Workshop at SIGGRAPH Asia*, pages 77–79. ACM, 2012.

[101] Sepp Hochreiter and Jürgen Schmidhuber. Long short-term memory. *Neural computation*, 9(8):1735–1780, 1997.

[102] Donald F Huelke. An overview of anatomical considerations of infants and children in the adult world of automobile safety design. In *Annual Proceedings/Association for the Advancement of Automotive Medicine*, volume 42, page 93. Association for the Advancement of Automotive Medicine, 1998.

[103] CAGJ Huijnen, MAS Lexis, and LP de Witte. Robots as new tools in therapy and education for children with autism. *Int J Neurorehabilitation*, 4(278):2376–0281, 2017.

[104] Claire AGJ Huijnen, Monique AS Lexis, Rianne Jansens, and Luc P de Witte. How to implement robots in interventions for children with autism? a co-creation study involving people with autism, parents and professionals. *Journal of autism and developmental disorders*, 47(10):3079–3096, 2017.

[105] Abdul Rashid Husain, Yaser Hadad, and Muhd Nazrul Hisham Zainal Alam. Development of low-cost microcontroller-based interface for data acquisition and control of microbioreactor operation. *Journal of Laboratory Automation*, 21(5):660–670, 2016.

[106] Tiffany L Hutchins and Patricia A Prelock. Using communication to reduce challenging behaviors in individuals with autism spectrum disorders and intellectual disability. *Child and Adolescent Psychiatric Clinics*, 23(1):41–55, 2014.

[107] Timothy Paul Hutchinson. Peak acceleration during impact with helmet materials: effects of impactor mass and speed. *European journal of sport science*, 14(sup1):S377–S382, 2014.

[108] Raul Igual, Carlos Medrano, and Inmaculada Plaza. Challenges, issues and trends in fall detection systems. *Biomedical engineering online*, 12(1):66, 2013.

[109] International Federation of Robotics. Executive summary world robotics 2016 industrial robots. (Date last accessed 1-Jan-2018).

[110] International Organization for Standardization. Iso 10218-1: 2011: Robots and robotic devices–safety requirements for industrial robots–part 1: Robots. *Geneva, Switzerland: International Organization for Standardization*, 2011.

[111] International Organization for Standardization. Iso 10218-2: 2011: Robots and robotic devices–safety requirements for industrial robots–part 2: Robot systems and integration. *Geneva, Switzerland: International Organization for Standardization*, 2011.

[112] International Organization for Standardization. Iso 13482: 2014: Robotic devices–safety requirements–nonmedical personal care robot. *Geneva, Switzerland: International Organization for Standardization*, 2014.

[113] International Organization for Standardization. Iso 8124-1: 2014: Safety of toys – part 1: Safety aspects related to mechanical and physical properties. *Geneva, Switzerland: International Organization for Standardization*, 2014.

[114] International Organization for Standardization. Iso/ts 15066:2016: Robots and robotic devices – collaborative robots. *Geneva, Switzerland: International Organization for Standardization*, 2016.

[115] Norah L Johnson, Joel Lashley, Alice V Stonek, and Annette Bonjour. Children with developmental disabilities at a pediatric hospital: Staff education to prevent and manage challenging behaviors. *Journal of pediatric nursing*, 27(6):742–749, 2012.

[116] Stephen M Kanne and Micah O Mazurek. Aggression in children and adolescents with asd: Prevalence and risk factors. *Journal of autism and developmental disorders*, 41(7):926–937, 2011.

[117] Nicky Kern, Bernt Schiele, and Albrecht Schmidt. Multi-sensor activity context detection for wearable computing. In *European Symposium on Ambient Intelligence*, pages 220–232. Springer, 2003.

[118] Young Shin Kim, Bennett L Leventhal, Yun-Joo Koh, Eric Fombonne, Eugene Laska, Eun-Chung Lim, Keun-Ah Cheon, Soo-Jeong Kim, Young-Key Kim, HyunKyung Lee, et al. Prevalence of autism spectrum disorders in a total population sample. *American Journal of Psychiatry*, 168(9):904–912, 2011.

[119] Hideki Kozima, Marek P Michalowski, and Cocoro Nakagawa. Keepon. *International Journal of Social Robotics*, 1(1):3–18, 2009.

[120] Hideki Kozima, Cocoro Nakagawa, Nobuyuki Kawai, Daisuke Kosugi, and Yoshio Yano. A humanoid in company with children. In *Humanoid Robots, 2004 4th IEEE/RAS International Conference on*, volume 1, pages 470–477. IEEE, 2004.

[121] Hideki Kozima, Cocoro Nakagawa, and Yuriko Yasuda. Children–robot interaction: a pilot study in autism therapy. *Progress in Brain Research*, 164:385–400, 2007.

[122] Alison M Kozlowski and Johnny L Matson. An examination of challenging behaviors in autistic disorder versus pervasive developmental disorder not otherwise specified: Significant differences and gender effects. *Research in Autism Spectrum Disorders*, 6(1):319–325, 2012.

[123] Rudolf Kruse, Christian Borgelt, Frank Klawonn, Christian Moewes, Matthias Steinbrecher, and Pascal Held. Multi-layer perceptrons. In *Computational Intelligence*, pages 47–81. Springer, 2013.

[124] Shashi Kuppa. Injury criteria for side impact dummies. *Washington, DC: National Transportation Biomechanics Research Center, National Highway Saftey Administration, US DOT*, 67, 2004.

[125] SB Kyle, P Adler, and RC Monticone. Reducing youth baseball injuries with protective equipment. *Consumer Product Saf Rev*, 1(1):1–4, 1996.

[126] Beibin Li, Laura Boccanfuso, Quan Wang, Erin Barney, Yeojin Amy Ahn, Claire Foster, Katarzyna Chawarska, Brian Scassellati, and Frederick Shic. Human robot activity classification based on accelerometer and gyroscope. In *2016 25th IEEE International Symposium on Robot and Human Interactive Communication (RO-MAN). Presented at the 2016 25th IEEE International Symposium on Robot and Human Interactive Communication (RO-MAN)*, pages 423–424, 2016.

[127] Paul Lukowicz, Jamie A Ward, Holger Junker, Mathias Stäger, Gerhard Tröster, Amin Atrash, and Thad Starner. Recognizing workshop activity using body worn microphones and accelerometers. In *International conference on pervasive computing*, pages 18–32. Springer, 2004.

[128] Wendy Machalicek, Mark F O'Reilly, Natasha Beretvas, Jeff Sigafoos, and Guilio E Lancioni. A review of interventions to reduce challenging behavior in school settings for students with autism spectrum disorders. *Research in Autism Spectrum Disorders*, 1(3):229–246, 2007.

[129] RB Martin, L Liptai, S Yerby, and KR Williams. The relationship between mass and acceleration for impacts on padded surfaces. *Journal of biomechanics*, 27(3):361–364, 1994.

[130] Giovanna Mascheroni and Donell Holloway. The internet of toys: A report on media and social discourses around young children and iotoys. 2017.

[131] Johnny L Matson, Melissa L Gonzalez, and Tessa T Rivet. Reliability of the autism spectrum disorder-behavior problems for children (asd-bpc). *Research in Autism Spectrum Disorders*, 2(4):696–706, 2008.

[132] Johnny L Matson and Mary Shoemaker. Intellectual disability and its relationship to autism spectrum disorders. *Research in developmental disabilities*, 30(6):1107–1114, 2009.

[133] Andrew S McIntosh and D Janda. Evaluation of cricket helmet performance and comparison with baseball and ice hockey helmets. *British journal of sports medicine*, 37(4):325–330, 2003.

[134] François Michaud and Serge Caron. Roball, the rolling robot. *Autonomous robots*, 12(2):211–222, 2002.

[135] Jason P Mihalik, J Troy Blackburn, Richard M Greenwald, Robert C Cantu, Stephen W Marshall, and Kevin M Guskiewicz. Collision type and player anticipation affect head impact severity among youth ice hockey players. *Pediatrics*, 125(6):e1394–e1401, 2010.

[136] Mehdi Moayyedian, Javad Farrokhi Derakhshandeh, and Sherif Said. Experimental investigations of significant parameters of strain measurement employing taguchi method. *SN Applied Sciences*, 1(1), dec 2018.

[137] Douglas C Montgomery. *Design and analysis of experiments*. John wiley & sons, 2017.

[138] Teruo Mori. *Taguchi methods: benefits, impacts, mathematics, statistics, and applications*. ASME Press, 2011.

[139] William C Moss, Michael J King, and Eric G Blackman. Towards reducing impact-induced brain injury: lessons from a computational study of army and football helmet pads. *Computer Methods in Biomechanics and Biomedical Engineering*, 17(11):1173–1184, 2014.

[140] Muhammad Mubashir, Ling Shao, and Luke Seed. A survey on fall detection: Principles and approaches. *Neurocomputing*, 100:144–152, 2013.

[141] Olivia Murphy, Olive Healy, and Geraldine Leader. Risk factors for challenging behaviors among 157 children with autism spectrum disorder in ireland. *Research in Autism Spectrum Disorders*, 3(2):474–482, 2009.

[142] Scott M Myers, Chris Plauché Johnson, et al. Management of children with autism spectrum disorders. *Pediatrics*, 120(5):1162–1182, 2007.

[143] National Instruments. Tdm excel add-in for microsoft excel download. (Date last accessed 22-Mar-2019).

[144] NICHD Early Child Care Research Network, William F Arsenio, et al. Trajectories of physical aggression from toddlerhood to middle childhood: Predictors, correlates, and outcomes. *Monographs of the Society for Research in Child Development*, pages i–143, 2004.

[145] Matthew K Nock, Alan E Kazdin, Eva Hiripi, and Ronald C Kessler. Lifetime prevalence, correlates, and persistence of oppositional defiant disorder: results from the national comorbidity survey replication. *Journal of Child Psychology and Psychiatry*, 48(7):703–713, 2007.

[146] Susanne Oberer and Rolf Dieter Schraft. Robot-dummy crash tests for robot safety assessment. In *Robotics and Automation, 2007 IEEE International Conference on*, pages 2934–2939. IEEE, 2007.

[147] Ewerton Oliveira, Davide Orrù, Tiago Nascimento, and Andrea Bonarini. Modeling player activity in a physical interactive robot game scenario. In *Proceedings of the 5th International Conference on Human Agent Interaction*, pages 411–414. ACM, 2017.

[148] Ewerton LS Oliveira, Davide Orrù, Luca Morreale, Tiago P Nascimento, and Andrea Bonarini. Learning and mining player motion profiles in physically interactive robogames. *Future Internet*, 10(3):22, 2018.

[149] Ewerton LS Oliveira, Davide Orrù, Tiago Nascimento, and Andrea Bonarini. Activity recognition in a physical interactive robogame. In *2017 Joint IEEE International Conference on Development and Learning and Epigenetic Robotics (ICDL-EpiRob)*, pages 92–97. IEEE, 2017.

[150] David M O'sullivan, Gabriel P Fife, Willy Pieter, and Insik Shin. Safety performance evaluation of taekwondo headgear. *Br J Sports Med*, 47(7):447–451, 2013.

[151] Salvatore Panduri, Valentina Dini, and Marco Romanelli. The durometer measurement of the skin: Hardware and measuring principles. *Agache's Measuring the Skin*, pages 1–7, 2016.

[152] Sarah Parsons, Peter Mitchell, and Anne Leonard. The use and understanding of virtual environments by adolescents with autistic spectrum disorders. *Journal of Autism and Developmental disorders*, 34(4):449–466, 2004.

[153] Fabian Pedregosa, Gaël Varoquaux, Alexandre Gramfort, Vincent Michel, Bertrand Thirion, Olivier Grisel, Mathieu Blondel, Peter Prettenhofer, Ron Weiss, Vincent Dubourg, et al. Scikit-learn: Machine learning in python. *Journal of machine learning research*, 12(Oct):2825–2830, 2011.

[154] J. T. Perry, S. Kellog, S. M. Vaidya, J. Youn, H. Ali, and H. Sharif. Survey and evaluation of real-time fall detection approaches. In *2009 6th International Symposium on High Capacity Optical Networks and Enabling Technologies (HONET)*, pages 158–164, Dec 2009.

[155] Giovanni Pioggia, ML Sica, Marcello Ferro, Roberta Igliozzi, Filippo Muratori, Arti Ahluwalia, and Danilo De Rossi. Human-robot interaction in autism: Face, an android-based social therapy. In *RO-MAN 2007-The 16th IEEE International Symposium on Robot and Human Interactive Communication*, pages 605–612. IEEE, 2007.

[156] Karen M Plant and Matthew R Sanders. Reducing problem behavior during care-giving in families of preschool-aged children with developmental disabilities. *Research in developmental disabilities*, 28(4):362–385, 2007.

[157] Thomas Plötz, Nils Y Hammerla, Agata Rozga, Andrea Reavis, Nathan Call, and Gregory D Abowd. Automatic assessment of problem behavior in individuals with developmental disabilities. In *Proceedings of the 2012 ACM Conference on Ubiquitous Computing*, pages 391–400. ACM, 2012.

[158] Sathiyaprakash Ramdoss, Russell Lang, Austin Mulloy, Jessica Franco, Mark O'Reilly, Robert Didden, and Giulio Lancioni. Use of computer-based interventions to teach communication skills to children with autism spectrum disorders: A systematic review. *Journal of Behavioral Education*, 20(1):55–76, 2011.

[159] Frederick P Rivara, Thomas D Koepsell, Jin Wang, Nancy Temkin, Andrea Dorsch, Monica S Vavilala, Dennis Durbin, and Kenneth M Jaffe. Incidence of disability among children 12 months after traumatic brain injury. *American journal of public health*, 102(11):2074–2079, 2012.

[160] Ben Robins, Kerstin Dautenhahn, and Paul Dickerson. From isolation to communication: a case study evaluation of robot assisted play for children with autism with a minimally expressive humanoid robot. In *Advances in Computer-Human Interactions, 2009. ACHI'09. Second International Conferences on*, pages 205–211. IEEE, 2009.

[161] Ben Robins, Kerstin Dautenhahn, Rene Te Boekhorst, and Aude Billard. Effects of repeated exposure to a humanoid robot on children with autism. In *Designing a more inclusive world*, pages 225–236. Springer, 2004.

[162] Ben Robins, Nuno Otero, Ester Ferrari, and Kerstin Dautenhahn. Eliciting requirements for a robotic toy for children with autism-results from user panels. In *Robot and Human interactive Communication, 2007. RO-MAN 2007. The 16th IEEE International Symposium on*, pages 101–106. IEEE, 2007.

[163] Hayley Robinson, Bruce MacDonald, and Elizabeth Broadbent. The role of healthcare robots for older people at home: A review. *International Journal of Social Robotics*, 6(4):575–591, 2014.

[164] Sally J Rogers. Brief report: Early intervention in autism. *Journal of autism and developmental disorders*, 26(2):243–246, 1996.

[165] Steven Rowson and Stefan M Duma. Development of the star evaluation system for football helmets: integrating player head impact exposure and risk of concussion. *Annals of biomedical engineering*, 39(8):2130–2140, 2011.

[166] Steven Rowson and Stefan M Duma. Brain injury prediction: assessing the combined probability of concussion using linear and rotational head acceleration. *Annals of biomedical engineering*, 41(5):873–882, 2013.

[167] KK Sadasivuni, AY Al Haddad, H Javed, WJ Yoon, and J-J Cabibihan. Strain, pressure, temperature, proximity, and tactile sensors from biopolymer composites. In *Biopolymer Composites in Electronics*, pages 437–457. Elsevier, 2017.

[168] Shinji Sakurai and Mitsumasa Miyashita. Developmental aspects of overarm throwing related to age and sex. *Human Movement Science*, 2(1):67–76, 1983.

[169] Tamie Salter, François Michaud, Dominic Létourneau, DC Lee, and Iain P Werry. Using proprioceptive sensors for categorizing human-robot interactions. In *Human-Robot Interaction (HRI), 2007 2nd ACM/IEEE International Conference on*, pages 105–112. IEEE, 2007.

[170] Nina Scarpinato, Jana Bradley, Kay Kurbjun, Xenia Bateman, Brenda Holtzer, and Beth Ely. Caring for the child with an autism spectrum disorder in the acute care setting. *Journal for Specialists in Pediatric Nursing*, 15(3):244–254, 2010.

[171] Brian Scassellati, Henny Admoni, and Maja Mataric. Robots for use in autism research. *Annual review of biomedical engineering*, 14:275–294, 2012.

[172] Kai-Uwe Schmitt, Peter F Niederer, Markus H Muser, and Felix Walz. *Trauma Biomechanics: Accidental injury in traffic and sports*. Springer Science & Business Media, 2009.

[173] Syamimi Shamsuddin, Hanafiah Yussof, Luthffi Idzhar Ismail, Salina Mohamed, Fazah Akhtar Hanapiah, and Nur Ismarrubie Zahari. Initial response in hri-a case study on evaluation of child with autism spectrum disorders interacting with a humanoid robot nao. *Procedia Engineering*, 41:1448–1455, 2012.

[174] Perry Share and John Pender. Preparing for a robot future? social professions, social robotics and the challenges ahead. *Irish Journal of Applied Social Studies*, 18(1):4, 2018.

[175] Oliver A Shergold and Norman A Fleck. Experimental investigation into the deep penetration of soft solids by sharp and blunt punches, with application to the piercing of skin. *Journal of biomechanical engineering*, 127(5):838–848, 2005.

[176] Takanori Shibata. Therapeutic seal robot as biofeedback medical device: Qualitative and quantitative evaluations of robot therapy in dementia care. *Proceedings of the IEEE*, 100(8):2527–2538, 2012.

[177] Bruno Siciliano and Oussama Khatib. *Springer handbook of robotics*. Springer, 2016.

[178] W-C So, MK-Y Wong, J-J Cabibihan, CK-Y Lam, RY-Y Chan, and H-H Qian. Using robot animation to promote gestural skills in children with autism spectrum disorders. *Journal of Computer Assisted Learning*, 32(6):632–646, 2016.

[179] Solutions, Humanetics Innovative. Hybrid iii 3 year old child. *Child Dummies, URL: http://www.humaneticsatd.com/crash-test-dummies/children/hiii-3yo*, 2017. (Date last accessed 1-Jan-2018).

[180] Angela Sucerquia, José David López, and Jesús Francisco Vargas-Bonilla. Real-life/real-time elderly fall detection with a triaxial accelerometer. *Sensors*, 18(4):1101, 2018.

[181] Denis G Sukhodolsky, Stephanie D Smith, Spencer A McCauley, Karim Ibrahim, and Justyna B Piasecka. Behavioral interventions for anger, irritability, and aggression in children and adolescents. *Journal of child and adolescent psychopharmacology*, 26(1):58–64, 2016.

[182] Lin Sun, Daqing Zhang, Bin Li, Bin Guo, and Shijian Li. Activity recognition on an accelerometer embedded mobile phone with varying positions and orientations. In *International conference on ubiquitous intelligence and computing*, pages 548–562. Springer, 2010.

[183] Carrie Sussman and Barbara M Bates-Jensen. *Wound care: a collaborative practice manual*. Lippincott Williams & Wilkins, 2007.

[184] Ilya Sutskever, Oriol Vinyals, and Quoc V Le. Sequence to sequence learning with neural networks. In *Advances in neural information processing systems*, pages 3104–3112, 2014.

[185] GenO̓ ichi Taguchi and Yuin Wu. *Introduction to off-line quality control*. Central Japan Quality Control Assoc., 1979.

[186] Alireza Taheri, Ali Meghdari, Minoo Alemi, and Hamidreza Pouretemad. Human–robot interaction in autism treatment: A case study on three pairs of autistic children as twins, siblings, and classmates. *International Journal of Social Robotics*, pages 1–21, 2017.

[187] T. Tamizharasan, N. Senthilkumar, V. Selvakumar, and S. Dinesh. Taguchi's methodology of optimizing turning parameters over chip thickness ratio in machining p/m AMMC. *SN Applied Sciences*, 1(2), jan 2019.

[188] Christopher A Taylor. Traumatic brain injury–related emergency department visits, hospitalizations, and deaths-united states, 2007 and 2013. *MMWR. Surveillance Summaries*, 66, 2017.

[189] Hong Tuan Teo and John-John Cabibihan. Toward soft, robust robots for children with autism spectrum disorder. In *FinE-R@ IROS*, pages 15–19, 2015.

[190] John Versace. A review of the severity index. Technical report, SAE Technical Paper, 1971.

[191] Rémy Willinger and Daniel Baumgartner. Human head tolerance limits to specific injury mechanisms. *International journal of Crashworthiness*, 8(6):605–617, 2003.

[192] John Z Wu, Christopher S Pan, Bryan M Wimer, and Charles L Rosen. Finite element simulations of the head–brain responses to the top impacts of a construction helmet: Effects of the neck and body mass. *Proceedings of the Institution of Mechanical Engineers, Part H: Journal of engineering in medicine*, 231(1):58–68, 2017.

[193] Agnieszka Wykowska, Jasmin Kajopoulos, Miguel Obando-Leiton, Sushil Singh Chauhan, John-John Cabibihan, and Gordon Cheng. Humans are well tuned to detecting agents among non-agents: examining the sensitivity of human perception to behavioral characteristics of intentional systems. *International Journal of Social Robotics*, 7(5):767–781, 2015.

[194] SHI Xingjian, Zhourong Chen, Hao Wang, Dit-Yan Yeung, Wai-Kin Wong, and Wang-chun Woo. Convolutional lstm network: A machine learning approach for precipitation nowcasting. In *Advances in neural information processing systems*, pages 802–810, 2015.

[195] Y Yamada, Y Hirasawa, SY Huang, and Y Umetani. Fail-safe human/robot contact in the safety space. In *Robot and Human Communication, 1996., 5th IEEE International Workshop on*, pages 59–64. IEEE, 1996.

[196] Nicholas H Yang, Kathleen Allen Rodowicz, and David Dainty. Baseball head impacts to the non-helmeted and helmeted hydrid iii atd. In *ASME 2014 International Mechanical Engineering Congress and Exposition*, pages V003T03A007–V003T03A007. American Society of Mechanical Engineers, 2014.

[197] Keith Owen Yeates, Erika Swift, H Gerry Taylor, Shari L Wade, Dennis Drotar, Terry Stancin, and Nori Minich. Short-and long-term social outcomes following pediatric traumatic brain injury. *Journal of the International Neuropsychological Society*, 10(3):412–426, 2004.

[198] Tyler J Young, Ray W Daniel, Steven Rowson, and Stefan M Duma. Head impact exposure in youth football: elementary school ages 7-8 years and the effect of returning players. *Clinical journal of sport medicine*, 24(5):416–421, 2014.

[199] Benjamin Zablotsky, Lindsey I Black, Matthew J Maenner, Laura A Schieve, and Stephen J Blumberg. Estimated prevalence of autism and other developmental disabilities following questionnaire changes in the 2014 national health interview survey. *National health statistics reports*, (87):1–21, 2015.

[200] Liying Zhang, King H Yang, and Albert I King. A proposed injury threshold for mild traumatic brain injury. *Transactions-American Society of Mechanical Engineers Journal of Biomechanical Engineering*, 126(2):226–236, 2004.

[201] Yu Zhao, Rennong Yang, Guillaume Chevalier, Ximeng Xu, and Zhenxing Zhang. Deep residual bidir-lstm for human activity recognition using wearable sensors. *Mathematical Problems in Engineering*, 2018, 2018.

[202] Chun Zhu and Weihua Sheng. Human daily activity recognition in robot-assisted living using multi-sensor fusion. In *Robotics and Automation, 2009. ICRA'09. IEEE International Conference on*, pages 2154–2159. IEEE, 2009.

[203] Lonnie Zwaigenbaum, Susan Bryson, Tracey Rogers, Wendy Roberts, Jessica Brian, and Peter Szatmari. Behavioral manifestations of autism in the first year of life. *International journal of developmental neuroscience*, 23(2-3):143–152, 2005.

APPENDIX $\mathcal{A}$

List of Publications

A.1 Journals

1. A. Y. Alhaddad, J.-J. Cabibihan, and A. Bonarini, "Head impact severity measures for small social robots thrown during meltdown in autism," International Journal of Social Robotics, Nov 2018.
2. A. Y. Alhaddad, J.-J. Cabibihan, A. Hayek, and A. Bonarini, "Safety experiments for small robots investigating the potential of soft materials in mitigating the harm to the head due to impacts," SN Applied Sciences, vol. 1, no. 5, p. 476, 2019.
3. A. Y. Alhaddad, J.-J. Cabibihan, A. Hayek, and A. Bonarini, "Influence of the shape and mass of a small robot when thrown to a dummy human head," SN Applied Sciences, vol. 1, no. 11, p. 1468, 2019.
4. A. Y. Alhaddad, J.-J. Cabibihan, and A. Bonarini, "Influence of Reaction Time in the Emotional Response of a Companion Robot to a Child's Aggressive Interaction," International Journal of Social Robotics, 2019.
5. A. Y. Alhaddad, J.-J. Cabibihan, A. Hayek, and A. Bonarini, "A low-cost test rig for impact experiments on a dummy head," HardwareX, p. e00068, 2019.
6. A. Y. Alhaddad, J.-J. Cabibihan, A. Hayek, and A. Bonarini, "Data on the impact of an object with different thicknesses of different soft materials at different impact velocities on a dummy head," Data in Brief, p. 103885, Apr. 2019.
7. A. Y. Alhaddad, J.-J. Cabibihan, A. Hayek, and A. Bonarini, "Data on the impact of objects with different shapes, masses, and impact velocities on a dummy head," Data in Brief, vol. 22, pp. 344–348, Feb 2019.

A.2 Conferences

1. A. Y. Alhaddad, J.-J. Cabibihan, and A. Bonarini, "Recognition of aggressive behaviors of children toward a robotic toy," IEEE International Conference on Robot-Human Interactive Communications, New Delhi, India, 2019.
2. A. Y. Alhaddad and J.-J. Cabibihan, "Reflex system for intelligent robotics," in Qatar Foundation Annual Research Conference Proceedings Volume 2016 Issue 1, vol. 2016, p. HBSP2914, Hamad bin Khalifa University Press (HBKU Press), 2016.

A.3 Book Chapters

1. A. Y. Alhaddad, H. Javed, O. Connor, B. Banire, D. Al Thani, and J.-J. Cabibihan, "Robotic trains as an educational and therapeutic tool for autism spectrum disorder intervention," in Robotics in Education (W. Lepuschitz, M. Merdan, G. Koppensteiner, R. Balogh, and D. Obdržálek, eds.), (Cham), pp. 249–262, Springer International Publishing, 2019.
2. J.-J. Cabibihan, R. Chellali, C. W. C. So, M. Aldosari, O. Connor, A. Y. Alhaddad, and H. Javed, "Social robots and wearable sensors for mitigating meltdowns in autism - a pilot test," in Social Robotics, pp. 103–114, Springer International Publishing, 2018.
3. K. Sadasivuni, A. Al Haddad, H. Javed, W. Yoon, and J.-J. Cabibihan, "Strain, pressure, temperature, proximity, and tactile sensors from biopolymer composites," in Biopolymer Composites in Electronics, pp. 437–457, Elsevier, 2017.
4. A. Y. Alhaddad, S. E. AlKhatib, R. A. Khan, S. M. Ismail, A.-S. S. Shehadeh, A. M. Sadeq, and J.-J. Cabibihan, "Toward 3D printed prosthetic hands that can satisfy psychosocial needs: Grasping force comparisons between a prosthetic hand and human hands," in Social Robotics (A. Kheddar, E. Yoshida, S. S. Ge, K. Suzuki, J.-J. Cabibihan, F. Eyssel, and H. He, eds.), (Cham), pp. 304–313, Springer International Publishing, 2017.

A.4 Patents

1. J. Cabibihan, H. Javed, K. Sadasivuni, and A. Al Haddad, "Smart robotic therapeutic learning toy," US 2019/0184299 A1, US Patent Office; Publication Date: 20 June 2019.
2. J.-J. Cabibihan, K. K. Sadasivuni, and A. Y. Alhaddad, "Biometric liveness detection through biocompatible capacitive sensor," US2019/0050622 A1, US Patent Office; Publication Date: 14 February 2019.
3. J. Cabibihan, H. Javed, K. Sadasivuni, and A. Al Haddad, "Smart robotic therapeutic learning toy," WO 2018/033857, World Intellectual Property Organization; Publication Date: 22 February 2018.
4. J.-J. Cabibihan, K. K. Sadasivuni, and A. Y. Alhaddad, "Biometric liveness detection through biocompatible capacitive sensor," WO 2019/030700, World Intellectual Property Organization; Publication Date: 14 February 2019.

APPENDIX B

Impact Test Rig

B.1 Hardware in context

Anthropomorphic test dummies (ATDs) are used to evaluate the potential harm to humans through the simulation of risky scenarios, for example, using ATD in car crash tests. Such dummies are equipped with sensors to measure different dynamics that occur due to impacts, such as accelerations and forces. Severity indices are used to assess the potential for an injury based on the measured dynamics. For example, the acceleration of the head due to impact is used to compute the Head Injury Criterion (HIC) numerical value, which in turn is used to predict the potential for harm based on the Abbreviated Injury Scale (AIS) [86].

The application of test dummies has been also considered in other areas, such as in sports. For the assessment of protective gears in sports, ATDs based setups were used [196] [133]. The evaluation was based on simulating impacts that might occur in actual scenarios. In a study evaluating concussion due to taekwondo kicks, a dummy head was used to measure the dynamics of the head due to impacts [76]. In that study, a 50th percentile ATD head (i.e. Hybrid II) with a mass of 5.1 kg attached to a neck was used. The internal structure of the head was made of aluminum covered with an artificial skin layer while the neck was made of rubber. The head setup was fitted with a taekwondo head guard that was then mounted on an aluminum support frame. A tri-axial accelerometer was embedded at the center of the head to obtain the linear acceleration of the head. The readings of the accelerometer was acquired through a three-channel sensor signal conditioner connected to a computer. A motion analysis system consisting of eight cameras was used to monitor the head's movement and to measure the peak velocity of the kicks through tracking reflective markers placed on the test head and the foot pads. The participants were requested to perform different kicks on the dummy head while wearing the foot pads.

Furthermore, such setups were also considered to assess harm in robotics by considering dif-

ferent scenarios where a robot is impacting a person at different body parts [90] [92]. Alternative approaches, such as low-cost sensors and body parts models, were also considered to conduct impact experiments [91] [189]. One study considered a low-cost developed head model to conduct impact experiments to characterize a safety index in robotics [60]. In that study, the impacts were performed by robotic arm (i.e. Scara Robot-Adept Cobra 600) at different impact speed conditions (i.e. 0.4 - 1.9 m/s). The developed head model was based on a leather ball filled with sand to reach a weight of 3 kg. A low-cost tri-axial accelerometer was placed at the head to measure the linear acceleration of the head. Furthermore, that study has considered a low-cost sensor to measure the impact force placed at the point of impact.

In this work, we present a low-cost method for the construction of a dummy head experimental setup to conduct impact experiments at low velocities. The impact rig is focused on investigating impacts due to thrown objects. The developed rig does not require expensive hardware (e.g. expensive camera system) and can be constructed using typical available facilities (e.g. 3D printer). Some suggested equipment can be substituted by cheaper alternatives.

B.2 Hardware description

The experimental setup is a device to examine the acceleration changes of the head due to impacts. It reports the head acceleration in the X, Y, and Z directions. The setup is suitable for the examination of low velocity impacts. The setup would be beneficial for researchers who have limited access to more expensive test dummies. The analysis of the acceleration data can report three severity indices. Modifications are possible to perform different forms of impact tests.

The setup offers the following:

- Reporting of the head accelerations (i.e. in X, Y, and Z axes) and the resultant acceleration
- Post processing of the raw data provides the analysis for three severity indices
- Adjustable to do different tests at different impact velocities
- The dummy head mass can be modified to meet different age groups
- The rig is adjustable to perform different tests (e.g. different impact areas)
- The artificial skin of the dummy head can be used as an indicator for tissue injuries

B.3 Design files

This section contains a summary to the design files that have been used to build the impact rig. All files can be found in their respective links in the online repository.

B.4 Bill of materials

This section contains the complete bill of materials that were used to construct the impact rig.

B.5 Build instructions

B.5.1 Experimental setup

The two files of the head design (i.e. human-head-part1 and human-head-part2) were developed by a 3D printer (Replicator 5th Generation, MakerBot Industries). The settings of the 3D printer were left at default. The infill option was set at 10%. If more robustness or higher mass is required, then

Table B.1: *Design Files Summary [11]*

Design file name	File type	Description	Open source license	Location of the file
human-head-part1	STL file	The modified front half of the original head design (Fig. B.1b)	CC BY 4.0	Link 1
human-head-part2	STL file	The modified back half of the original head design (Fig. B.1c)	CC BY 4.0	Link 2
Exp_bench	PDF	A reference drawing of the experimental bench that was used showing the dimensions.	CC BY 4.0	Link 3
labview_ script	National instruments VI file	A script that reads the accelerometer that is connected to the data acquisition card and stores the readings.	CC BY 4.0	Link 4
Matlab_ script_multi	MATLAB code	A code to calculate the three severity indices, namely, the HIC, 3 ms, and peak acceleration.	CC BY 4.0	Link 5

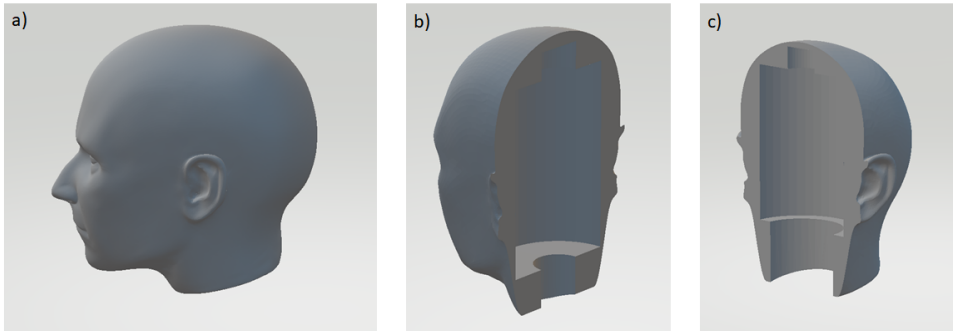

Figure B.1: *The 3D head design that was used to develop the dummy head [11]. a) Complete view of the original design (Source: Link). b) Part 1 view (i.e. front). c) Part 2 view (i.e. back).*

Table B.2: *Bill of Materials [11]*

Designator	Component	Units	Unit Cost (US$)	Total cost(US$)	Source of materials	Material type
ACC	ADXL 377	1	$ 25.95	$ 25.95	SparkFun	Electronics
DAQ	PCI-6031E	1	$ 2,895.00	$ 2,895.00	National Instrument	Electronics
Camera	FDR-X1000V	1	$ 500.00	$ 500.00	Sony	Electronics
Tripod	Amazon Basics 50-Inch Lightweight Tripod	1	$ 15.00	$ 15.00	Amazon	Aluminum
Wires	Ribbon Cable -6 wires 15ft	2	$ 2.95	$ 5.90	SparkFun	Cables
3D printing material	PLA Material Large Spool	2	$ 48	$ 96	MakerBot Industries	Polylactic acid
Soft material	Ecoflex 00-30 (2 lbs)	1	$ 32.21	$ 64.42	Smooth-On	Silicone rubber
Mass	Modeling clay	2	∼$ 10	∼$ 20	Locally	Polymer clay
Frame	Custom-made bench	1	∼$ 150	∼$ 150	Locally	
Rope	Coated ropes	1	$ 5	$ 5	Locally	Nylon
Velcro	Velcro Elastic Straps (36" x 1")	2	∼$ 7	∼$ 14	Locally	Nylon, Polyester
PVC	Plastic Saddle Elbow (1")	2	$ 2	$ 4	Locally	Plastic

Figure B.2: *The 3D printed head parts after applying the soft material [11].*

this option should be set at higher percentages. However, this will increase the time required to print the parts considerably. Soft materials can be added to make the skin more lifelike [42] [44] [50] [43] [40]. Hence, a 2 mm layer of a soft material made of silicone was added to the head [49]. The soft material (Ecoflex, Smooth-On, USA) was prepared by mixing equal volume (i.e. 1A:1B) of the two material parts for around 4 mins. The soft material was then applied to both parts of the head then left to cure for 4 hours at room temperature (Fig. B.2). Other soft materials can also be considered (e.g. PDMS [105]). Furthermore, embedding other sensors (e.g. pressure or force [51] [167] [1]) inside the soft material is also a viable option. This will allow the detection of other modalities.

As part of our research toward safer social robots for children with autism, this experimental setup was developed to investigate safety in social robots by considering a scenario where a small robot is thrown to the child′s head [9]. Hence, a head mass of 3 kg was selected to make the developed dummy head comparable to that of children's dummy heads [179]. Both head parts were augmented with clay to reach this mass (Fig. B.3). The masses of the parts were measured using a weight scale (Fig. B.4). If the goal is to study an adult's head, then a higher dummy head mass should be considered (e.g. 4.5 kg).

A tri-axial accelerometer (ADXL 377, SparkFun Electronics, USA) was embedded inside the clay at the center of the front part of the dummy head (Fig. B.5). This accelerometer will be used to measure the linear acceleration of the dummy head. The ribbon cable of the accelerometer was routed out of the head through the opening at the bottom (Fig. B.6). Pressure was applied to merge the two parts of the head together. The plastic elbows were attached to the head with the Velcro straps (Fig. B.6). The straps should provide more pressure to keep the head intact. Next, the dummy head was placed inside the experimental frame with the nylon coated ropes. The ropes should be arranged so that the head is at the center of the experimental setup.

B.5.2 Sensor calibration

The accelerometer was interfaced to a computer through a data acquisition card (DAQ). The ribbon cable of the accelerometer was connected to the appropriate pins of the DAQ (Fig. B.7). These pins

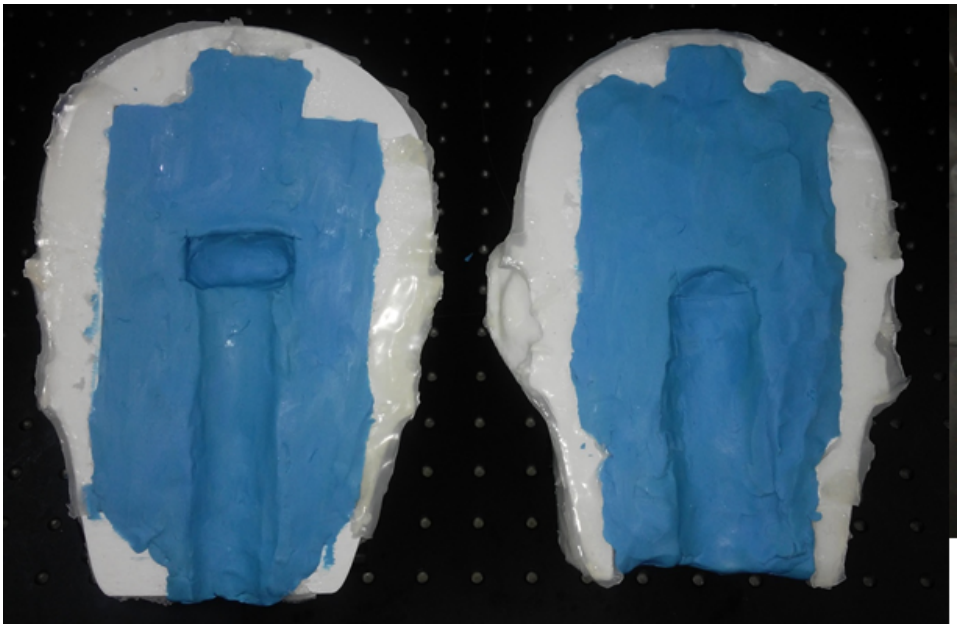

Figure B.3: *The 3D printed head parts after adding the clay to reach the desirable mass [11].*

Figure B.4: *The measured mass of the dummy head parts [11].*

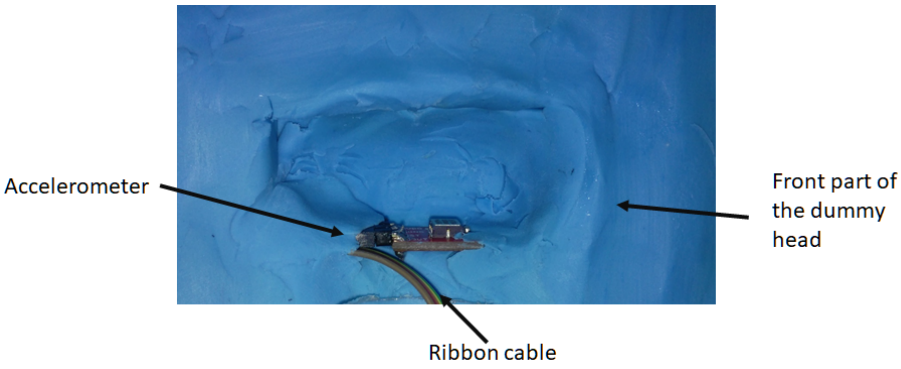

Figure B.5: *The accelerometer placed inside the dummy head [11].*

Figure B.6: *The dummy head after assembling it with the Velcro straps [11].*

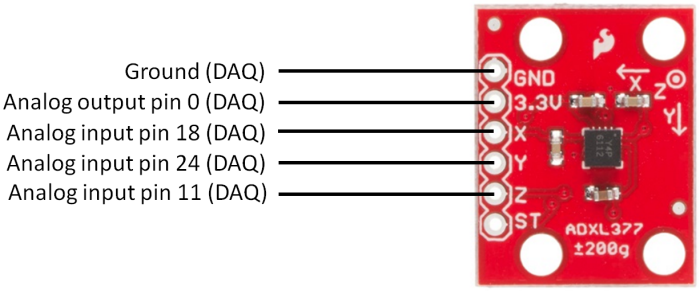

Figure B.7: *The mapping of the accelerometer pins to the data acquisition card (DAQ). The analog output pin 0 of the DAQ was used to provide 3.3 V to power up the accelerometer. Alternatively, an external power supply can be used [11].*

were matched with the configuration of the LabView script (Fig. (B.8)). Different configurations and pins can be considered depending on the DAQ model being used. A microcontroller-based DAQ that is capable of acquiring the data at a high rate can also be considered [105]. The LabView script read the voltages of the DAQ pins that were connected to the X, Y, and Z pins of the accelerometer at a sampling rate of 20 kHz and then filtered according to Channel Frequency Class 60 [58]. The readings were then converted to acceleration values (g) for each axis based on the following relation:

$$A_{axis} = \frac{|V_{current} - V_{zero}|}{Sensitivity_{axis}} \tag{B.1}$$

where $V_{current}$ is the current reading of the voltage of an axis (e.g. X, Y, and Z), V_{zero} is the voltage value of that axis at 0 g, and the sensitivity of an axis is the amount of voltage change that corresponds to gravitational change of one unit (g). The typical sensitivity of the accelerometer is around 6.5 mV/g based on the datasheet. More accurate sensitivity can be obtained experimentally by finding the voltage difference at 1 g and 0 g for each axis. The 0 g voltage was found by setting the axis studied parallel to ground surface while 1 g voltage by setting the axis perpendicular to the ground surface, for example, making the top surface of the accelerometer facing upward will give 1 g at the z axis while rotating it 90° will give 0 g. The sensitivity for each axis can be obtained accordingly. The sensitivity and V_{zero} values for each axis should be updated in the LabView script (i.e. labview_script.ni) by updating the formula vi (Fig. B.9).

The magnitude of the resultant acceleration is based on the square root of the sum of the squares of the individual accelerations. The relation is represented as follows:

$$|A| = \sqrt{A_x^2 + A_y^2 + A_z^2} \tag{B.2}$$

where A_x is the magnitude of acceleration in the X direction, A_y is the magnitude of acceleration in the Y direction, and A_z is the magnitude of acceleration in the Z direction.

B.6 Operation instructions

B.6.1 Preparation of the test rig

There are some steps that need to done before conducting any impact experiment. The steps are as follows:

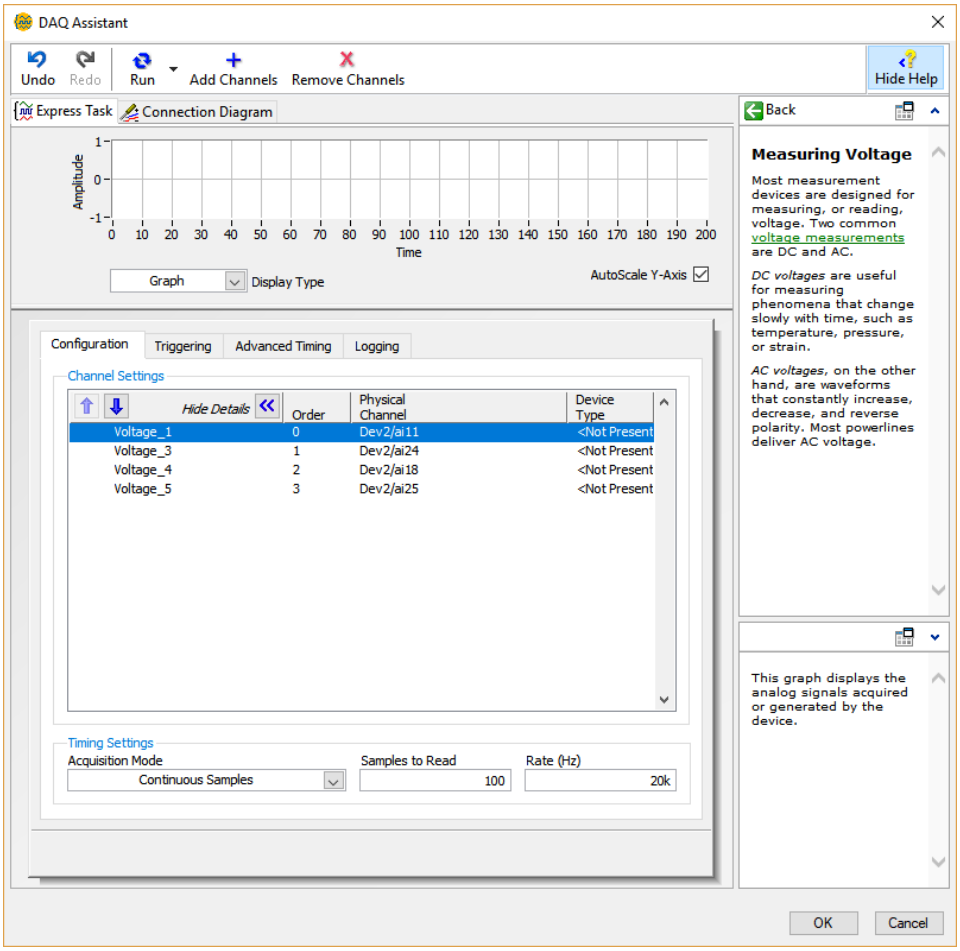

Figure B.8: *The analog input pins configuration of the data acquisition card (DAQ) within the LabView script. Reading the analog input pin 25 is optional and it was used for testing purposes [11].*

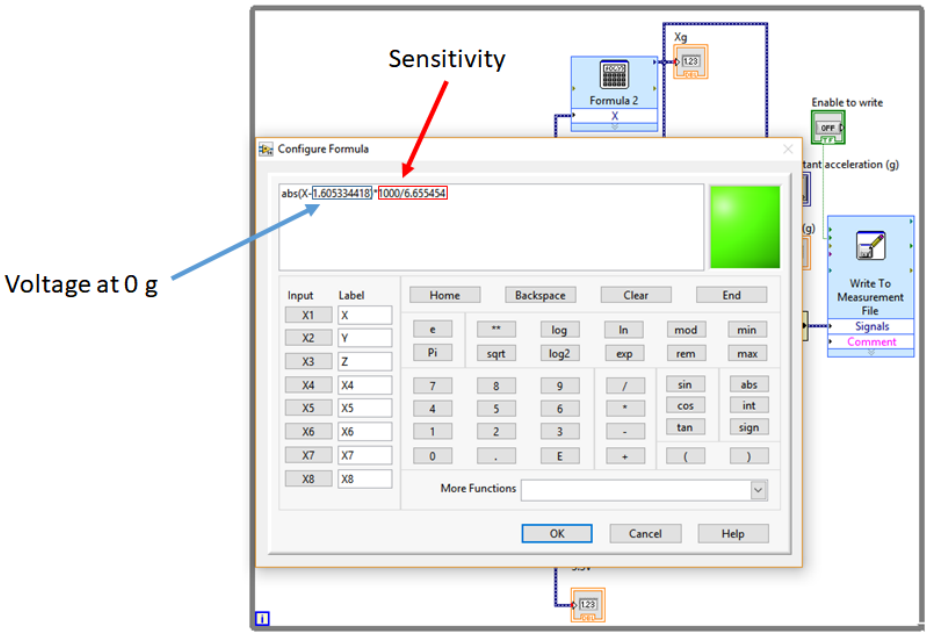

Figure B.9: *Updating the formula vi for the X-axis [11].*

- Check the connections of the DAQ and the accelerometer and their functionality. This can be achieved by running the LabView script and performing a test experiment (e.g. light nudge to the head) and checking the response.
- Ensure that there is a fixed reference (e.g. ruler) with a known dimension that is placed along the direction of impacts and perpendicular to the head (Fig. B.10). An ideal location would be under the head. This reference will be used to scale the dimensions in the video analysis software to determine the impact velocity.
- Set up the camera on the tripod in such way so that it faces the experimental setup from the side. The center view of the camera should be as centered and close to the head (Fig. B.10). The reference rod and the impactor should be visible.

B.6.2 Conducting an experiment

Two experimenters are recommended to conduct an experiment. One is in charge of performing the impact tests while the other is in charge of recording the videos. The operations involved are as follows:

1. Load the LabView script (i.e. labview_script.ni) and configure the *Write to Measurement File* to specify the folder and the appropriate file name (Fig. B.11).
2. Run the script and click *Enable to write* to start acquiring the acceleration data. Concurrently, start the video recording.
3. While conducting an experiment, the experimenter, who is releasing the impactor, should be aligned to the center of the setup and targeting the front side of the dummy head.

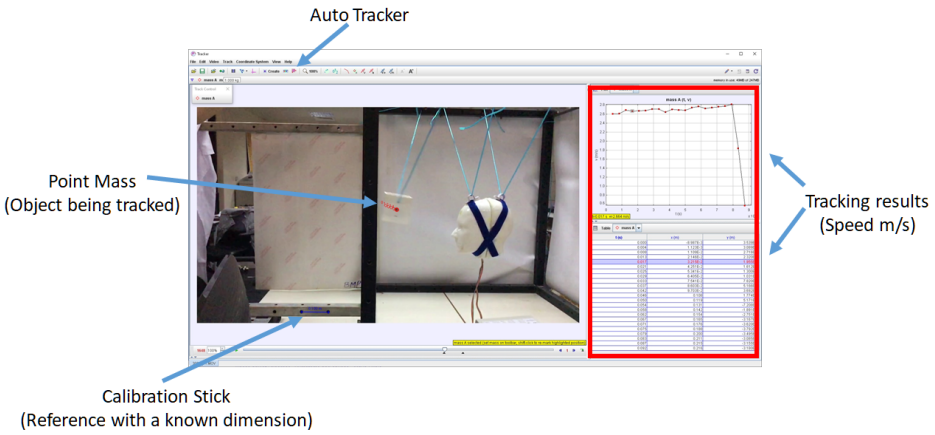

Figure B.10: *A video of an impact test being analyzed for the velocity of impact in the video analysis software [11].*

4. After conducting an experiment, the *Enable to write* should be clicked again to stop writing to the file. The script and the video recording should be stopped.
5. Repeat the same steps for multiple experiments.

The LabView script saves the data in Technical Data Management Streaming (TDMS) file format. Hence, an Add-In package need to be installed to be able to read the file in Microsoft Excel [143].

B.6.3 Video analysis

The video recordings of experiments were analyzed to obtain the impact velocities. An open-source video analysis software (Version 5.0.7, Douglas Brown, Open Source Physics) was used[1]. The steps involved in analyzing a video are as follows:

1. Run the software and load the video file. Move the *start frame* arrow to the start of the experiment and the *end frame* arrow after the impactor hits the dummy head. It is best to mark the start of an experiment after the impactor passes through the frame.
2. Add the *Calibration Stick* and mark both ends to the reference measurement (Fig. B.10).
3. Create *Point Mass* by clicking *Create* in the menu bar. This will be used to track the object in the next step.
4. Click *Auto Tracker* icon to open the menu for autotracking. Press *Shift* + *Ctrl* and click on a feature on the impactor to select a feature to track.
5. After selecting a feature to track on the current frame, press *Search* to allow the software to automatically track the feature in the next frames of the video. Manual intervention might be needed to correctly track the feature in the next frame.
6. To view the velocity plot, change the Y-axis on the plot to *v: velocity magnitude*.

[1] Visit the software website for more details about the options and settings of the software [38].

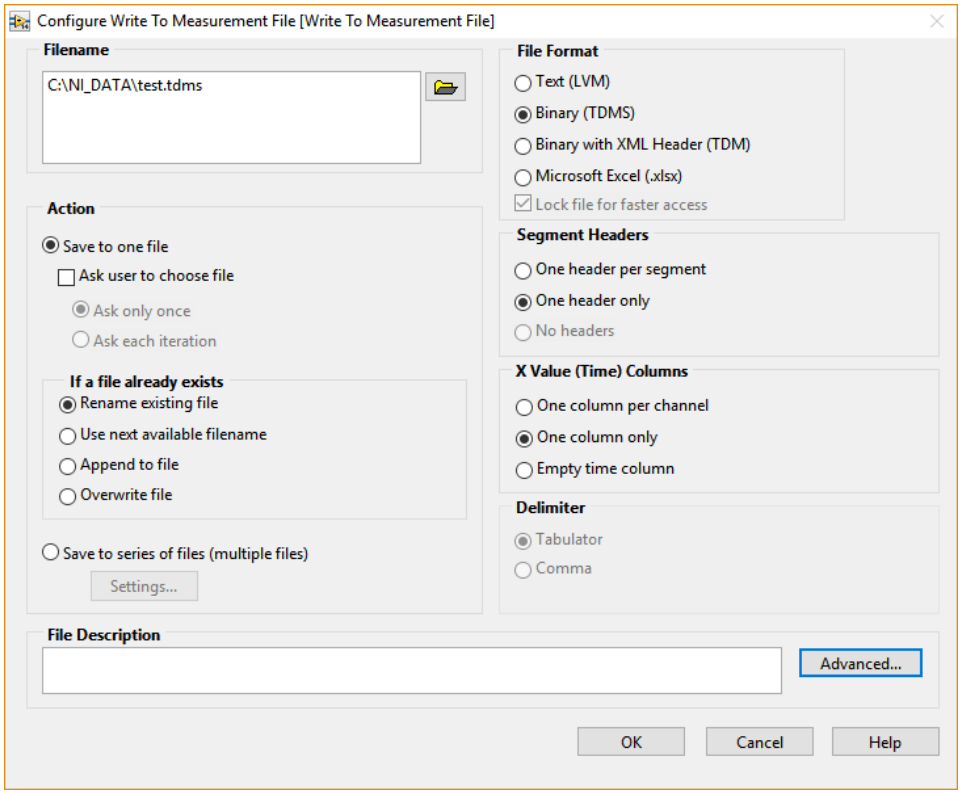

Figure B.11: *Specifying a folder and file name in the LabView script to store the acquired data [11].*

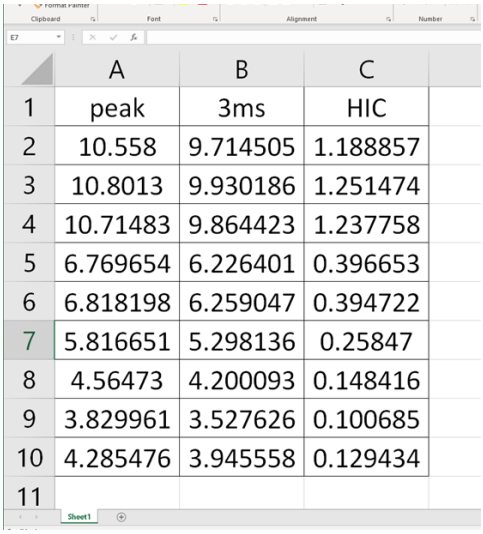

	A	B	C
1	peak	3ms	HIC
2	10.558	9.714505	1.188857
3	10.8013	9.930186	1.251474
4	10.71483	9.864423	1.237758
5	6.769654	6.226401	0.396653
6	6.818198	6.259047	0.394722
7	5.816651	5.298136	0.25847
8	4.56473	4.200093	0.148416
9	3.829961	3.527626	0.100685
10	4.285476	3.945558	0.129434
11			

Figure B.12: *A sample of a generated analysis for 9 experiments [11].*

B.6.4 Data analysis

The data analysis involves calculating the three severity indices from the acceleration data. A MATLAB script (i.e. Matlab_script_multi.m) was used to find the Head Acceleration Criterion (HIC), 3 ms criterion, and peak head acceleration. It can process multiple files and store the results in a spreadsheet file. The steps involved to analyze the data are as follows:

1. An excel file (i.e. xlsx) should be created for each experiment that contains the time and the resultant acceleration columns of the TDMS files from the experiments.
2. Each excel file should be named *trial_%d.xlsx* where *%d* is the experiment number (e.g. 1, 2, etc) placed with the script in the same folder.
3. The script is set to read 9 files. However, line 5 in the MATLAB script can be changed to match the number of files that are needed to be analyzed.
4. After running the script, the code creates a file *processed_new.xlsx* that contains the results of the analysis (Fig. B.12).

B.6.5 Limitations

This test rig is a suitable platform to evaluate the level of harm due to impacts, especially when considered for small objects (i.e. less than 3 kg) thrown at low velocities (i.e. less than 10 m/s). Furthermore, it can be used to investigate a relationship between the severity indices employed in the setup and some of the parameters (e.g. mass) of impactors. The artificial skin could also be used as an indicator for tissue injuries. However, re-applying the soft material might be needed in case of a tear or damage. Heavy impactors with sharp features should be avoided as it might penetrate the 3D printed structure of the dummy head.